EOSINOPHILIC RHINITIS AND NASAL EPITHELIAL REMODELING IN MICE EPISODICALLY EXPOSED TO OZONE

By

Chee Bing Ong

A THESIS

Submitted to
Michigan State University
in partial fulfilment for the requirement
for the degree of

Pathobiology – Master of Science

2014

ABSTRACT

EOSINOPHILIC RHINITIS AND NASAL EPITHELIAL REMODELING IN MICE EPISODICALLY EXPOSED TO OZONE

By

Chee Bing Ong

Ozone is an oxidant air pollutant in photochemical smog. Though nasal epithelial remodeling has been well-documented in laboratory animals repeatedly exposed to ozone, associated inflammatory responses have not been fully characterized. In this study, I investigated if the onset of ozone-induced nasal epithelial remodeling is related to temporal changes in granulocytic influx and cytokine gene expression. Mice exposed to 24 weekdays of inhaled ozone developed marked eosinophilic rhinitis with epithelial hyperplasia, mucous cell metaplasia and hyalinosis. Repeated subacute ozone exposures in mice induced an eosinophilic rhinitis with epithelial remodeling that resembled the pathology of human eosinophilic rhinitis. Ozone-induced eosinophilic rhinitis was associated with an initial T helper cell 1 (Th1)-inflammatory response, followed by T helper cell 2 (Th2)-inflammatory response. Based on these findings, a study was conducted to investigate the role of lymphocytes (hypothesized cellular sources of Th1- and Th2-cytokines) in the development of eosinophilic rhinitis and associated nasal epithelial remodeling. In Rag2 x common gamma chain (γc) - deficient [RAG2(-/-) x γc(-/-)] mice, which lack T- and B- lymphocytes as well as NK cells, ozone nasal epithelial remodeling and eosinophilic rhinitis did not develop, thus supporting the hypothesis that lymphocytes are a crucial component to ozone induced eosinophilic rhinitis and associated epithelial changes in mice. These results suggest that chronic exposure to air pollutants, like ozone, may contribute to rising incidence of eosinophilic rhinitis.

To Estella Liew, my wife.
For your sacrifice, unconditional love and
being by my side through good and bad times

ACKNOWLEDGEMENTS

I would like to thank all the past and present members of Dr Harkema's laboratory, who have contributed into this project, assisted me tremendously, and had made this research project a fulfilling learning journey. I am grateful to my mentor, Dr Jack Harkema, for his guidance, patience, his willingness to share his expertise and knowledge, and in directing the path which this research project took. My graduate research and training experience in his laboratory exposed me to the realm of toxicological pathology which I will continue to connect with and pursue in my future endeavours. My gratitude also goes to my Master committee members, namely Dr Matti Kiupel, Dr Ingeborg Langohr and Dr Colleen Hegg, for their professional guidance and advice.

My research project would not have been possible without the help, guidance, patience and expertise of the fellow laboratory members, Christina Brandenberger, Lori Bramble, Katryn Allen, Ryan Lewandowski, Daven Jackson and James Wagner. They have all been extremely helpful in sharing and teaching me the works in the laboratory, and made my research enjoyable and enriching. Appreciation also goes to Rance Nault, Echo Hansen, Dennis Shubitowski and all the summer students for helping with their respective contributions to the project.

I would also like to thank the Agency for Science, Technology and Research (A*STAR), Singapore, for funding my graduate degree and veterinary pathology residency training. My journey to United States and attainment of this specialized training would not have been possible without this sponsorship.

Last but not least, I would also like to thank my family for their support and love, and especially to my wife who has always been with me, supportive of me, physically or in spirit, hence allowing my achievement of this milestone.

To all the above-mentioned, I owe the success of this research project.

TABLE OF CONTENTS

LIST OF TABLES ix

LIST OF FIGURES x

KEY TO SYMBOLS AND ABBREVIATIONS xiii

CHAPTER 1
INTRODUCTION 1
- **A. Ozone Toxicity** 2
  - **1. Ozone-Induced Adverse Health Effects in Humans** 2
  - **2. Ozone Inhalation Toxicity Studies in Animals** 5

REFERENCES 8

CHAPTER 2
TEMPORAL DEVELOPMENT OF EOSINOPHILIC RHINITIS AND NASAL EPITHELIAL REMODELING IN MICE EPISODICALLY EXPOSED TO OZONE 13
- **A. Introduction** 14
- **B. Materials and Methods** 17
  - **1. Laboratory Animals** 17
  - **2. Experimental Design and Inhalation Exposures** 17
  - **3. Necropsies and Nasal Tissue Collection** 19
  - **4. Tissue Processing for Light Microscopy, Histochemistry and Immunohistochemistry** 19
  - **5. Nasal Mucosal Morphometry** 22
  - **6. Transmission Electron Microscopy** 23
  - **7. Total RNA Isolation from Nasal Mucosa** 24
  - **8. Gene Expression Analysis** 26
  - **9. Statistical Analysis** 26
- **C. Results** 27
  - **1. 24-weekday Inhalation Exposures** 27
    - **i. Histopathology and Morphometry** 27
      - **a. Granulocyte Infiltration** 27
      - **b. Epithelial Thickness** 29
      - **c. Intraepithelial Mucosubstances** 29
      - **d. Intraepithelial Ym1/2 protein** 30
      - **e. Epithelial DNA Synthesis** 34
  - **2. 1, 2, 4 or 9 Weekdays of Inhalation Exposures** 36
    - **i. Histopathology and Morphometry** 36
      - **a. Granulocyte Infiltration** 36
      - **b. Epithelial Thickness** 39
      - **c. Intraepithelial Mucosubstances** 39
      - **d. Intraepithelial Ym1/2 Protein** 40

e. Epithelial DNA Synthesis 44
ii. Ultrastructural Changes in Nasal Mucosa of Mice 46
iii. Cytokine Gene Expression in Nasal Mucosa 48
a. Temporal Changes in Cytokine Gene Expression 48
b. Unsupervised Hierarchical Clustering of Gene Expression and Morphometric Parameters 48
c. Th2 Cytokine Gene Expression 50
d. Th1 Cytokine Gene Expression 51
e. Muc5AC and Gob5 Cytokine Gene Expression 53
D. Discussion 54
APPENDICES 62
Appendix A 63
Appendix B 64
REFERENCES 65

CHAPTER 3
ROLE OF LYMPHOCYTES IN OZONE-INDUCED EOSINOPHILIC RHINITIS, USING RAG2(-/-) x γc(-/-) MICE AND C57BL/6 MICE 71
A. Introduction 72
B. Materials and Methods 74
1. Laboratory Animals 74
2. Experimental Design and Inhalation Exposures 74
3. Necropsies and Nasal Tissue Collection 75
4. Tissue Processing for Light Microscopy, Histochemistry and Immunohistochemistry 75
5. Nasal Mucosal Morphometry 77
6. Total RNA Isolation from Nasal Mucosa 78
7. Gene Expression Analysis 79
8. Statistical Analysis 80
C. Results 81
1. Histopathology and morphometry 81
i. Eosinophil Infiltration 81
ii. Neutrophil Infiltration 83
iii. Epithelial Remodeling 85
ix. Intraepithelial Mucosubstances 86
x. Intraepithelial Ym1/2 Protein 88
2. Cytokine Gene Expression in Nasal Mucosa 90
i. Cytokine Gene Expression in Nasal Mucosa of RAG2(-/-) x γc(-/-) Mice and C57BL/6 Mice 90
ii. Unsupervised Hierarchical Clustering of Gene Expression 90
iii. Th2 Cytokine Gene Expression 92
ix. Gob5, Muc5AC and Muc5b Cytokine Gene Expression 94
D. Discussion 95
APPENDIX 101
REFERENCES 103

CHAPTER 4
SUMMARY, CONCLUSIONS AND FUTURE DIRECTIONS 107
REFERENCES.....117

LIST OF TABLES

Table 1. Ozone chamber concentrations during inhalation exposures 63

Table 2. Temporal fold changes in gene expression in nasal mucosa of C57BL/6 mice after 1, 2, 4 or 9 days of inhalation exposure to ozone. 64

Table 3. Gene expression in nasal mucosa of RAG2(-/-) x γc(-/-) mice and C57BL/6 mice after 9 days of ozone inhalation exposure.....102

LIST OF FIGURES

Figure 1: Experimental Design 18

Figure 2: Site of nasal tissue extraction for mRNA analysis, histopathology and morphometry 25

Figure 3: Light photomicrographs of granulocyte infiltration within nasal mucosa of mice after 24-weekday exposure 28

Figure 4. Morphometry of granulocyte influx in the mucosa lining the proximal nasal airways after 24-weekday exposure 28

Figure 5. Light photomicrographs of nasal mucosa of mice after 24 weekdays of ozone exposure 31

Figure 6. Morphometry of nasal epithelial thickness after 24 weekdays of ozone exposure 32

Figure 7. Morphometry of intraepithelial mucosubstances in the mucosa lining the proximal nasal airways after 24-weekday exposure to ozone 32

Figure 8. Morphometry of intraepithelial Ym1/2 in the mucosa lining the proximal nasal airways after 24-weekday exposure to ozone 33

Figure 9. Light photomicrographs of BrdU immunolabeling in nasal mucosa of mice after 24-weekday exposure to ozone 34

Figure 10. Morphometry of epithelial BrdU in the mucosa lining the proximal nasal airways after 24-weekday exposure to ozone 35

Figure 11. Light photomicrographs of granulocyte infiltration within nasal mucosa of mice after 1, 2, 4 or 9 weekdays of ozone exposure 37

Figure 12. Morphometry of granulocytic influx in nasal lateral wall of mice exposed to 1, 2, 4 or 9 weekdays of ozone or filtered air 38

Figure 13. Light photomicrographs of nasal mucosa of mice with 1, 2, 4 or 9 weekdays of ozone exposure 41

Figure 14: Morphometry of airway epithelial thickness in the mucosa lining the proximal nasal airways after single or repeated exposures 42

Figure 15. Morphometry of intraepithelial mucosubstances in the mucosa lining the proximal nasal airways after single or repeated exposures..... 42

Figure 16. Morphometry of airway epithelial Ym1/2 in the mucosa lining the proximal nasal airways after single or repeated exposures 43

Figure 17: Light photomicrographs of BrdU immunolabeling in nasal mucosa of mice after 1-day exposure 44

Figure 18: Morphometry of epithelial BrdU in the mucosa lining the proximal nasal airways after 1 and 2-day exposure 45

Figure 19: Transmission electron photomicrographs of ultrastructural changes in nasal mucosa of mice due to ozone 47

Figure 20: Unsupervised hierarchical clustering of temporal changes in ozone-induced gene expression and morphometric phenotypes (*) in nasal mucosa of ozone-exposed mice relative to air-exposed control mice 49

Figure 21: Temporal fold changes in gene expressions in nasal lateral wall of mice exposed to 1, 2, 4 or 9 weekdays of ozone exposure, for selected Th2 genes 50

Figure 22. Temporal fold changes in gene expressions in nasal lateral wall of mice exposed to 1, 2, 4 or 9 weekdays of ozone exposure, for selected Th1 genes 52

Figure 23: Temporal fold changes in gene expressions in nasal lateral wall of mice exposed to 1, 2, 4 or 9 weekdays of ozone exposure, for Muc5AC and Gob5 genes 53

Figure 24. Eosinophil infiltration within nasal mucosa of C57BL/6 mice and RAG2(-/-) x γc(-/-) mice after 9 weekdays of air (0 ppm) and ozone (0.5 ppm) exposures 82

Figure 25. Morphometry of eosinophil infiltration in the mucosa of RAG2(-/-) x γc(-/-) and C57BL/6 mice after 9-weekday inhalation exposure....82

Figure 26. Neutrophils, immunohistochemistically labelled with rat anti-mouse neutrophil allotypic marker, within nasal mucosa of C57BL/6 mice and RAG2(-/-) x γc(-/-) mice after 9 weekdays of air (0 ppm) and ozone (0.5 ppm) exposures 83

Figure 27. Morphometry of neutrophil infiltration in the mucosa of RAG2(-/-) x γc(-/-) and C57BL/6 mice after 9-weekday inhalation exposure 84

Figure 28. Light photomicrographs of nasal mucosa of C57BL/6 mice and RAG2(-/-) x γc(-/-) mice after 9-weekday inhalation exposure 85

Figure 29. Intraepithelial mucosubstances in the mucosa lining the proximal nasal airways of RAG2(-/-) x γc(-/-) mice and C57BL/6 mice after 9-weekday inhalation exposure 86

Figure 30. Morphometry of intraepithelial mucosubstances in the mucosa lining the proximal nasal airways of RAG2(-/-) x γc(-/-) mice and C57BL/6 mice after 9-weekday inhalation exposures 87

Figure 31. Epithelial Ym1/2 protein in nasal mucosa of C57BL/6 mice and RAG2(-/-) x γc(-/-) mice with 9-weekday inhalation exposures 88

Figure 32. Morphometry of epithelial Ym1/2 in nasal mucosa of RAG2(-/-) x γc(-/-) mice and C57BL/6 mice with 9-weekday inhalation exposures 89

Figure 33. Unsupervised hierarchical clustering of changes in ozone-induced gene expression in nasal mucosa of RAG2(-/-) x γc(-/-) mice and C57BL/6 mice, relative to air-exposed C57BL/6 mice....91

Figure 34. Fold changes in gene expressions in nasal lateral wall of RAG2(-/-) x γc(-/-) mice and C57BL/6 mice after 9-weekday inhalation exposure, for selected Th2 cytokine genes....92

Figure 35. Fold changes in gene expressions in nasal lateral wall of RAG2(-/-) x γc(-/-) mice and C57BL/6 mice after 9-weekday inhalation exposures, for Muc5AC, Muc5b and Gob5 genes ...94

Figure 36. Ozone-Induced Airway Inflammation & Remodeling in Mice....113

KEY TO SYMBOLS AND ABBREVIATIONS

AB/PAS	Alcian Blue/Periodic Acid Schiff
Arg1	Arginase 1
AZ	Arizona
BALF	Bronchoalveolar lavage
BrdU	5-bromo-2-deoxyuridine
CA	California
Ccl2	Chemokine (C-C motif) ligand 1
Ccl8	Chemokine (C-C motif) ligand 8
Chi3l3	Chitinase 3-like 3, Ym1
Chi3l4	Chitinase 3-like 4, Ym2
Cxcl1	Chemokine (C-X-C motif) ligand 1
COPD	Chronic Obstructive Pulmonary Disease
Cxcl2	Chemokine (C-X-C motif) ligand 2
EIB	Exercise-induced bronchial
GM-CSF	Granulocyte macrophage colony-stimulating factor
H&E	Hematoxylin and eosin
Hmox	Heme oxygenase 1
IFN-γ	Interferon gamma
Ig	Immunoglobulin
IHC	Immunhistochemistry
Il2rg or γc	Common gamma chain
IL-1β	Interleukin 1 beta
IL-4	Interleukin 4

IL-2	Interleukin 2
IL-4	Interleukin 4
IL-5	Interleukin 5
IL-6	Interleukin 6
IL-7	Interleukin 7
IL-8	Interleukin 8
IL-9	Interleukin 9
IL-10	Interleukin 10
IL-13	Interleukin 13
IL-15	Interleukin 15
IL-25	Interleukin 25
IL-33	Interleukin 33
IgE	Immunoglobulin E
KC	Keratinocyte chemoattractant
MBP	Major basic protein
MIP-2	Macrophage inflammatory protein 2
MCP-1	Monocyte chemoattractant protein 1
MCP-2	Monocyte chemoattractant protein 2
MMP	Matric metalloproteins
MO	Missouri
MSU	Michigan State University
Muc5AC	Mucin 5AC
NC	North Carolina
NJ	New Jersey
NK	Natural Killer cells

NK-kb	nuclear factor kappa-light-chain-enhancer of activated B cells
NOD	Non-obese diabetic
PDGF	Platelet-derived growth factor
RAG	Recombinase activating gene
RANTES	Regulated on activation, normal T cell expressed and secreted
RNA	Ribonucleic Acid
Saa-3	Serum amyloid A 3
TCR	T-cell receptor
TGF	Transforming Growth Factor
TNF-α	Tumor ncerosis factor alpha
TEM	Transmission Electron Microscopy.
Th1	T-helper 1
Th2	T-helper 2
TSLP	Thymic stromal lymphopoietin
WI	Wisconsin

CHAPTER 1

INTRODUCTION

A. Ozone Toxicity

Ground level ozone, or tropospheric ozone, formed through the photochemical interaction of nitrogen oxides, volatile organic compound and sunlight, is a common secondary gaseous air pollutant and a principal oxidant air pollutant of photochemical smog. Ozone is a very reactive chemical and a highly irritating airway toxicant. The mechanism of ozone toxicity in humans and experimental animals is related to its oxidizing properties, mediated through effects of free-radicals and lipid-peroxide induced damage on the conducting airways and lungs (Menzel, 1984). Due to the anatomical location of the nose at the most proximal part of the respiratory tract, the nasal passages are in close proximity to the external environment, and hence a major site of ozone-induced injury. The nasal passages have functions of air filtration, humidification, and metabolism of airborne xenobiotics, thereby acting as an 'air-conditioner' and 'defender' of the lower respiratory tract (Harkema et al., 2006). This makes the nasal airways, however, prone to injury from exposure to inhaled airborne toxicant such as ozone.

1. Ozone-Induced Adverse Health Effects in Humans

It has been well documented in human epidemiologic studies that exposures to elevated ambient concentrations of ozone are associated with increases in both morbidity and mortality (Bell et al., 2004; Burnett et al., 2001; Gryparis et al., 2004; Jerrett et al., 2013), causing respiratory health effects, such as impairment of pulmonary function (Bromberg et al., 1995) and exacerbations of chronic respiratory diseases such as asthma and allergic rhinitis (Peden, 1995; Jenerowicz et al., 2012). Approximately 40% of the U.S. population still lives in counties where annual ambient ozone levels exceed the U.S. Environmental Protection Agency's national ambient air quality standards (American Thoracic Society's State of the Air 2013 Report).

While healthy adults and children are not spared, the most susceptible group of people to the detrimental effects of ozone include outdoor workers, athletes and asthmatics, patients with COPD, with clinical consequences of decreased pulmonary function, increased pneumonia, airway reactivity, decreased exercise tolerance and increased hospital admissions (Bascom et al., 1996; Burnett et al., 1997; Jenerowicz et al., 2012). Elevated ground level ozone has been associated with increased exercise-induced bronchial (EIB) reactivity, lifetime allergic rhinitis, allergic sensitization and asthma in children, as well as increased prevalence of atopy (Kim et al., 2012; Pénard-Morand et al.; 2005; Peden et al., 2001). With predicted future climate changes, ambient ozone concentrations will likely increase rather than decrease, resulting in more exposure-related health effects (Ebi et al., 2009).

Specific to the nasal airways, humans acutely exposed to ozone develop nasal epithelial injury and remodeling, accompanied by acute rhinitis dominated by an influx of polymorphonuclear leukocytes (i.e., neutrophils) (Bascom et al., 1990; Koren et al., 1989). The acute inflammatory response in human is characterized by an increase in neutrophils in nasal lavage and bronchioalveolar fluid (Graham et al., 1990), as well as increased expression of NK-kB, TNF-a, IL-1β, IL-8, IL-6 and GM-CSF by the mucosal epithelial cells (Dokic et al., 2006; Jaspers et al., 1997; Chang et al., 1998). With chronicity of ozone exposure in humans, mucosal epithelial cell changes are characterized initially by loss of cilia, basal cell hyperplasia and mild dysplasia, which eventually progress to squamous cell metaplasia, marked basal cell hyperplasia, and loss of respiratory epithelium in the nasal airways (Calderon-Garcidueñas et al., 1992).

Children and infants are at higher risk to the adverse effects of airway injury from air pollution, due to greater airway exposure as a result of higher ventilation rates compared to adults (Kim, 2004). Eighty percent of the pulmonary alveoli are developed post-natally and

maturation continues through adolescence. Hence, the developing lung of children is prone to damage from inhaled airborne toxicants such as ozone (Kim, 2004). In children acutely exposed to ozone, changes in the nasal passage consist of nasal mucosal atrophy, neutrophilic influx and abnormal nasal cytology (Calderón-Garcidueñas et al., 1995). Exposure of children to unhealthy levels of ozone at a young age can have pathologic ramifications to the respiratory system resulting in adverse health effects later in life.

2. Ozone Inhalation Toxicity Studies in Animals

Comparative aspects of the nasal airways of laboratory animal species and human are well-described, and there are species-specific differences in gross structure and distribution of nasal epithelium. While the human nasal cavity consists of relatively simple superior, middle and inferior turbinates, the nose of laboratory rodents have evolved to adapt for more developed olfactory function and dentition, and contain complex nasoturbinates, maxilloturbinates and ethmoturbinates. These differences and variations in nasal anatomy between species are important when reviewing comparative studies (Harkema, 1991). While animal models are useful in the study of the pathogenesis of allergic and non-allergic rhinitis, interspecies variation in dose-response relationship, anatomy and route of exposure are important factors to be considered when designing an in vivo experimental study.

Controlled inhalation exposures to high ambient concentrations of ozone cause airway epithelial injury and acute airway inflammation in both the upper and lower airways of laboratory animals (Harkema et al., 2005). The magnitude of ozone-induced airway epithelial toxicity (e.g., cell necrosis and loss of airway cilia) and acute inflammation (e.g., influx of neutrophils) are concentration, time (exposure duration) and species dependent (Carey et al., 2011; Dormans et al.; 1999, Harkema et al., 2006; Vancza et al., 2009). In regards to the latter, using controlled inhalation exposures in rats and human subjects, it takes approximately four-five times the airborne concentrations of ozone in laboratory rodents to induce the same amount of pulmonary inflammation that is induced in exposed human subjects (Hatch et al., 1994).

Repeated daily, long-term exposures to high ambient concentrations of ozone cause marked remodeling of the airway epithelium lining both the nasal and bronchiolar airways in laboratory rodents (Wagner et al., 2001; Wagner et al., 2002; Harkema et al., 2005; Harkema et

al., 2006) and nonhuman primates (Harkema et al., 1987). The epithelial remodeling in nasal airways is characterized by epithelial cell hyperplasia/hypertrophy and mucous cell metaplasia. Ozone-induced nasal epithelial lesions are bilateral and located predominantly in the proximal aspects of the nasal passages. At these intranasal locations, the airways are normally lined by a pseudostratified epithelium that contains sparse numbers of ciliated and mucus-secreting (goblet) cells, and is principally composed of non-ciliated, cuboidal and basal cells (i.e., nasal transitional epithelium) (Harkema et al., 2006). Along with nasal epithelial injury and remodeling, there is an accompanying acute rhinitis dominated by an influx of polymorphonuclear leukocytes (i.e., neutrophils) in rodents (Harkema et al., 2006) and nonhuman primates (Carey et al., 2011) acutely exposed to ozone (e.g., commonly 1-8 hours per day for 1-5 days in rodent studies). Like in control human exposure studies (Koren et al, 1989; Graham et al, 1990), acute ozone exposures cause an increase in neutrophil numbers in the bronchoalveolar lavage fluid (BALF) of animals (Hotchkiss et al., 1989). In the lung, this neutrophilic inflammatory response to acute ozone exposure is often accompanied by elevated levels of inflammatory cytokines, such as macrophage inflammatory protein (MIP-2) in mice (Driscoll et al., 1993; Zhao et al., 1998; Johnston et al., 1999).

In studies using rodent models of acute allergic rhinitis, nasal mucosal and submucosal changes have not been extensively studied. Site-specific epithelial changes in the nasal airways of allergic rats and mice have been described, but not completely characterized (Wagner et al., 2007). Specifically, the temporal changes in the nature of inflammatory cell infiltration, mucosal epithelial remodeling, as well as localized cytokine expression in the nasal cavity of mice, induced by subacute ozone exposure, have not been thoroughly investigated. These data gaps

were basis for my overall hypothesis and experimental studies, described in the following chapters.

REFERENCES

REFERENCES

1. Bascom R, Naclerio RM, Fitzgerald TK, Kagey-Sobotka A, Proud D: Effect of ozone inhalation on the response to nasal challenge with antigen of allergic subjects. Am Rev Respir Dis. 1990 Sep;142(3):594-601.

2. Bascom R. et al. Health effects of outdoor air pollution. Committee of the Environmental and Occupational Health Assembly of the American Thoracic Society. Am J Respir Crit Care Med. 1996 Jan;153(1):3-50.

3. Bell M, McDermott A, Zeger S, Samet J, Dominici F. Ozone and short-term mortality in 95 US urban communities, 1987–2000. *JAMA* 2004;292:2372–2378

4. Bromberg PA, Koren HS: Ozone-induced human respiratory dysfunction and disease. *Toxicol Lett.* 1995 Dec;82-83:307-16.

5. Burnett RT, Smith-Doiron M, Stieb D, Raizenne ME, Brook JR, Dales RE, Leech JA, Cakmak S, Krewski D. Association between ozone and hospitalization for acute respiratory diseases in children less than 2 years of age. *Am J Epidemiol* 2001;153:444–452.

6. Burnett RT, Brook JR, Yung WT, Dales RE, Krewski D. Association between ozone and hospitalization for respiratory diseases in 16 Canadian cities. Environ Res. 1997 Jan;72(1):24-31.

7. Calderon-Garcidueñas L, Osorno-Velazquez A, Bravo-Alvarez H, Delgado-Chavez R, Barrios-Marquez R. Histopathologic changes of the nasal mucosa in southwest Metropolitan Mexico City inhabitants. Am J Pathol. 1992 Jan;140(1):225-32.

8. Calderón-Garcidueñas L, Rodriguez-Alcaraz A, García R, Ramírez L, Barragan G. Nasal inflammatory responses in children exposed to a polluted urban atmosphere. J Toxicol Environ Health. 1995 Aug;45(4):427-37.

9. Carey SA, Ballinger CA, Plopper CG, McDonald RJ, Bartolucci AA, Postlethwait EM, Harkema JR. Persistent rhinitis and epithelial remodeling induced by cyclic ozone exposure in the nasal airways of infant monkeys. Am J Physiol Lung Cell Mol Physiol. 2011 Feb;300(2):L242-54.

10. Chang MM, Wu R, Plopper CG, Hyde DM. IL-8 is one of the major chemokines produced by monkey airway epithelium after ozone-induced injury. Am J Physiol. 1998 Sep;275(3 Pt 1):L524-32.

11. Dokic D, Howarth HP. Effects of ozone on the nasal mucosa (epithelial cells). Prilozi. 2006 Dec;27(2):115-25.

12. Dormans JA, van Bree L, Boere AJ, Marra M, Rombout PJ. Interspecies differences in time course of pulmonary toxicity following repeated exposure to ozone. Inhal Toxicol. 1999 Apr;11(4):309-29.

13. Driscoll KE, Simpson L, Carter J, Hassenbein D, Leikauf GD. Ozone inhalation stimulates expression of a neutrophil chemotactic protein, macrophage inflammatory protein 2. Toxicol Appl Pharmacol. 1993 Apr;119(2):306-9.

14. Ebi K, McGregor G: Climate change, tropospheric ozone and particulate matter, and health impacts. Cien Saude Colet. 2009 Nov-Dec;14(6):2281-93.

15. Graham DE, Koren HS. Biomarkers of inflammation in ozone-exposed humans. Comparison of the nasal and bronchoalveolar lavage. Am Rev Respir Dis. 1990 Jul;142(1):152-6.

16. Gryparis A, Forsberg B, Katsouyanni K, Analitis A, Touloumi G, Schwartz J, Samoli E, Medina S, Anderson HR, Niciu EM, et al. Acute effects of ozone on mortality from the "Air Pollution and Health: A European Approach" project. *Am J Respir Crit Care Med* 2004;28:28.

17. Harkema JR, Plopper CG, Hyde DM, St George JA, Dungworth DL: Effects of an ambient level of ozone on primate nasal epithelial mucosubstances. Quantitative histochemistry. Am J Pathol. 1987 Apr;127(1):90-6.

18. Harkema JR. Comparative aspects of nasal airway anatomy: relevance to inhalation toxicology. Toxicol Pathol. 1991;19(4 Pt 1):321-36.

19. Harkema JR, Wagner JG: Epithelial and inflammatory responses in the airways of laboratory rats coexposed to ozone and biogenic substances: enhancement of toxicant-induced airway injury. Exp Toxicol Pathol. 2005 Jul;57 Suppl 1:129-41.

20. Harkema JR, Carey SA, Wagner JG: The nose revisited: a brief review of the comparative structure, function, and toxicologic pathology of the nasal epithelium. Toxicol Pathol. 2006;34(3):252-69.

21. Hatch GE, Slade R, Harris LP, McDonnell WF, Devlin RB, Koren HS, Costa DL, McKee J: Ozone dose and effect in humans and rats. A comparison using oxygen-18 labeling and bronchoalveolar lavage. 1994. Am J Respir Crit Care Med. 150(3):676-83.

22. Hotchkiss JA, Harkema JR, Sun JD, Henderson RF: Comparison of acute ozone-induced nasal and pulmonary inflammatory responses in rats. Toxicol Appl Pharmacol. 1989 Apr;98(2):289-302.

23. Jaspers I, Flescher E, Chen LC. Ozone-induced IL-8 expression and transcription factor binding in respiratory epithelial cells. Am J Physiol. 1997 Mar;272(3 Pt 1):L504-11.

24. Jerrett M, Burnett RT, Beckerman BS, Turner MC, Krewski D, Thurston G, Martin R, von Donkelaar A, Hughes E, Shi Y, Gapstur SM, Thun MJ, Pope CA 3rd. Spatial Analysis of Air Pollution and Mortality in California. *Am J Respir Crit Care Med*. 2013 Jun 27.

25. Jenerowicz D, Silny W, Dańczak-Pazdrowska A, Polańska A, Osmola-Mańkowska A, Olek-Hrab K: Environmental factors and allergic diseases. Ann Agric Environ Med. 2012;19(3):475-81

26. Johnston CJ, Stripp BR, Reynolds SD, Avissar NE, Reed CK, Finkelstein JN. Inflammatory and antioxidant gene expression in C57BL/6J mice after lethal and sublethal ozone exposures. Exp Lung Res. 1999 Jan-Feb;25(1):81-97.

27. Kim BJ, Hong SJ. Ambient air pollution and allergic diseases in children. Korean J Pediatr. 2012 Jun;55(6):185-92.

28. Kim JJ; Ambient air pollution: health hazards to children. American Academy of Pediatrics Committee on Environmental Health. Pediatrics. 2004 Dec;114(6):1699-707.

29. Koren HS, Devlin RB, Graham DE, Mann R, McGee MP, Horstman DH, Kozumbo WJ, Becker S, House DE, McDonnell WF: Ozone-induced inflammation in the lower airways of human subjects. Am Rev Respir Dis. 1989 Feb;139(2):407-15.

30. Menzel DB. Ozone: an overview of its toxicity in man and animals. J Toxicol Environ Health. 1984;13(2-3):183-204.

31. Peden DB, Setzer RW Jr, Devlin RB: Ozone exposure has both a priming effect on allergen-induced responses and an intrinsic inflammatory action in the nasal airways of perennially allergic asthmatics. Am J Respir Crit Care Med. 1995 May;151(5):1336-45.

32. Peden DB. Effect of pollutants in rhinitis. Curr Allergy Asthma Rep. 2001 May;1(3):242-6.

33. Pénard-Morand C, Charpin D, Raherison C, Kopferschmitt C, Caillaud D, Lavaud F, Annesi-Maesano I. Long-term exposure to background air pollution related to respiratory and allergic health in schoolchildren. Clin Exp Allergy. 2005 Oct;35(10):1279-87.

34. *State of the Air 2013*; American Lung Association: Washington, DC, USA, 2013.

35. Vancza EM, Galdanes K, Gunnison A, Hatch G, Gordon T. Age, strain, and gender as factors for increased sensitivity of the mouse lung to inhaled ozone. Toxicol Sci. 2009 Feb;107(2):535-43.

36. Wagner JG, Hotchkiss JA, Harkema JR. Effects of ozone and endotoxin coexposure on rat airway epithelium: potentiation of toxicant-induced alterations. Environ Health Perspect. 2001 Aug;109 Suppl 4:591-8.

37. Wagner JG, Hotchkiss JA, Harkema JR. Enhancement of nasal inflammatory and epithelial responses after ozone and allergen coexposure in Brown Norway rats. Toxicol Sci. 2002 Jun;67(2):284-94.

38. Wagner JG, Harkema JR. Rodent models of allergic rhinitis: relevance to human pathophysiology. Curr Allergy Asthma Rep. 2007 May;7(2):134-40.

39. Zhao Q, Simpson LG, Driscoll KE, Leikauf GD: Chemokine regulation of ozone-induced neutrophil and monocyte inflammation. Am J Physiol. 1998 Jan;274(1 Pt 1):L39-46.

CHAPTER 2

TEMPORAL DEVELOPMENT OF EOSINOPHILIC RHINITIS AND NASAL EPITHELIAL REMODELING IN MICE EPISODICALLY EXPOSED TO OZONE

A. Introduction

Ozone is a very reactive and highly irritating airway toxicant. In both humans and laboratory animals, experimental inhalation exposures to ozone cause inflammation and epithelial injury in the upper and lower respiratory tract, which is dependent on the concentration and duration of exposure.

In laboratory rats and mice, daily exposures to high ambient concentrations of ozone have been shown to cause epithelial pathology in the nasal airways. This ozone-induced nasal pathology consists of epithelial remodeling that is characterized by epithelial cell hyperplasia, hypertrophy and mucous cell metaplasia (Wagner et al., 2001; Wagner et al., 2002; Harkema et al., 2005; Harkema et al., 2006), as well as an acute rhinitis dominated by an influx of neutrophils (Harkema et al., 2006). Neutrophilic rhinitis is also accompanied by a neutrophilic inflammatory response, and elevated levels of inflammatory cytokines in the lungs of mice experimentally exposed to ozone (Driscoll et al., 1993; Zhao et al., 1998; Johnston et al., 1999). Ozone-induced nasal airway lesions are bilateral and located in proximal nasal passages, where the airways are lined by predominantly non-ciliated, pseudostratified, cuboidal epithelial cells, interspersed with few ciliated cells and goblet cells (Harkema et al., 1989). The extent and location of pathological changes in the nasal passages are dependent, at least in part, on regional differences in ozone concentration and airflow pattern in the nasal passages. The intranasal difference in susceptibility to ozone-induced airway injury may also be due to differences in epithelial cells populations, local vasculature, innervation and metabolic capacity (Harkema et al., 2006).

While acute rhinitis induced by short-term ozone exposure has been well documented in animal and human inhalation studies, the nasal inflammatory cell and cytokine responses to more long-term ozone exposures (i.e., subacute and chronic) in laboratory animals have not been

thoroughly investigated and characterized. Interestingly, human epidemiological studies have reported associations of elevated ambient ozone concentrations with increases in eosinophil-derived proteins (e.g., eosinophil cationic protein and eosinophil protein X) in the urine of both asthmatic and non-asthmatic children, supporting the hypothesis that repeated ozone exposures is associated with eosinophilic, rather than neutrophilic, airway inflammation (Frischer et al., 2001; Hiltermann et al., 1997). Frischer et al. (1993) reported that ambient ozone causes upper airway inflammation in children characterized by a nasal mucosal influx of eosinophils and elevations in eosinophil cationic protein in collected nasal lavage fluid. Rhinitis, in children or adults, with a granulocytic influx dominated by eosinophils is most often diagnosed as allergic rhinitis, with lesser reported cases of non-allergic eosinophilic rhinitis (Ellis et al., 2006).

To investigate granulocytic inflammatory cell responses to repeated ozone exposures, I conducted a series of related studies designed to determine the type of granulocytic inflammatory cells (e.g., neutrophils, eosinophils) and associated nasal epithelial changes (i.e., epithelial remodeling) that occur over time with repeated daily exposures (i.e., 1, 2, 4, 9 or 24 consecutive weekdays, for four hours/day). Results from preliminary study showed that ozone exposure caused an eosinophilic rather than neutrophilic influx in the nasal airway of mice. This eosinophilic rhinitis accompanied the epithelial hyperplasia/hypertrophy, hyalinosis as well as mucous cell metaplasia. Eosinophilic inflammation and mucous cell metaplasia have been associated with a Th2 cytokine (e.g. IL-4, IL-5, IL-13) response such as that described in allergic rhinits and asthma. Hence, in mice experimentally exposed to ozone, phenotypic changes of the nasal airway epithelium and associated eosinophilic rhinitis, appear to favour a Th2 cytokine response. I further hypothesize that the temporal development of ozone-induced nasal epithelial

remodeling and inflammation are associated with an early temporal Th1 cytokine response followed by a later Th2 profile in the nasal mucosa.

B. Materials and Methods

1. Laboratory Animals

Specific pathogen free male C57BL/6 mice (6–8 weeks of age; Charles River Breeding Laboratories, Portage) were used in this study. Mice were housed in stainless steel wire cages, whole body inhalation exposure chambers (H-1000; Lab Products Marywood, NJ). Animals were provided free access to food (Harlan Teklad Irradiated 8940, Madison, WI) and water. Mice were maintained in Michigan State University (MSU) animal housing facilities accredited by the Association for Assessment and Accreditation of Laboratory Animal Care and according to the National Institutes of Health guidelines as overseen by the MSU Institutional Animal Care and Use Committee. Rooms were maintained at temperatures of 21°C–24°C and relative humidities of 45–70%, with a 12-h light/dark cycle starting at 7:30 A.M.

2. Experimental Design and Inhalation Exposures

In the first part of this study, 8 mice per group were exposed for 24 days to 0.5 ppm ozone or filtered air (0 ppm ozone). In the second part, 6 mice per group were exposed to filtered air or 0.5 ppm ozone for 1, 2, 4 and 9 weekdays, at two groups (air control and ozone) per time point, 4 hours of exposure per day. Mice were euthanized 24 hours after end of the exposures. 6-8 mice in both 0.5 ppm ozone and filtered air groups in the 1, 2 and 24 weekdays time points were given bromodeoxyuridine (BrdU) via intraperitoneal injections, 2 hours before euthanasia. An additional group of 6 mice was exposed for 4 hours of 0.5 ppm ozone for 1 day and euthanized 2 hours after end of exposure. Figure 1 provides a visual representation of the experimental design. An additional 6 mice per group (both air control and ozone groups) in the 1, 2, 4 and 9 weekdays time point, as well as in the 1 day 2 hours time point, were exposed and processed for nasal RNA

extraction. Three additional mice per exposure group in the 4-day and 9-day time points, were processed for transmission electron microscopy (TEM).

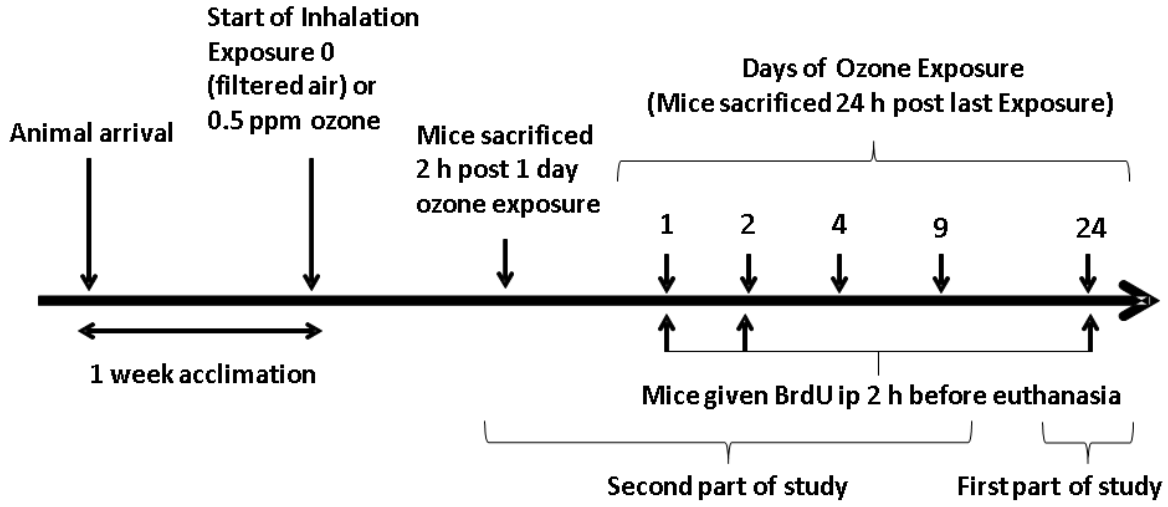

Figure 1. Experimental Design

Mice were housed individually in stainless steel wire cages, and exposed to whole body inhalation exposure chambers (H-100; Lab Products Marywood, NJ). Ozone was generated with an OREC 03V1-Clone ozone generator (Ozone Research and Equipment Corp., AZ) using compressed air as a source of oxygen. Total airflow through the exposure chambers was 250 l/min (15 chamber air changes per hour). Dasibi 1003 AH ambient air ozone monitor (Dasibi Environmental Corp., Glendale, CA) was used to monitor the ambient ozone concentration in the air chamber. Two ozone sampling probes were placed in the middle of the ozone chambers, 10–15 cm above cage racks, for monitoring the ozone concentration in ozone chamber, with a Dasibi 1003 AH ambient air ozone monitor during the exposures. Table 1 (Appendix A) shows the ozone chamber concentrations during the daily inhalation exposures.

3. Necropsies and Nasal Tissue Collection

Mice in the 1, 2, 4, 9 and 24 weekdays exposure groups were killed at 24 h after inhalation exposures. Mice in the 1-day exposure groups were killed 2 or 24 hours after the inhalation exposures. Two hours before necropsies, mice in the 1-, 2-, and 24-day groups (sacrificed 24h post-exposure), were injected intraperitoneally with bromodeoxyuridine (BrdU) to label epithelial cells undergoing DNA synthesis (S-phase of the cell cycle). At designated times post exposure (2 or 24h post last exposure), mice were anesthetized with sodium pentobarbital (Vortech Pharmaceuticals, Ltd. Dearborn, MI) and sacrificed by exsanguination via the abdominal aorta. Immediately after death, the head of each animal was removed from the carcass. After the lower jaw and skin were removed, formalin or RNA-Later fluid was infused retrograde through the nasopharyngeal meatus. The head was immersed in 10% neutral buffered formalin for routine histology of the nasal cavity, or in RNA-Later (Sigma-Aldrich, an ammonium sulfate based RNA fixative/stabilizer) for nasal mucosal RNA extraction.

4. Tissue Processing for Light Microscopy, Histochemistry and Immunohistochemistry

Transverse tissue blocks of four anatomic sites from the heads of the mice were selected for light microscopy as previously described (Young 1981; Harkema et al. 2006; Islam et al. 2006). Briefly, the proximal section (T1) was taken immediately caudal to the upper incisor teeth; the middle section (T2) was taken at the level of the incisive papilla of the hard palate; the third nasal section (T3) was taken at the level of the second palatal ridge; and the most caudal nasal section (T4) was taken at the level of the intersection of the hard and soft palate, through the proximal portion of the olfactory bulb of the brain (see Figure 2 on page 25). Nasal tissue blocks were processed for histopathologic, immunohistochemical, and morphometric analyses. All of

these blocks were embedded in paraffin, and the anterior face of each block was sectioned at a thickness of 5 microns and stained with hematoxylin and eosin for routine light microscopic examination. Additional slides were stained with Alcian Blue (pH 2.5)/Periodic Acid Schiff (AB/PAS) to identify acidic and neutral mucosubstances stored in mucus-secreting cells of nasal airway surface epithelium.

For immunohistochemistry, slides were placed in Tris Buffered Saline for pH adjustment, followed by Heat Induced or Enzyme Induced Epitope Retrieval, and subsequently blocked for endogenous peroxidase using 3% Hydrogen Peroxide/Methanol. Following pretreatments standard Avidin, Biotin complex staining steps were performed at room temperature on the Dako Autostainer. Slides were blocked for non-specific protein in Normal Goat / Normal Rabbit Serum (Vector Labs – Burlingame, CA). Endogenous Biotin was blocked by incubation in Avidin D (Vector) and d-Biotin (SigmaAldrich – St.Louis, MO).

Sections were immunostained for mouse eosinophil specific major basic protein (MBP) using a rat antibody directed against murine MBP (1:10,000; Mayo Clinic, Scottsdale, AZ), and for neutrophils using Rat Anti-Mouse Neutrophil 7/4 Allotypic Marker (1:2500 AbD Serotec Raleigh, NC). Sections were subsequently covered with secondary biotinylated antibodies, treated with alkaline phosphatase and visualized with Fast Red (Substrate Kit 1). For Ym1/2 immunohistochemistry, unstained and hydrated paraffin sections were incubated for one hour with rabbit polyclonal anti-Ym1 antibody at a dilution of 1:3,000. This antibody was a generous gift from Dr. Shioko Kimura (National Cancer Institute, Bethesda, MD) and was prepared by immunizing rabbits with 2 peptide sequences derived from eosinophilic crystals in gastric

epithelium of CYP1A2 deficient mice. Immunoreactivity of Ym1/2 was visualized with Vector R.T.U. Elite ABC Peroxidase Reagent followed by Nova Red (Vector Laboratories Inc., Burlingame, CA).

After immunohistochemistry, slides were dehydrated through ascending grades of ethanol; cleared through several changes of xylene and cover-slipped using permanent mounting media. Routine immunohistochemical techniques were used for nasal epithelial detection of nuclear BrdU. Nasal sections were deparaffinized in xylene and rehydrated through descending grades of ethanol and immersed in 3% hydrogen peroxide to block endogenous peroxides. Sections were incubated with normal horse sera to inhibit nonspecific proteins (Vector Laboratories Inc., Burlingame, CA) followed by specific dilutions of primary antibodies (1:40, monoclonal mouse anti-BrdU antibody, BD Biosciences). Tissue sections were subsequently covered with secondary biotinylated antibodies, and immunostaining was developed, with the Vector RTU Elite ABC kit (Vector Laboratories Inc.) 3,3#-diaminobenzidine (SigmaChemicals) chromogens.

5. Nasal Mucosal Morphometry

Mucosal epithelial thickness, amounts of epithelial mucosubstances, eosinophils and neutrophils in the mucosa, as well as epithelial Ym1/2 protein, were estimated by standard morphometry techniques. All histological slides were scanned and digitalized with a slide scanner (VS110, Olympus) prior to quantification. Analysis of the virtual slides was performed with the newCast system (Visiopharm, Denmark). Briefly, images for analysis were sampled at the region of interest, i.e. entire length of the lateral walls in the T1 section, with a 100 % meander sampling at a 40x magnification. In Figure 2B, the yellow segmented lines indicate lateral wall mucosa that was morphometrically analysed in this study.

For estimation of epithelial thickness and the amount of intraepithelial mucosubstances per length of basal lamina, a point-intercept grid was superimposed over the selected images. The point grids had an area/point of 105.60 μm^2 and 16.90 μm^2 for estimating the area of cells or mucosubstances, respectively, over the length of basal lamina. A line grid with a length/line of 25.69 μm and an area/point of 563.20 μm^2 was used to estimate the corresponding surface density of the basal lamina.

The formula for the estimation of epithelial mucosubstances and cellular volume per basal lamina are the same and described here in detail for mucosubstances.

Density of mucosubstances ($\hat{V}_M$) was estimated by counting the number of points falling on epithelial areas staining positively for AB/PAS (P_M) multiplied by the area/point (a/p) and divided by the total number of point in all images (n) as shown in equation 1 (EQ1) .

$$\hat{V}_M = \frac{\sum P_M \times a/p}{n} \qquad \text{EQ 1}$$

The surface density of the basal lamina ($\hat{S}_{BL}$) in the selected images was estimated by counting the number of intercepts (I) of the line probe with the basal lamina of the lateral wall divided by the length per point (l/p) and the number of points in all sampled images (n) as described in equation 2 (EQ2).

$$\hat{S}_{BL} = \frac{2 \times \sum I}{l / p \times n} \qquad \text{EQ2}$$

Stained mucosubstances per basal lamina of the lateral wall was then estimated by dividing $\hat{V}_M$ by $\hat{S}_{BL}$.

For quantification of BrdU and Ym1/2 labelling within nasal epithelium of lateral wall, the same formula and image analysis settings as that for mucus, with point grids area/point of 105.60 μm^2, were used.

The influx of neutrophil and eosinophil influx in the nasal mucosa was estimated by quantifying the amount of Major Basic Protein (MBP) immunolabelling for eosinophils, and the amount of rat anti-mouse neutrophil allotypic marker (clone 7/4) for neutrophils in the nasal mucosa of the lateral wall. A point grid with an area/point of 16.90 μm^2 was used to estimate the area of MBP and neutrophil marker respectively and a point grid with an area/point of 563.20 μm^2 was used to measure the reference space, i.e. the lamina propria and the epithelium of the lateral wall. The total number of points was the multiplied by the area/point for either MBP stain or neutrophil marker and for the reference space. The percentage of MBP or neutrophil marker per mucosa was calculated by dividing the area of the stain by the area of the reference space.

6. Transmission Electron Microscopy

Nasal cavities of mice designated for transmission election microscopy were fixed for transmission electron microscopy with 2.5% glutaraldehyde in 0.03 M potassium phosphate buffer at 4˚C for at least 48 hours. The heads were then decalcified with IHC-Tek Bone Decal Solution (IHC World, MD) for 2 month under continuous shaking and changing the solution on a weekly basis. Sufficient decalcification was tested prior to further processing of TEM sample embedding (D.J. Seilly, Medical Laboratory Sciences 1982, 39, 71-73). For TEM embedding, samples were then postfixed in 1% osmium tetroxide and dehydrated in a graded acetone series. Samples were infiltrated and embedded in Spurr resin (Polysciences). Thin sections (70 nm thickness) were obtained with a PTXL ultramicrotome (RMC, Boeckeler Instruments, Tucson, AZ) on 200 mesh copper grids stained with uranyl acetate and lead citrate. Sections were imaged using a JEOL 100CX Transmission Electron Microscope (Japan) at a 100kV accelerating voltage.

7. Total RNA Isolation from Nasal Mucosa

A longitudinal incision was made along the midline of individual RNA-Later preserved head of ozone-exposed and filtered air control group mice. The median septum was removed and the turbinates and lateral wall tissues were microdissected from both left and right nasal cavities. The tissues removed for analysis consist of the region between T1 and T2 in Figure 2A.

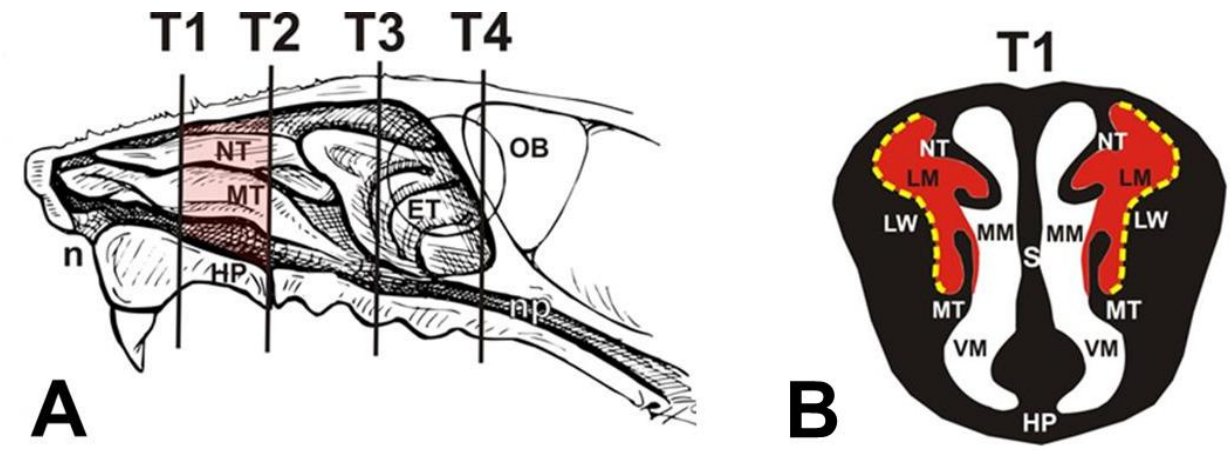

Figure 2: Site of nasal tissue extraction for mRNA analysis, histopathology and morphometry. **(A)** Illustration of the sites of anterior faces processed for histology (T1-T4). **(B)** Anterior face of T1. The yellow segmented line indicates lateral wall mucosa that was morphometrically analysed in this study. *(NT = nasoturbinate: MT = maxilloturbinate; HP = hard palate; ET= ethmoturbinate; OB = olfactory bulb; np= nasopharynx; S = septum; VM = ventral meatus; MM = middle meatus; LM = lateral meatus; NT= nasoturbinate; LW= lateral wall)*

Tissues samples were removed and placed in RNALater and kept at 4ºC for 24 hours then transferred to -80ºC until processed. Total RNA was extracted using RNeasy Mini Kit according to manufacturer's instructions (Qiagen, Valencia, CA). Briefly, tissues were homogenized in buffer RLT containing β -Mercaptoethanol with a 5mm rotor-sator Homogenizer (PRO Scientific, Oxford, CT) and centrifuged at 12,000g for 3 minutes. RNA was purified from the supernatant using the RNeasy capture column. Samples were treated with Qiagens Rnase-Free Dnase Set on the column (2X recommended concentration for 30min). Eluted RNA was quantified using a Genequant pro spectrophotometer (BioCrom, Cambridge, England).

8. Gene Expression Analysis

Reverse Transcription was performed using High Capacity cDNA archive Kit reagents (Applied Biosystems, Foster City, CA). RNA was incubated in GeneAmp PCR System 9700 Thermocycler PE (Applied Biosystems, Foster City, CA) at 25ºC for 10 Minutes, 37ºC for 2 hours and held at 4ºC. cDNA was diluted to 5ng/ul and 384 well reaction plates were set up robotically using the BioMek 2000 Automated Workstation (Beckman Coulter, Fullerton, Ca). Quantitative mRNA expression analysis was performed using the ABI PRISM 7900 HT Sequence Detection System using Taqman Gene Expression Assay reagents (Applied Biosystems). The cycling parameters were 48ºC for 2min, 95ºC for 10 min and 40 cycles of 95ºC for 15sec and 60ºC for 1min. The real-time PCR reaction was relatively quantified using the ΔΔCT method normalized to 18S, GAPDH and β-actin. Statistical analysis was performed in individual relative fold increase values using Sigma Stat (SPSS Inc, Chicago, IL). Hierarchical clustering of nasal mucosal gene expressions, together with morphometry parameters less Ym1/2, was performed in the TM4 Multiexperiment Viewer (MeV 4.8.1; (http://www.tm4.org) using Pearson correlation metric.

9. Statistical Analysis

Data are reported as mean ± SEM. Exposure related effects between air and ozone were assessed by a T-test for single comparisons where appropriate. Exposure and time related effects were determined by ANOVA, followed by Student-Newman-Keuls post hoc test, for multiple comparisons. Non-normal distributed data was analyzed by Kruskal-Wallis ANOVA on ranks. Specific statistical analysis for each data set is provided in each figure. Significance was assigned to p-values less than or equal to 0.05.

C. Results

1. 24-weekday Inhalation Exposures

i. Histopathology and Morphometry

Ozone-induced nasal lesions were present in mice after 24 weekdays of inhalation exposure, and this was seen in the lateral walls of the lateral meatus of both proximal nasal passages (Figure 2A). At this site, represented in T1 section, the lateral walls are lined by low cuboidal pseudostratified airway epithelium dominated by cuboidal non-ciliated cells, basal cells, lesser numbers of cuboidal ciliated cells and very few mucous goblet cells.

a. Granulocyte Infiltration

After 24 days of exposure, ozone-exposed mice had ozone-induced rhinitis, characterized by marked mucosa granulocyte infiltration predominated by eosinophils. The majority of eosinophils, immunohistochemically labelled with major basic protein (MBP), were present in the lamina propria with only a few extending into the basal layers of the overlying hyperplastic nasal epithelium. Scant neutrophils were present in the lamina propria of 24-day ozone-exposed mice. In air-control mice (0 ppm ozone), neither neutrophils nor eosinophils were present in significant numbers in the lamina propria or epithelium of the nasal mucosa (Figure 3).
The morphometrically estimated quantities of eosinophils and neutrophils are shown in Figure 4. There was a statistically significant increase in the infiltration of eosinophils as well as neutrophils, in the lateral wall mucosa of the ozone-exposed mice, compared to mice exposed to filtered air. The eosinophilic accumulation was significantly higher than that of neutrophils.

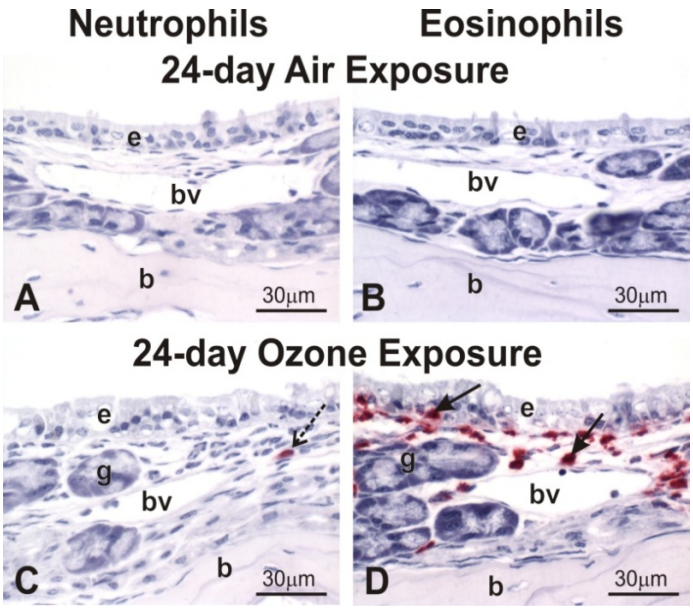

Figure 3: Light photomicrographs of granulocyte infiltration within nasal mucosa of mice after 24-weekday exposure. **(A, B)** Insignificant number of eosinophils and neutrophils were present in the air-exposed animals. **(C)** There were scant neutrophils (dotted arrow, rat anti-mouse neutrophil allotypic marker) present in the lamina propria of ozone-exposed mice. **(D)** Eosinophils, immunohistochemically labelled with Major Basic Protein (MBP) (solid arrows), predominate the granulocytes of the nasal mucosa of ozone-exposed animals and were not present in the control animals (0 ppm ozone). *(bv: blood vessel; e: epithelium; b:bone; g: gland)*

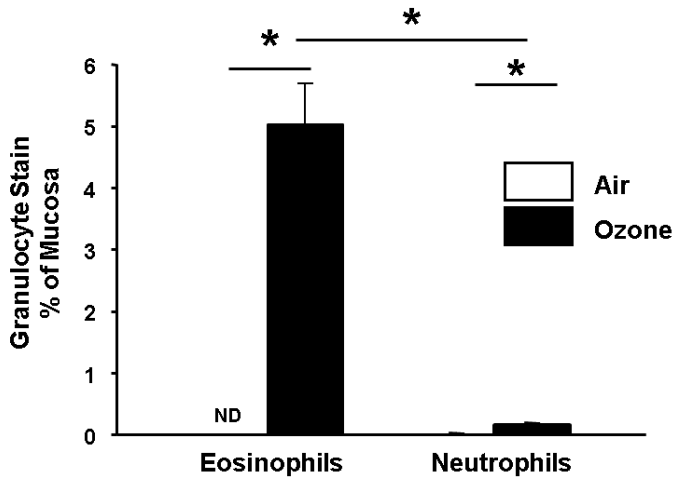

Figure 4. Morphometry of granulocyte influx in the mucosa lining the proximal nasal airways after 24-weekday exposure. There was a significant increase in infiltration of eosinophils as well as neutrophils in the lateral wall mucosa of the ozone-exposed mice, compared to mice exposed to filtered air. The eosinophilic influx was significantly higher than that of neutrophils. *Statistically different, $p \leq 0.05$, by way of T tests. Data are expressed as mean ± SEM.

b. Epithelial Thickness

Examination of H&E sections of mice with 24 days of inhalation exposure revealed a marked increase in epithelial thickness in the lateral wall of the proximal nasal mucosa in the ozone (0.5 ppm)-exposed mice. This epithelial remodeling comprised of hypertrophy, hyperplasia and accumulation of cytoplasmic hyaline material. Ciliated cuboidal to columnar epithelial cells were present in the hyperplastic epithelium. The granulocytic infiltration expanded the lamina propria in the ozone-exposed animals, observed both within blood vessels and lamina propria. There was no epithelial hyperplasia/hypertrophy in the air control (0.5 ppm) animals (Figure 5A, B). Morphometrically estimated quantities of increases in epithelial thickness are shown in Figure 6. Morphometrically estimated thickness (microns) of the airway surface epithelium revealed statistically significant increase in airway epithelial thickness in mucosa lining the proximal nasal passages of mice exposed to ozone, compared to air control animals.

c. Intraepithelial Mucosubstances

Using Alcian Blue PAS (pH 2.5) histochemical stain to highlight mucosubstances, an increase in amount of apical intraepithelial mucosubstances was observed in the proximal nasal transitional epithelium lining lateral wall in mice exposed to ozone for 24 days, consistent with mucous cell metaplasia. Mucous cell metaplasia of lateral wall mucosal epithelial was not seen in the mucosa of air control (0 ppm ozone) animal (Figure 5C, D). The morphometrically estimated quantities of the epithelial mucosubstances are shown in Figure 7. There was a significant increase in epithelial mucosubstances in the ozone-exposed animals.

d. Intraepithelial Ym1/2 Protein

Within the thickened epithelium of ozone (0.5 ppm)-exposed animals, abundant Ym1/2 protein was present in the apical and basilar aspects of transitional nasal epithelium. This marked Ym1/2 expression was not observed in the air control (0 ppm ozone) animals, in which only very weak expression of Ym1/2 was present in the apical aspect of the ciliated epithelial cells (Fig. 5E, F). The morphometrically estimated quantity of intraepithelial Ym1/2 protein showed a significant and marked increase in epithelial cell cytoplasmic Ym1/2 protein in the ozone-exposed compared to air control animals (Figure 8).

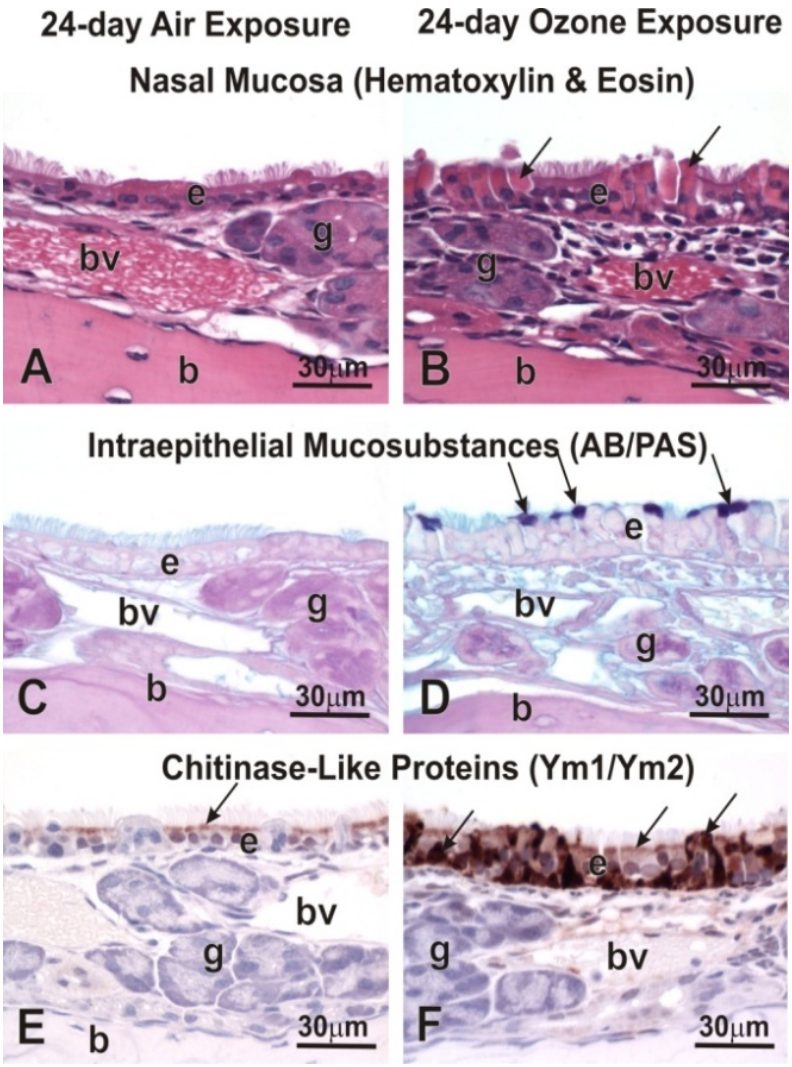

Figure 5. Light photomicrographs of nasal mucosa of mice after 24 weekdays of ozone exposure. **(A, B)** There was epithelial hypertrophy, hyperplasia and accumulation of eosinophilic hyaline material (hyalinosis, solid arrow) within epithelial cytoplasm in the ozone (0.5 ppm)-exposed animals, compared to the air-exposed (0 ppm ozone) animals. (Hematoxylin and Eosin). **(C, D)** Increased amount of apical intraepithelial mucosubstances was present in the ozone-exposed animals (solid arrow), not seen in the mucosa of air control (0 ppm ozone) animals. (Alcian Blue, pH 2.5 PAS). **(E, F)** In the air control (0 ppm ozone) animals, there was expression of Ym1/2 in the apical aspect of the ciliated epithelial cells. Within the thickened epithelium of ozone (0.5 ppm) exposed animals, abundant Ym1/2 protein was present in the apical and basilar aspects of epithelial cell cytoplasm, and faintly along subcilial apical cytoplasm. (solid arrows, rabbit polyclonal anti-Ym1 antibody). *(bv: blood vessel; e: epithelium; b:bone; g: gland)*

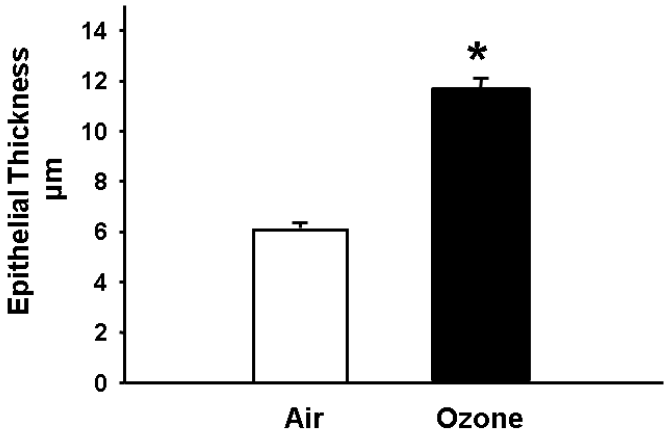

Figure 6. Morphometry of nasal epithelial thickness after 24 weekdays of ozone exposure. There was a significant increase in airway epithelial thickness in mucosa lining the proximal nasal passages of mice exposed to ozone, compared to air control animals. *Statistically different, $p \leq 0.05$, by way of T tests. Data are expressed as mean ± SEM.

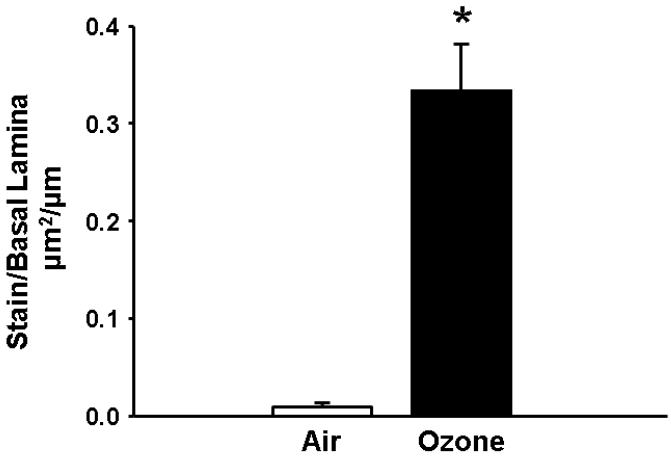

Figure 7. Morphometry of intraepithelial mucosubstances in the mucosa lining the proximal nasal airways after 24-weekday exposure to ozone. There was significant increase in epithelial mucosubstances in the ozone-exposed animals compared to air control animals. *Statistically different, $p \leq 0.05$, by way of T tests. Data are expressed as mean ± SEM.

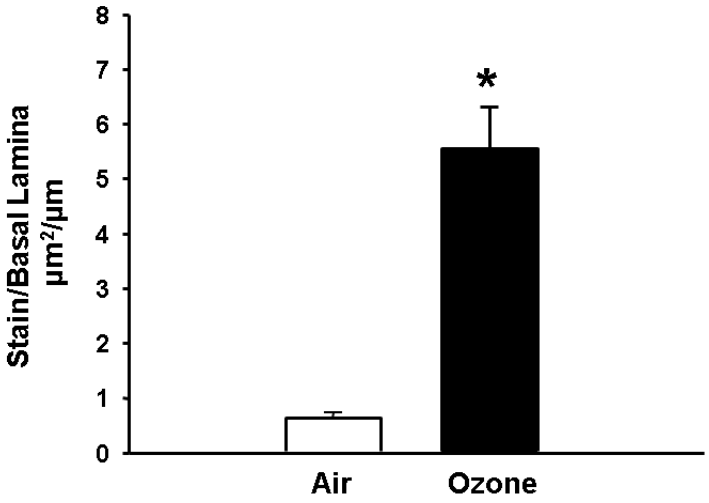

Figure 8. Morphometry of intraepithelial Ym1/2 in the mucosa lining the proximal nasal airways after 24-weekday exposure to ozone. There was significant increase in epithelial cell cytoplasm Ym1/2 material in the ozone-exposed compared to air control animals. *Statistically different, $p \leq 0.05$, by way of T tests. Data are expressed as mean ± SEM.

e. Epithelial DNA Synthesis

Increased DNA synthesis in nasal epithelium is a reliable marker of injury/repair processes after exposure to ozone. Exposure to 0.5 ppm ozone for 24 days caused significant DNA synthesis in the nasal mucosal lining of the lateral wall, as indicated by an increase in epithelial cell staining positive for nuclear BrdU (Fig. 9). The morphometrically estimated quantity of epithelial BrdU showed a significant increase in labeling in the ozone-exposed compared to air control animals (Figure 10).

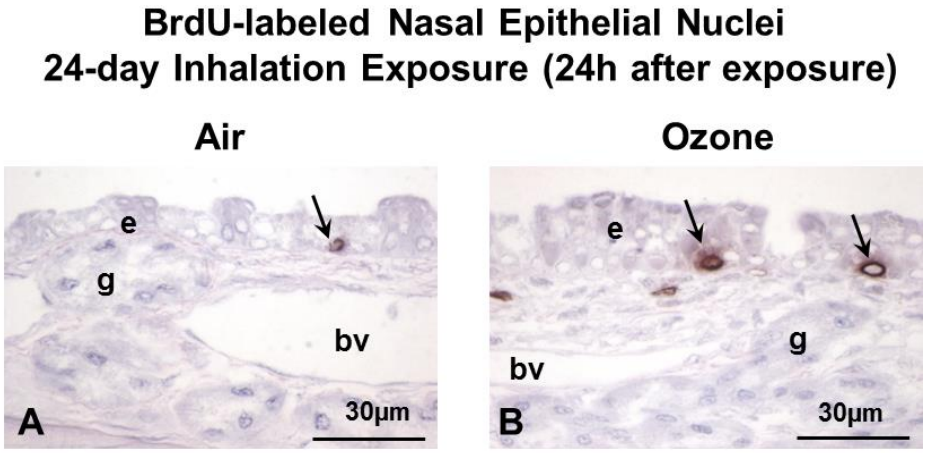

Figure 9. Light photomicrographs of BrdU immunolabeling in nasal mucosa of mice after 24-weekday exposure to ozone. **(A,B)** More BrdU nuclear labelling (solid arrow) was present in the mucosa lining of the ozone-exposed animals compared to air control animals. *(bv: blood vessel; e: epithelium; b:bone; g: gland)*

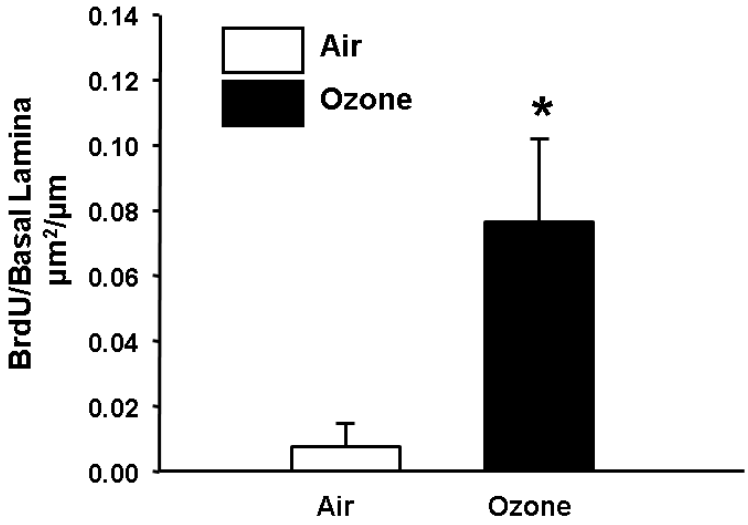

Figure 10. Morphometry of epithelial BrdU in the mucosa lining the proximal nasal airways after 24-weekday exposure to ozone. There was a significant increase in epithelial BrdU in the ozone-exposed compared to air control animals. *Statistically different, $p \leq 0.05$, by way of T tests. Data are expressed as mean ± SEM.

2. 1, 2, 4 or 9 Weekdays of Inhalation Exposure

i. Histopathology and Morphometry

Site specific and temporal changes in ozone-induced nasal pathology were present in mice after 1, 2, 4 and 9 weekdays of inhalation exposure. Similar to mice with 24-day inhalation exposure, these changes were seen in the lateral walls of the both lateral meatus of the proximal nasal passages of the ozone exposed animals, but not in the air-exposed animals.

a. Granulocyte Infiltration

There was a decrease in neutrophil infiltrate and concomitant increase in eosinophilic influx in the nasal mucosa of ozone treated mice from 1 to 9 days of ozone exposure (Figure 11). The early onset neutrophil infiltration in the lamina propria, most significant at the 1-day (2h post-exposure) time point, subsequently decreased in the latter time points. In contrast, eosinophilic influx within the mucosa increased with chronicity of ozone exposures, with the most dramatic increase seen at 9 days of ozone exposure. While neutrophils were the main granulocytes at 1-day (2h post-exposure), 1- and 2-days (24h post-exposure) within the lamina propria of nasal lateral wall, eosinophils predominated in the 4-day and 9-day ozone-exposed mice. The degree of eosinophilic rhinitis at 9 days surpassed the extent of neutrophilic infiltration across all individual time points.

The densities of granulocytes evaluated morphometrically were graphed in Figure 12. The trend of decrease in neutrophils and increase in eosinophils could be appreciated by the respective bars at the different time points. In the 1-day (2h post-exposure) time point, there was a significant increase in neutrophil within the nasal mucosa compared to air control animals. Statistically

significant increase in eosinophilic infiltrate was observed in the 9 day ozone-exposed animals compared to air control animals (Figure 12).

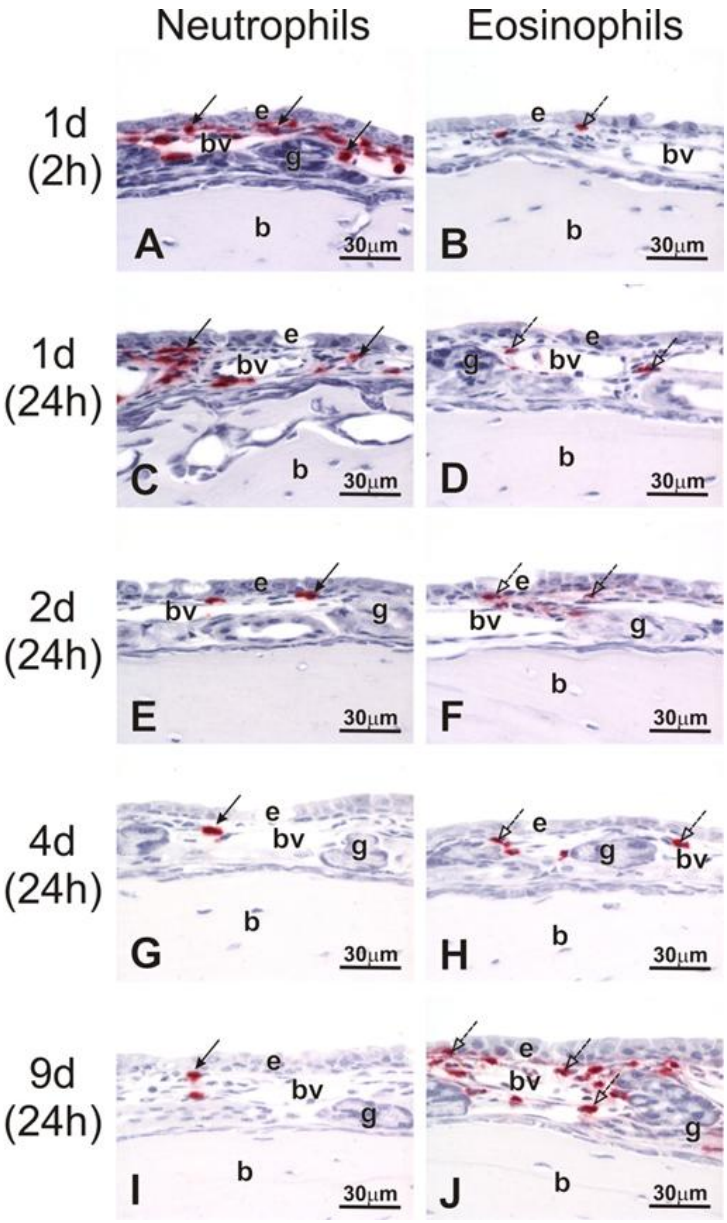

Figure 11. Light photomicrographs of granulocyte infiltration within nasal mucosa of mice after 1, 2, 4 or 9 weekdays of ozone exposure. **(A, C, E, G, I)** There was an acute neutrophilic influx (solid arrows) in the nasal mucosa, which decreased with chronicity of intermittent ozone exposure. (rat anti-mouse neutrophil allotypic marker stain). **(B, D, F, H, J**) The density of eosinophils (non-solid arrows) increased with time of ozone exposures. (Major Basic Protein stain) *(bv: blood vessel; e: epithelium; b:bone; g: gland) (bv: blood vessel; e: epithelium; b:bone; g: gland)*

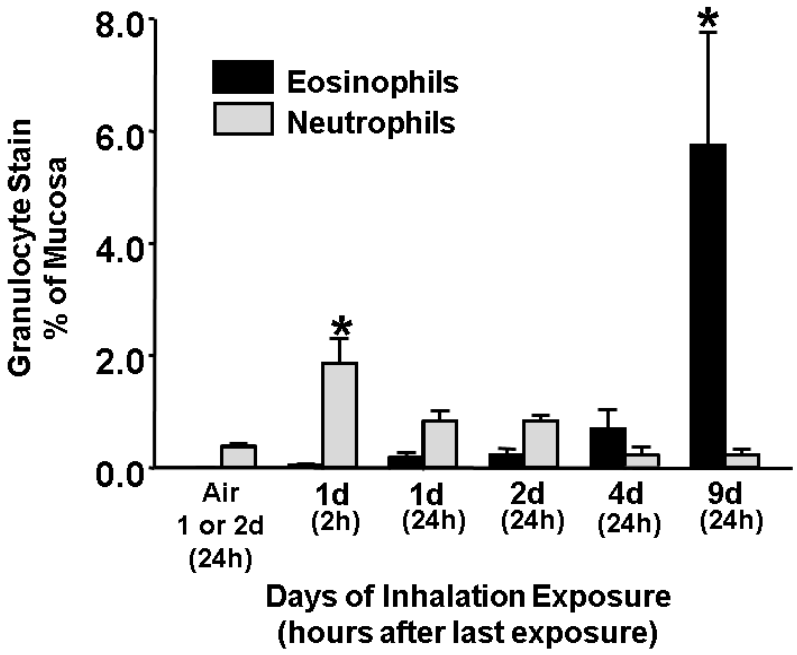

Figure 12. Morphometry of granulocytic influx in nasal lateral wall of mice exposed to 1, 2, 4 or 9 weekdays of ozone or filtered air. Graphic representations of the morphometric determinations of neutrophil and eosinophil densities expressed as percentage of mucosa presented in the same scale. *Statistically different from air-control group, $p \leq 0.05$, by two-way ANOVA and Student-Newman-Keuls post hoc test. Data are expressed as mean ± SEM.

b. Epithelial Thickness

There was an acute loss of epithelial cilia and epithelial degeneration/necrosis at 1-day (sacrifice 2 hours after exposure), before a gradual increase in epithelial thickness after 1- to 9-day ozone exposure (Figure 13 A, D, G, J, M). The initial loss of epithelium in response to ozone was characterized by cell vacuolar degeneration, cell necrosis and exfoliation, particularly involving few widely scattered ciliated cells of the nasal transitional epithelium. Subsequent increase in epithelial thickness was attributed to cellular hyperplasia and hypertrophy. After 9 days of ozone exposure, there were few epithelial cells with early cytoplasmic hyalinosis. The temporal changes in epithelial thickness are quantitated morphometrically and graphed (Figure 14). Initial decrease in epithelial thickness was observed at the earlier time points (reflecting the early epithelial degeneration and loss), although not significantly different from air control animals. In the 9-day ozone-exposed mice, there was a significant increase in nasal mucosal epithelial thickness compared to air control animals.

c. Intraepithelial Mucosubstances

The amount of mucosubstances in the mucosal epithelium also increased with time of ozone exposure (Figure 13 C, F, I, L, O). Intraepithelial mucosubstances were not present significantly after 1, 2 or 4 days, but was most prominent after 9 days of ozone exposure. Amounts of intraepithelial mucosubstances (area of AB/PAS-stained glycoproteins per length of airway basal lamina) were morphometrically estimated (Figure 15). There was a marked and statistically significant increase in mucosubstances in the ozone-exposed animals compared to air control animals at 9 days.

d. Intraepithelial Ym1/2 Protein

The amount of intraepithelial Ym1/2 increased with the duration of ozone exposure (Figure 13 B, E, H, K, N). Ym1/2 protein was present in the apical aspect of the ciliated epithelial cells at 1 day of ozone exposure. At 2 days, there was an increase in Ym1/2 at the basal portion of epithelial cells in lateral wall mucosa. Ym1/2 protein was more diffusely distributed, perinuclear and apical in the mucosal epithelium at 4 days of ozone exposure. This became more intense, diffusely cytoplasmic and apically distributed at 9 days of ozone exposure, and was accompanied by mucosa epithelial hyperplasia/hypertrophy. Amounts of intraepithelial Ym1/2 were morphometrically estimated (Figure 16). A marked increase in Ym1/2 protein was present in the 9 days ozone-exposed animals, and this was significantly elevated at this day compared to air control animals.

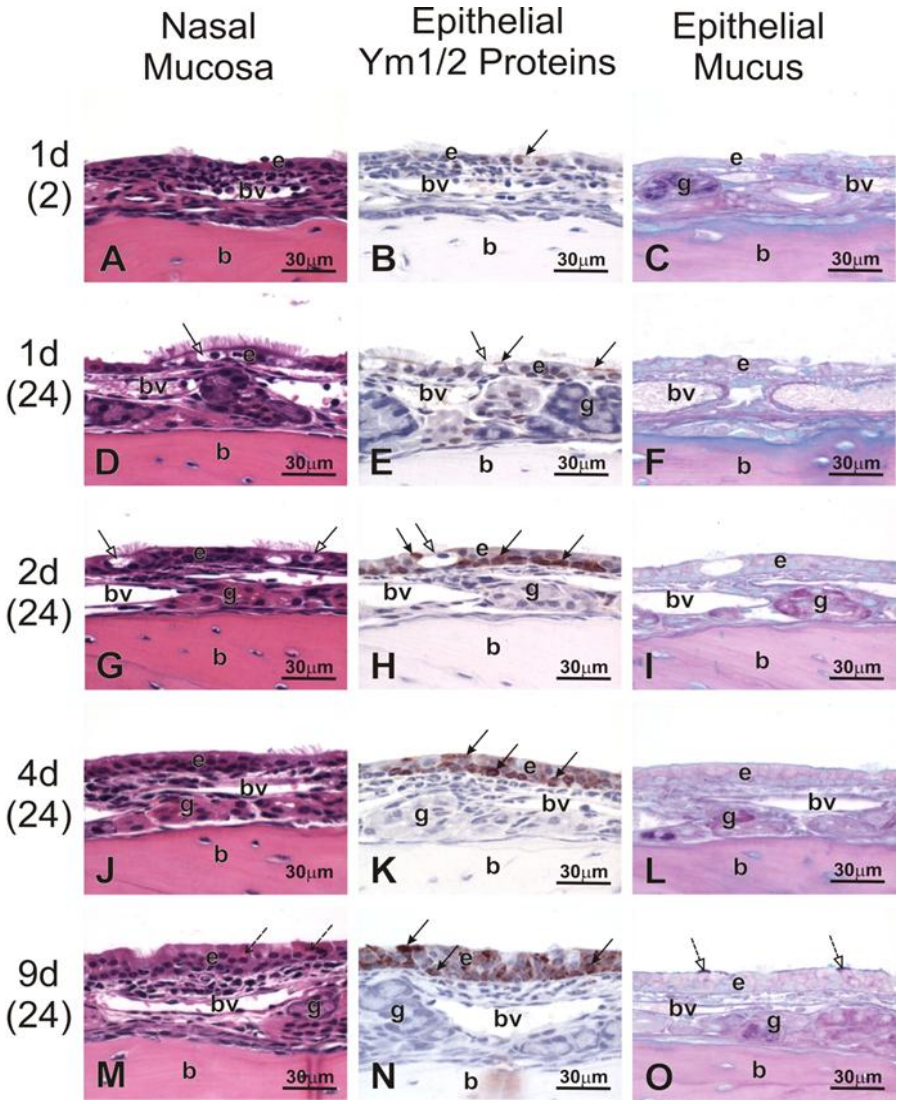

Figure 13. Light photomicrographs of nasal mucosa of mice with 1, 2, 4 or 9 weekdays of ozone exposure. **(A, D, G, J, M)** There was acute epithelial degeneration, vacuolation (clear arrow) and loss of cilia in the nasal mucosa of mice exposed to 1 to 2 days of ozone. After 9 days, there were few epithelial cells with early cytoplasmic hyalinosis. **(B, E, H, K, N)** The production of Ym1/2 increases and varies in distribution within the mucosal epithelial cells, with time of ozone exposure. It was present in the apical aspect of the ciliated epithelial cells at 1 day of ozone exposure (solid arrow). After 2 days, there was increase in Ym1/2 in the basal portion of epithelial cells in lateral wall mucosa. Ym1/2 protein was more diffusely distributed, perinuclear and apical in the mucosal epithelium at 4 days of ozone exposure. This and became more intense, diffusely cytoplasmic and apically distributed after 9 days of ozone exposure, accompanied by the thickened mucosa epithelium (solid arrow). (rabbit polyclonal anti-Ym1 antibody). **(C, F, I, L, O**) Intraepithelial mucosubstances were not present significantly at 1-4 days, and was most prominent after 9 days of ozone exposure. Initial epithelial damage followed by remodeling, mucous cell metaplasia and Ym1/2 protein expression in nasal mucosa of mice from 1 to 9 days of ozone exposure. (Alcian Blue, pH 2.5 PAS) *(bv: blood vessel; e: epithelium; b:bone; g: gland)*

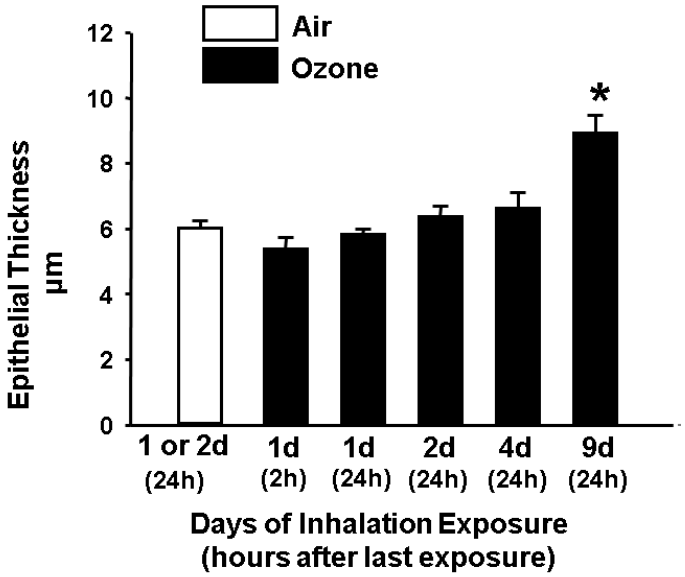

Figure 14. Morphometry of airway epithelial thickness in the mucosa lining the proximal nasal airways after single or repeated exposures. There was an initial decrease in epithelial thickness at the earlier time points, reflecting the early epithelial degeneration and loss. In the 9-day ozone-exposed animals, there was a significant increase in nasal mucosal epithelial thickness compared to air control animals. *Statistically different from air-control group, $p \leq 0.05$, by two-way ANOVA and Student-Newman-Keuls post hoc test. Data are expressed as mean ± SEM.

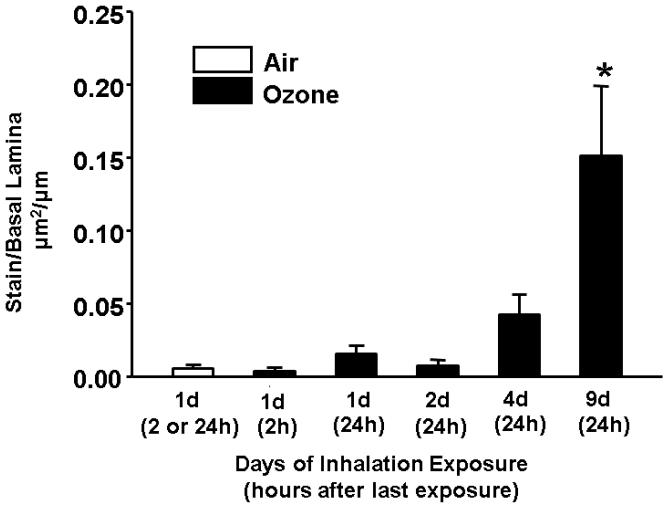

Figure 15. Morphometry of intraepithelial mucosubstances in the mucosa lining the proximal nasal airways after single or repeated exposures. There was a marked and statistically significant increase in mucosubstances in the ozone-exposed animals compared to air control animals after 9 days. *Statistically different from air-control group, $p \leq 0.05$, by two-way ANOVA and Student-Newman-Keuls post hoc test. Data are expressed as mean ± SEM.

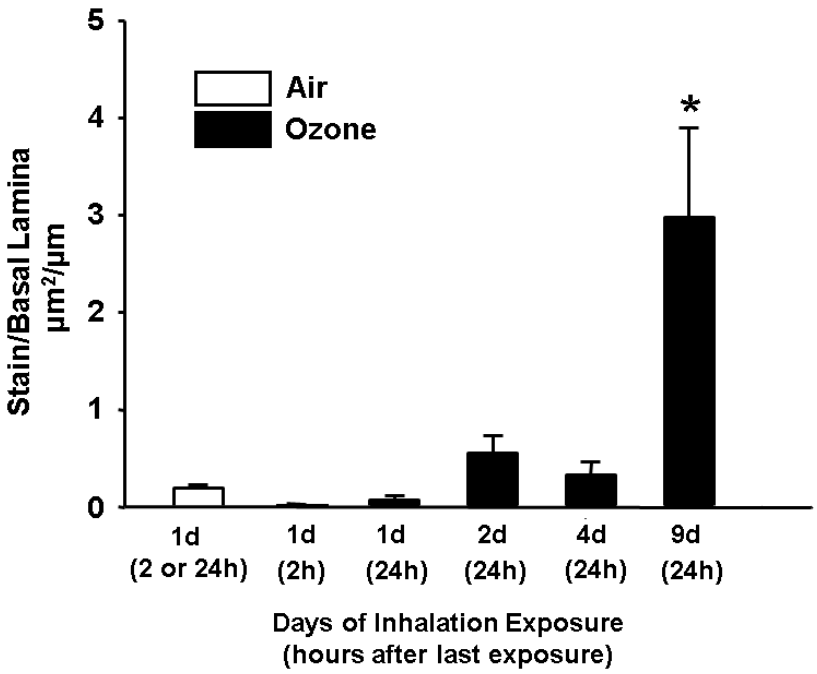

Figure 16. Morphometry of airway epithelial Ym1/2 in the mucosa lining the proximal nasal airways after single or repeated exposures. There was a marked increase in epithelial Ym1/2 protein in the 9-day ozone-exposed animals compared to air control animals. *Statistically different from air-control group, $p \leq 0.05$, by two-way ANOVA and Student-Newman-Keuls post hoc test. Data are expressed as mean ± SEM.

e. Epithelial DNA Synthesis

Exposure to 0.5 ppm ozone for 1 and 2 days caused significant DNA synthesis in the nasal mucosal lining of the lateral wall. Photomicrographs in Figure 17 illustrate the nuclear BrdU labelling in the 1 day air and ozone-exposed animals. Amounts of intranuclear BrdU in the 1- and 2-day mice were morphometrically estimated (Figure 18). At both time points, there was significant increase in BrdU labeling in the ozone-exposed compared to air control animals. There was also a significant decrease in BrdU labelling in the 2-day ozone-exposed animals compared to 1-day ozone-exposed animals, as shown in Figure 18.

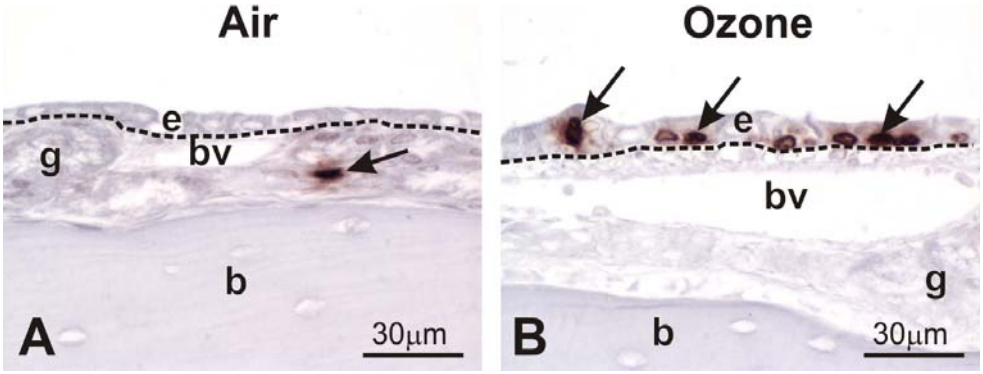

Figure 17: Light photomicrographs of BrdU immunolabeling in nasal mucosa of mice after 1-day exposure. **(A,B)** More BrdU nuclear labelling (solid arrow) was present in the mucosa lining of the ozone-exposed animals compared to air control animals. *(bv: blood vessel; e: epithelium; b:bone; g: gland)*

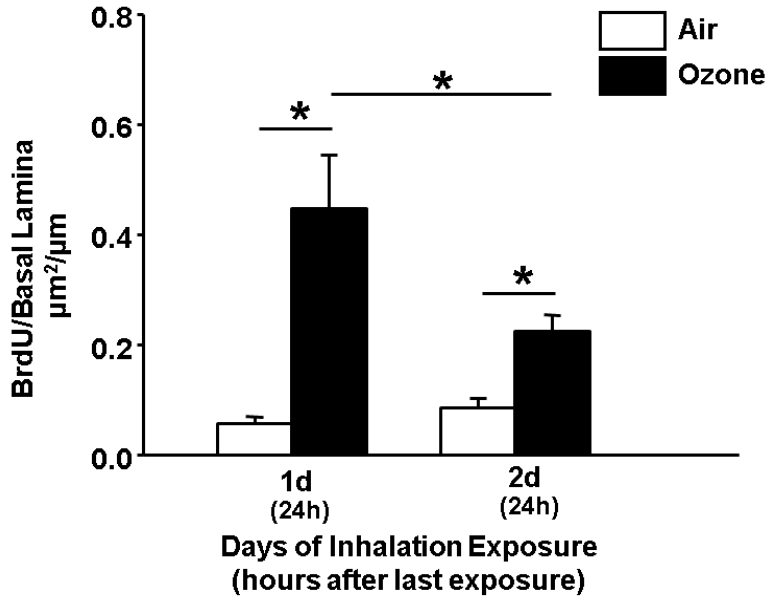

Figure 18. Morphometry of epithelial BrdU in the mucosa lining the proximal nasal airways after 1 and 2-day exposure. At both time points, there was significant increase in labeling in the ozone exposed compared to air control animals. There was also a significant decrease in BrdU labelling in the 2-day ozone-exposed animals compared to 1-day ozone-exposed animals. *Statistically different, $p \leq 0.05$, by way of T tests. Data are expressed as mean ± SEM.

ii. Ultrastructural Changes in Nasal Mucosa of Mice

At 4-day ozone (0.5 ppm) exposure, there were few eosinophils present in the lamina propria of nasal mucosa (Figure 19B), not seen in the air control animals (Figure 19A). After 9 days of ozone (0.5 ppm) exposure, there was intercellular edema in the mucosal epithelium characterized by separation of epithelial cells by electron-lucent spaces, as well as eosinophilic infiltration in lamina propria (Figure 19C). Ultrastructurally, the eosinophils in lamina propria of mice exposed 4 and 9 days of ozone contained cytoplasmic specific/secondary granules with internal electron-dense crystalline core, as well as bilobed nucleus (Figure 19C, D), that distinguished these granulocytes from neutrophils. There was minimal to mild cytoplasmic vacuolation in the 4 day and 9-day ozone exposed animals. No eosinophils or ultrastructural epithelial changes were present in air control mice (Figure 19A).

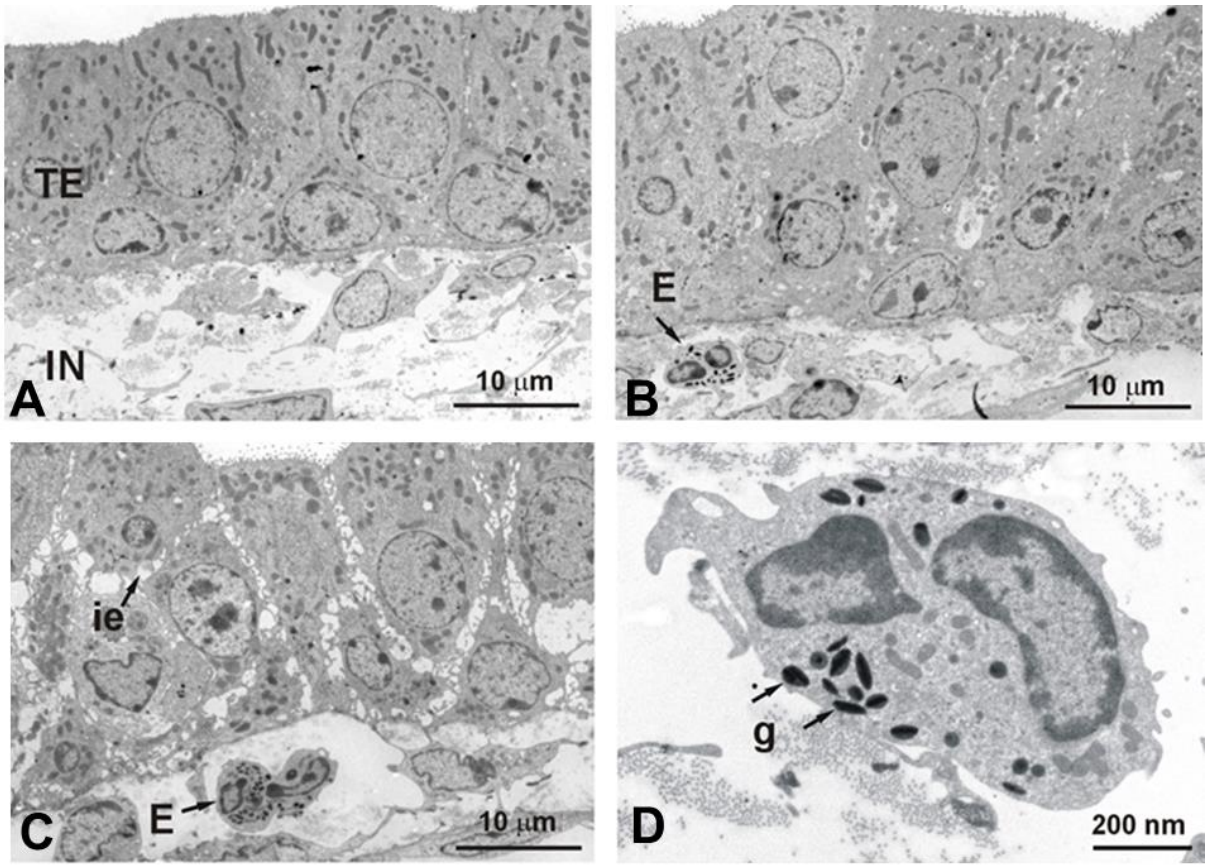

Figure 19. Transmission electron photomicrographs of ultrastructural changes in nasal mucosa of mice due to ozone. **(A).** Air control animals. **(B).** 4 day ozone exposed animals. **(C).** 9 day ozone exposed animals. **(D).** Higher magnification of an eosinophil within lamina propria. (*TE = transitional epithelium; IN = interstitium; E = eosinophil; ie = intercellular edema; g = eosinophil secondary granules*)

iii. Cytokine Gene Expression in Nasal Mucosa

a. Temporal Changes in Cytokine Gene Expression

Fold changes in cytokine gene expression in nasal mucosa of C57BL/6 mice after 1, 2, 4, 9-weekday ozone exposure are shown in Table 2 (Appendix B). Values were expressed as mean ± standard error of the mean, relative to air group within each individual time point.

b. Unsupervised Hierarchical Clustering of Gene Expression and Morphometric Parameters

There were two fairly distinct main branches within the hierarchical tree of gene expressions combined with morphometric parameters (Figure 20). Th1 cytokine genes were clustered with neutrophil density, while Th2 cytokine genes were clustered with increases in eosinophil density, epithelial Ym1/2 proteins and mucosubstances. There was marked over expression of Cxcl2 (MIP-2), IL-1β, IL-6, Tnf-α, Cxcl1 (KC) and Ccl2 (MCP-1) mRNAs after a single day ozone exposure. In contrast, 9-day exposure to ozone induced conspicuous over expression of Ccl11 (Eotaxin), Muc5AC, IL-13, IL-10, Arg1, Ccl8 (MCP-2), Chi3l4 (YM2), Clca3 (Gob5), Saa-3, Chi3l3 (YM1) mRNAs. Hmox and MCP1 were only expressed at the early 1-day (2 h post-exposure) time point. Expressions of Saa3 and Ym1 were reduced at the earliest time point and not significantly different from air control in the later time points. There was a biphasic expression of IL-5 and IL-13, with increased expression seen after 1-day and 9-days of ozone exposure.

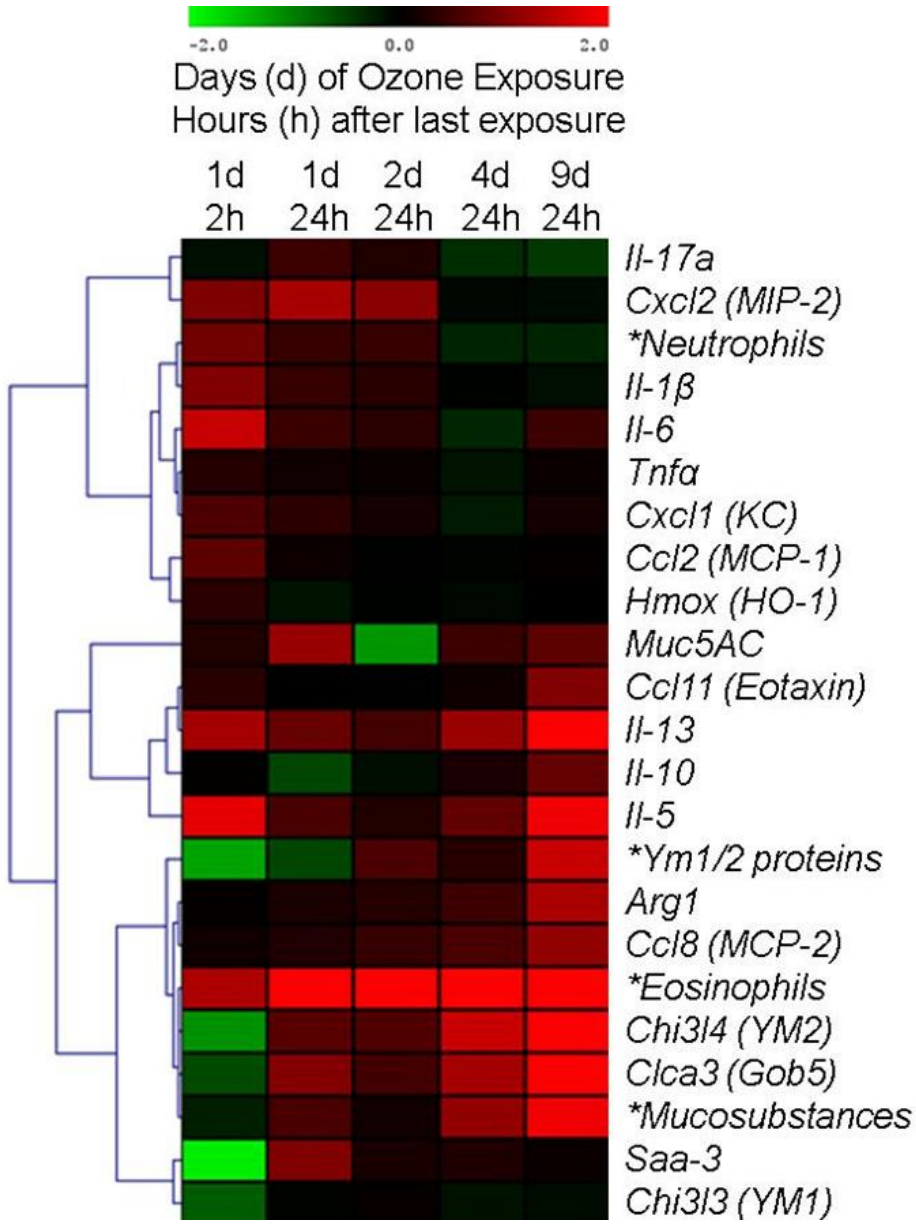

Figure 20. Unsupervised hierarchical clustering of temporal changes in ozone-induced gene expression and morphometric phenotypes (*) in nasal mucosa of ozone-exposed mice relative to air-exposed control mice.
Red intensity = Degree of up-regulation vs. air-exposed controls.
Green intensity = Degree of down-regulation vs. air-exposed controls.
Hierarchical clustering was performed in the TM4 Multiexperiment Viewer (MeV 4.8.1; (http://www.tm4.org) using Pearson correlation metric.

c. Th2 Cytokine Gene Expression

The temporal fold changes in IL-5, IL-13 and Ym2 gene expressions, relative to air controls within each time point, were statistically analysed and graphically represented (Figure 21). There was a biphasic expression of IL-5, with most significant increase present in mice exposed to ozone for 1 day (2h post-exposure), 1 day (24h post-exposure) and 9 days (24h post-exposure) of ozone (Figure 21A). The most significant increase in IL-13 and Ym2 expression was in the 9 day ozone exposed mice (Figure 21B, C).

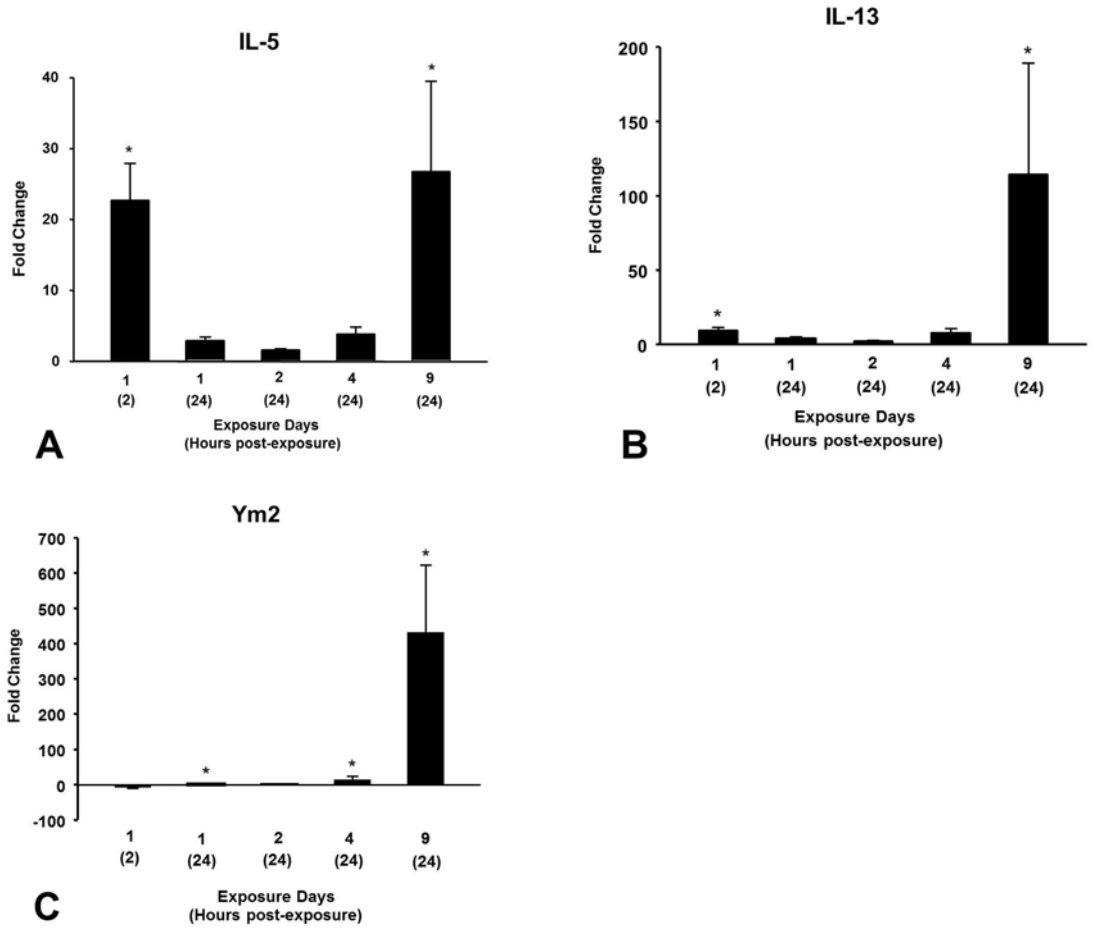

Figure 21: Temporal fold changes in gene expressions in nasal lateral wall of mice exposed to 1, 2, 4 or 9 weekdays of ozone exposure, for selected Th2 genes. **(A)** There was a biphasic expression of IL-5, most significant at 1 day and 9 day of ozone exposure. **(B)** and **(C)** IL-13 and Ym2 gene expressions showed significant fold increases at 9 day of ozone exposure. *Statistically different from air-control group, $p \leq 0.05$, by two-way ANOVA and Student-Newman-Keuls post hoc test. Data are expressed as mean ± SEM.

d. Th1 Cytokine Gene Expression

The temporal fold changes in MIP-2, IL-1β, IL-6 and Tnf-α gene expression, relative to air controls within each time point, were statistically analysed and graphically represented (Figure 22). The relative fold changes in the expression of these genes were greatest in mice exposed to ozone for 1 day (2h post-exposure), 1 day (24h post-exposure) and 2 days (24h post-exposure) ozone. Expressions of these Th1 genes by the ozone exposed animals were not significantly different from air control animals at the 4-day and 9-day time points. The expression of Th1 cytokines decreased with increasing days of ozone exposure.

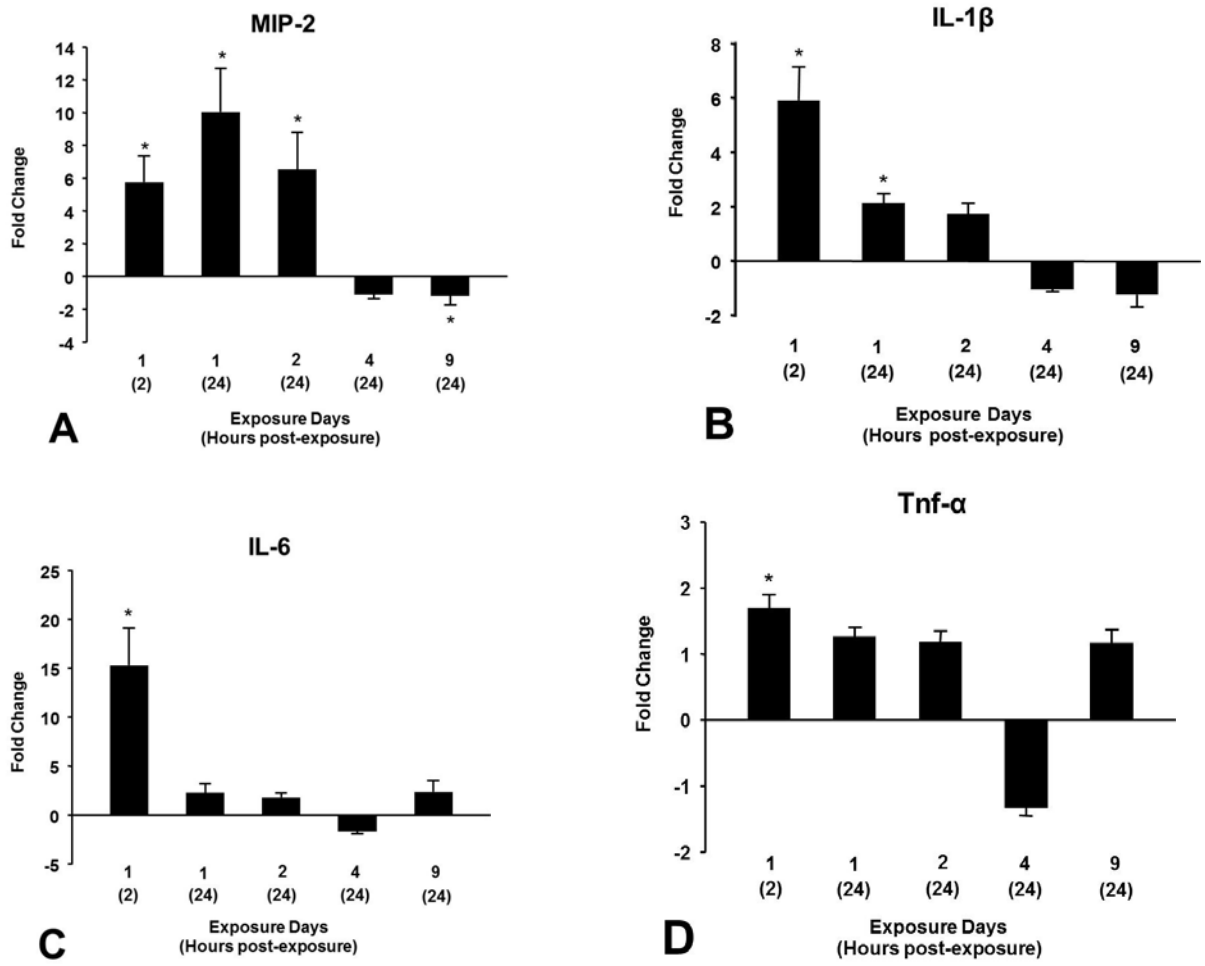

Figure 22. Temporal fold changes in gene expressions in nasal lateral wall of mice exposed to 1, 2, 4 or 9 weekdays of ozone exposure, for selected Th1 genes. **(A)** Expression of MIP-2 was significantly increased in 1 day (2h post-exposure), 1 day (24h post-exposure) and 2 days (24h post-exposure) ozone exposed animals. **(B)** Expression of IL-1β was significantly increased in the 1 day (2h post-exposure), 1 day (24h post-exposure) ozone exposed animals. **(C, D)** Expressions of IL-6 and Tnf-α were significantly increased only at the 1 day (2hr) timepoint. *Statistically different from air-control group, $p \leq 0.05$, by two-way ANOVA and Student-Newman-Keuls post hoc test. Data are expressed as mean ± SEM.

e. Muc5AC and Gob5 Cytokine Gene Expression

The temporal fold changes in Muc5AC and Gob5 gene expression were statistically analysed and graphically represented (Figure 23). The greatest increase in Muc5AC expression was at the 1 day (24h post-exposure) time point, and the greatest fold increase for Gob5 gene expression was in the 9-day ozone exposed animals.

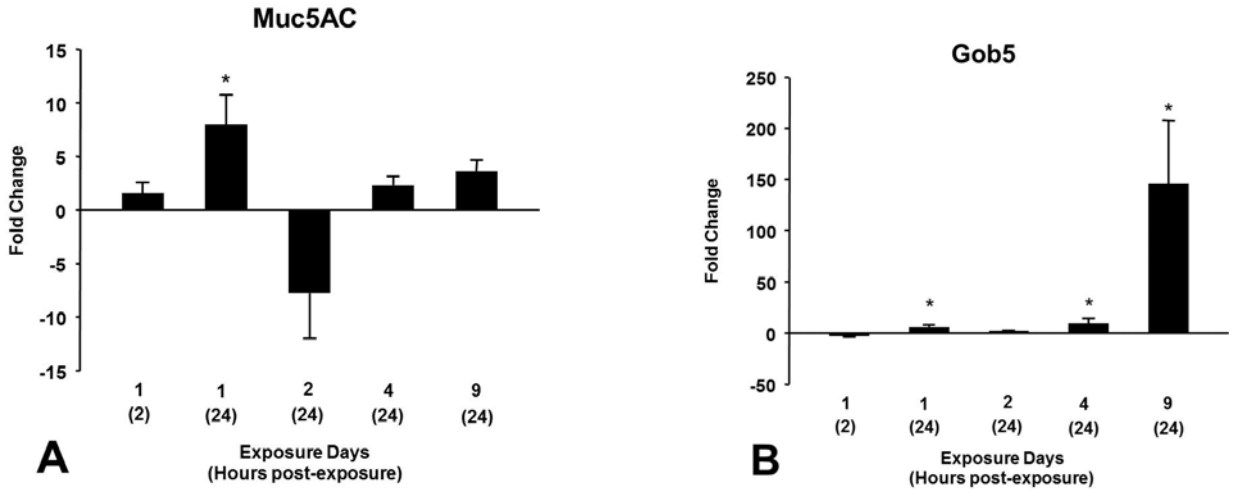

Figure 23: Temporal fold changes in gene expressions in nasal lateral wall of mice exposed to 1, 2, 4 or 9 weekdays of ozone exposure, for Muc5AC and Gob5 genes. **(A)** Expression of Muc5AC was significantly increased in 1 day (24h post-exposure) ozone exposed animals. **(B)** Expression of Gob5 was significantly increased in the 1 day (24h post-exposure), 4-day and 9-day ozone exposed animals. *Statistically different from air-control group, $p \leq 0.05$, by two-way ANOVA and Student-Newman-Keuls post hoc test. Data are expressed as mean ± SEM.

D. Discussion

In the present study, the nasal lesions caused by ozone in these mice were restricted to proximal nasal passages (bilateral lesions) in a region that is lined by nasal transitional epithelium, a low cuboidal pseudostratified airway epithelium, that is normally dominated by cuboidal non-ciliated cells and basal cells and lesser numbers of cuboidal ciliated cells and very few, if any, mucous goblet cells (Harkema et al., 2006). The few widely scattered ciliated cells of the nasal transitional epithelium were most affected by the acute ozone exposures, undergoing vacuolar degeneration, oncotic cell death (necrosis) and exfoliation. The intranasal distribution and character of these epithelial and inflammatory lesions in mice were very similar to those previously reported in rats and nonhuman primates acutely exposed to similar ozone regimens (Hotchkiss et al., 1989; Carey et al., 2011). The novel finding in this study, however, was the marked eosinophilic rhinitis in mice that received the longer-term episodic exposures to ozone for 9 or 24 consecutive weekdays, four hours per day (subacute exposure). The remodeled nasal epithelium was characterized by mucous cell metaplasia and epithelial hyperplasia/hypertrophy. This was similar to that previously reported in laboratory rats and mice (Harkema et al., 2006) and nonhuman primates (Carey et al., 2011) exposed to daily ozone exposures for several days, weeks or even months. By using specific immunohistochemical markers for murine neutrophils and eosinophils, these two infiltrating granulocytic populations could be easily distinguished by light microscopy. To further confirm the ozone-induced eosinophilic inflammatory influx, transmission electron microscopy was used to identify the unique ultrastuctural features of eosinophils, i.e., cytoplasmic specific granules with an internal electron-dense, crystalline core surrounded by an electron-lucent matrix, and the bilobed nucleus, that ultrastructurally distinguishes these granulocytes from neutrophils.

T lymphocytes that express the CD4 cell surface molecule are important sources of Th1 and Th2 cytokines, and these cytokines play important roles in immune and inflammatory diseases. Th1 cytokines, primary IL-2, IFN-γ and TNF-β, direct a cell-mediated immune response and are responsible for killing intracellular viruses, bacteria and fungal organisms, and some autoimmune responses (Berger et al., 2000). Th2 cytokines include IL-4, IL-5 and IL-13. IL-4 is the major factor that regulates IgE production by B-cells, and is required for optimal Th2 lymphocyte differentiation. IL-5 is an interleukin that is produced by T-helper 2 cells and mast cells. It is a major factor for the maturation, activation, recruitment and survival of eosinophils and is hence responsible for eosinophilic influx in diseases such as asthma and atopy. IL-13 has partial gene sequence homology to and similar function as IL-4, and is also a cytokine that is elevated in allergic diseases. IL-10 is another Th2 cytokine, which has more of an anti-inflammatory role. The cytokines produced by Th1 or Th2 subsets of lymphocytes not only enhance the activation and function of the subset that produces them (via autocrine effect), but also diminishes the development and activity of the other subset, known as cross-regulation.

Besides lymphocytes, other cells such as monocytes, macrophages, endothelial cells and epithelial cells are also sources of cytokines. While the primary function of the airway epithelium was thought to be that of a protective barrier that prevents entry of harmful inhaled substances, past studies have shown that airway epithelial cells are an important source of cytokines such as RANTES, MCP-1 and other factors that are chemotactic for T-cells and eosinophils. Hence, airway epithelial cells could mediate the inflammatory events in the respiratory system (Renauld JC, 2001).

In the present study, relative changes in the expression of genes that are often associated with eosinophilic or neutrophilic inflammatory responses further substantiated the dramatic shift

in the nasal inflammatory cell and cytokine profiles with increasing days of ozone exposure. As expected, elevations in mucosal gene expression for IL-1β, IL-6, TNF-α, KC, and MIP-2, all cytokines that are known to respond quickly to cell/tissue injury, were restricted to mice that had received 1- or 2-days exposures to ozone and had neutrophilic rhinitis with nasal epithelial degeneration and necrosis. Similar innate inflammatory cell and cytokine responses have been well documented in the pulmonary airways of laboratory animals and human subjects acutely exposed to ozone (Lu et al., 2006; Johnston et al., 2000; Devlin et al., 1996; Bosson et al., 2003).

In contrast to the innate neutrophilic rhinitis caused by acute ozone exposures, the eosinophilic inflammatory influx in the nasal mucosa of mice that received subacute episodic exposures correlated with the exposure-related increases in gene expressions of IL-5, IL-13, and CCL11 (eotaxin), which are Th2 cytokines that have been well documented to promote the tissue recruitment and accumulation of eosinophils (Li et al., 1999).

In this study, there was an early and late marked biphasic pattern of expression in IL-5, IL-13 and eotaxin genes, especially in the former two genes. The development of eosinophils within the bone marrow is under the control of critical transcription factors such as GATA-1 and PU-1. IL-3, IL-5 and GM-CSF are eosinophilopoietins that regulate the expansion of eosinophil population (Rothenberg et al., 2006; Gonlugur et al., 2006). IL-5 plays a major role in migration of eosinophils out of bone marrow (Rothenberg et al., 2006), and can be expressed in T-lymphocytes, airway epithelial cells as well as in enterocytes in the gastrointestinal tract (Rothenberg et al., 2006). Eotaxin, on the other hand, could be produced by a variety of cells such as epithelial cells, endothelial cells, fibroblasts, eosinophils, T-lymphocytes, monocytes and macrophages (Van CE, 1999). In this study, the expression of eotaxin (chemotaxic agent in recruitment of eosinophils), IL-5, IL-10 and IL-13, fits into a Th2 directed immune response that

peaked after 9 days of ozone exposure. The temporal development of eosinophilic rhinitis accompanied this Th2 cytokine expression. The initial IL-5 and IL-13 gene expressions observed at 1- and 2-days, however, were intriguing and warrant further investigation. Innate lymphoid cells, a recently described specific immune cell population, could be responsible for this early IL-5 and IL-13 expressions. This early IL-5 and IL-13 expressions could be an early innate immune response, which subsequently drives the eosinophilic rhinitis and epithelial remodeling. Group 2 innate lymphoid cells (ILC 2) produce Th2 cytokines such as IL-5 and IL-13, and are seen in acute pulmonary inflammation, acute hypersensitivity reaction and viral infections (Kumar et al., 2014). The over expression of these two cytokines suggest the potential role of ILC2s in the early time points of this study.

Mechanisms of acute ozone-induced toxicity are due to lipid peroxidation of cellular membranes, resulting in epithelial degeneration and necrosis due to oxidative stress and injury, along with generation of free radicals and their related damage. In the present study, increase in Hmox gene expression is accompanied by marked TNF-α and IL-6 expressions at 2 hr of ozone exposure, due to an acute ozone-induced damage to nasal mucosa epithelial cells. Heme oxygenase (Hmox) is an antioxidative enzyme that serves a protective role against TNF-α associated airway inflammation via down regulation of IL-6 (Lee et al., 2009). In this study, Hmox expression was restricted to the 1-day (2h post-exposure) time point, and the expression of this gene was not elevated in subsequent days of ozone exposures, as epithelial remodeling ensued.

I demonstrated, for the first time, the accumulation of Ym1/2 protein within nasal epithelium that line the proximal nasal passage, in mice subjected to ozone inhalation exposure. Ym2 was expressed alongside the nasal mucosal eosinophilic influx in response to increased

period of ozone exposure. In mice, chitinase 3-like-3 (Ym1) and chitinase 3-like-4 (Ym2) are chitinase-like proteins with 95% of nucleotide sequence homology, the expression of which are both dependent on IL-13 (Jin et al., 1998; Dianne et al., 2001). Ym1 is a homolog of YKL40 in human, and is normally expressed in the spleen, bone marrow and lung, and has been shown to be an eosinophil chemotactic chemokine in mice (Lee et al., 2011; Jin et al., 1998; Nio et al., 2004; Owhashi et al., 2000). Ym1 has been reported to be strongly upregulated in the mucus producing cells of upper airways of the lung, in response to allergic inflammation (Homer et al., 2006), while Ym2 is expressed by keratinocytes of the squamous portion in the stomach of mice, and increased expression of Ym2 is also seen in the lung in allergies (Nio et al., 2004; Jin et al., 1998). Ym1 and Ym2 protein have been shown to be upregulated along with inflammation in neoplastic transformation of the epidermis, and have been suggested to be autoantigens in mice, with serum immunoglobulin G reactivity (Qureshi et al., 2011). Chitin, a polymer of N-acetylglycosamine, is the major component of fungal, arthropod, nematode and crustacean organisms and is the second most abundant polysaccharide in the world, but do not exist in mammals (Brinchmann et al., 2011). The family of chitinase proteins includes chitinases and chitinase-like proteins. The former exists in mammals with a defense function against chitinous parasites, and are glycoproteins that cleave B-glycosidic bonds between N-acetyleglucosamine residues of chitin (Nio et al., 2004). Environmental exposure to chitin and immune activation of chitinase pathway in human is implicated in development of allergic conditions such as asthma (Brinchmann et al., 2011; Goldman et al., 2011). Chitinase-like proteins, on the other hand, lack enzymatic activities but still bind to chitin and glysosaminoglycans The up-regulation of Ym2 expression with increasing time of ozone exposure in this study could have been initiated by IL-13 expression, and is at least in part responsible for the eosinophilic rhinitis. In this study, a

temporal increase in Ym1/2 protein was evident in the nasal mucosal epithelium, and this was accompanied by Ym2 gene over expression. Interestingly, Ym1 gene expression was not significantly elevated in the initial and later time points, and it appeared that it was the Ym2 gene that is driving Ym1/2 epithelial protein accumulation in the ozone exposed mice.

Ozone exposure causes nasal epithelial hyperplasia and mucous cell metaplasia in rats and also enhances airway hyperresponsiveness allergen-sensitized mice (Hotchkiss et al., 1991; Larsen et al., 2010). In our study, nasal epithelial hyperplasia and mucous cell metaplasia was similarly seen in the lateral wall epithelium of mice exposed to ozone, in a time dependent manner, along with increased IL-13, Gob5 and Muc5AC expressions. IL-13 has also been shown to be involved in tissue eosinophilia and mucous cell metaplasia (Zhu et al., 1999). Gob5 is a member of the calcium-activated chloride channel family, and is the primary protein responsible for the mucus hypersecretion and goblet cell metaplasia in mice allergic asthma model (Nakanishi et al., 2001). The expression pattern of IL-13, Gob5 and Muc5AC is in agreement with the histological increase in epithelial mucosubstances of the nasal passage in this study, and indicates that ozone induces a phenotype that resembles an allergic/non-allergic rhinitis and asthma. In humans, allergic and non-allergic rhinitis had been described. Allergic rhinitis is mediated by IgE, with associated mast cell histamine release and eosinophilic infiltration in the nasal mucosa. IL-4 and IL-5 production (Th2 response) occurs in allergic rhinitis, which have immediate and late phase responses to the allergen. Non-allergic rhinitis on the other hand, is associated with chronic nasal symptoms in response to a non-allergen (e.g. cigarette smoke), negative allergen test and is less well-understood (Tran et al., 2011). Even though ozone is not thought to be a chemical sensitizer or allergen, the ozone induced eosinophilic rhinitis and localized Th2 cytokine response in this study most resemble non-allergic rhinitis with

eosinophilia syndrome (NARES) in humans. In the present study, I did not determine IgE levels in the blood of these the air or ozone-exposed mice. Hence, whether the observed ozone-induced eosinophilic rhinitis seen in these mice more resembles that of allergic or non-allergic rhinitis in humans needs to be further elucidated.

There is an intimate relationship between upper and lower airways. In some diseases, such as allergic rhinitis and asthma in humans, similar lesions can be seen in both parts of the respiratory tract (Passalacqua et al., 2000). In experimentally allergen-sensitized mice, nasal mucosal changes and eosinophilic rhinitis occurred alongside similar bronchiolar mucosa changes and pulmonary inflammation. The upper airway plays a role in being the 'first responder' to an allergic stimulation, with subsequent trickle-down effects on the lower bronchial tree and lung. Hence, the nose could be the primary site in driving the pulmonary and systemic allergic responses (Hellings et al., 2001; McCusker et al., 2002). Previous studies have already showed exposure to ozone causes pulmonary eosinophilic inflammation and hyperreactivity, as well as epithelial adaptation with chronicity of exposure (Kierstein et al., 2008; Jang et al., 2006). The nasal epithelial changes and mucosal inflammation described in the current studies followed a similar trend of changes. The nose should be viewed as having an active integral immunological role in the pathophysiology of diseases, affecting the lower respiratory tract.

In summary, the results of these studies clearly showed a dramatic shift in cytokine expression, from an early Th1 to a late Th2 gene profile, accompanied by a temporal shift from a neutrophilic to an eosinophilic granulocytic influx nasal mucosa, due to prolonged ozone exposure. This Th2 cytokine expression due to subacute ozone exposure occurred without previous or concurrent inhalation exposures to a known aeroallergen. These studies showed that

subacute intermittent ozone exposures, in the absence of aeroallogen, caused eosinophilic rhinitis, Th2 inflammatory cytokine release, as well as epithelial remodeling and mucous cell metaplasia in C57BL/6 mice. In humans, Th2 cytokine overexpression is typically associated with allergies and atopic diseases. In asthma patients, Th2 cytokines such as IL-4, IL-5 and IL-13 are overexpressed by T cells (Renauld JC, 2001). Allergic and non-allergic rhinitis in humans are also associated with eosinophilic influx in the nasal airways and Th2 immune response. The present study showed that repeated ozone exposures induce Th2 cytokine expression, epithelial remodeling and eosinophilic rhinitis that mimic changes seen in these human respiratory diseases. Results of the present study provide biological plausibility to the epidemiological associations between eosinophilic airway and systemic inflammation previously reported by Frischer and colleagues (Frischer et al., 2001; Frischer et al., 1993). As lymphocytes and associated leukocytes are responsible for orchestrating immune response to allergens, infectious agents and otherwise adverse acute or chronic insults to the body, these mononuclear inflammatory cells are likely sources of the Th2 cytokines associated with the influx of eosinophils in the nasal mucosa of mice exposed to zone. In the next chapter, I will describe studies that were designed to test the hypothesis that ozone-induced eosinophilic rhinitis is dependent on Th2 cytokines produced by lymphoid cells.

APPENDICES

Appendix A

Inhalation Exposures (necropsy time after last exposure)	Air Chamber (ppm) *	Ozone Chamber (ppm) *
1 day (2 hours)	0.005 ± 0.0005	0.517 ± 0.002
1 day (24 hours)	0.005 ± 0.0005	0.517 ± 0.002
2 days (24 hours)	0.003 ± 0.0007	0.498 ± 0.002
4 days (24 hours)	0.008 ± 0.0004	0.493 ± 0.004
9 days (24 hours)	0.008 ± 0.0003	0.485 ± 0.002
24 days (24 hours)	0.004 ± 0.0002	0.503 ± 0.006

Table 1. Ozone chamber concentrations during inhalation exposures. (ppm; *mean ± standard error of the mean)

Appendix B

Gene	1d 2h O3	1d 24h O3	2d 24h O3	4d O3	9d O3
Arg1	1.07+/-0.09	1.49+/-0.28	2.69+/-0.35	2.32+/-0.49	10.33+/-4.02
MCP1	3.59+/-0.44	1.20+/-0.23	1.27+/-0.16	-1.05+/-0.10	1.09+/-0.16
MCP2	1.27+/-0.18	1.58+/-0.34	3.50+/-0.61	2.81+/-0.58	7.53+/-2.93
Eotaxin	1.79+/-0.24	-1.01+/-0.12	1.20+/-0.08	1.25+/-0.16	5.90+/-2.07
YM1	-3.51+/-0.82	-1.06+/-0.17	1.23+/-0.26	-1.27+/-0.28	-1.18+/-0.24
YM2	-7.24+/-2.20	3.38+/-1.40	3.66+/-0.61	15.57+/-9.97	431.34+/-192.17
Gob5	-2.80+/-0.88	6.12+/-2.29	3.90+/-0.39	9.56+/-4.85	145.82+/-61.93
KC	2.96+/-0.45	1.88+/-0.55	1.75+/-0.49	-1.44+/-0.08	1.34+/-0.49
MIP2	5.75+/-1.61	10.04+/-2.67	3.23+/-1.12	-1.10+/-0.24	-1.17+/-0.57
Hmox	1.84+/-0.25	-1.29+/-0.11	1.37+/-0.08	-1.12+/-0.04	1.04+/-0.10
Ifng	1.34+/-0.21	1.54+/-0.47	-1.61+/-0.24	-1.39+/-0.11	-1.34+/-0.26
IL1b	5.93+/-1.22	2.14+/-0.34	1.52+/-0.33	-1.03+/-0.09	-1.24+/-0.44
IL2				1.07+/-0.23	1.31+/-0.25
IL4				1.15+/-0.23	3.62+/-2.15
IL5	22.70+/-5.21	2.83+/-0.59	1.91+/-0.25	3.79+/-1.06	26.74+/-12.71
IL6	15.31+/-3.77	2.25+/-0.96	2.09+/-0.52	-1.66+/-0.24	2.35+/-1.17
IL9				-2.49+/-0.07	#DIV/0!
IL10	1.06+/-0.14	-2.57+/-0.29	1.27+/-0.13	1.45+/-0.31	4.04+/-1.37
IL12a				-1.26+/-0.26	-1.46+/-0.28
IL12b				-1.41+/-0.42	-1.47+/-0.25
IL13	9.63+/-1.96	4.11+/-1.29	3.01+/-0.65	8.11+/-2.94	114.67+/-74.74
IL17a	-1.23+/-0.38	2.31+/-0.46	1.18+/-0.36	-1.86+/-0.34	-2.15+/-1.80
Mmp8				-1.75+/-0.46	-3.83+/-1.27
Mmp12	1.59+/-0.27	1.45+/-0.19	1.15+/-0.22	1.49+/-0.26	2.43+/-0.60
Muc5AC	1.60+/-0.97	8.02+/-2.73	-13.32+/-7.32	2.31+/-0.83	3.63+/-1.01
Saa3	-25.26+/-6.78	5.85+/-3.60	1.05+/-0.34	1.56+/-0.16	1.19+/-0.39
Tnfa	1.70+/-0.20	1.26+/-0.14	1.46+/-0.21	-1.33+/-0.12	1.17+/-0.21

Table 2. Temporal fold changes in gene expression in nasal mucosa of C57BL/6 mice after 1, 2, 4 or 9 days of inhalation exposure to ozone. Values are expressed as fold changes (mean ± SEM), relative to C57BL/6 air group within individual timepoint. Values highlighted in yellow are significantly different.

REFERENCES

REFERENCES

1. Berger A. Th1 and Th2 responses: what are they? BMJ. 2000 Aug 12;321(7258):424.

2. Bosson J, Stenfors N, Bucht A, Helleday R, Pourazar J, Holgate ST, Kelly FJ, Sandström T, Wilson S, Frew AJ, Blomberg A. Ozone-induced bronchial epithelial cytokine expression differs between healthy and asthmatic subjects. Clin Exp Allergy. 2003 Jun;33(6):777-82.

3. Brinchmann BC, Bayat M, Brøgger T, Muttuvelu DV, Tjønneland A, Sigsgaard T. A possible role of chitin in the pathogenesis of asthma and allergy. Ann Agric Environ Med. 2011 Jun;18(1):7-12.

4. Carey SA, Ballinger CA, Plopper CG, McDonald RJ, Bartolucci AA, Postlethwait EM, Harkema JR. Persistent rhinitis and epithelial remodeling induced by cyclic ozone exposure in the nasal airways of infant monkeys. Am J Physiol Lung Cell Mol Physiol. 2011 Feb;300(2):L242-54.

5. Devlin RB, McDonnell WF, Becker S, Madden MC, McGee MP, Perez R, Hatch G, House DE, Koren HS. Time-dependent changes of inflammatory mediators in the lungs of humans exposed to 0.4 ppm ozone for 2 hr: a comparison of mediators found in bronchoalveolar lavage fluid 1 and 18 hr after exposure. Toxicol Appl Pharmacol. 1996 May;138(1):176-85.

6. Dianne C. Webb, McKenzie AN, Foster PS. Expression of the Ym2 lectin-binding protein is dependent on interleukin (IL)-4 and IL-13 signal transduction: identification of a novel allergy-associated protein. J Biol Chem. 2001 Nov 9;276(45):41969-76.

7. Driscoll KE, Simpson L, Carter J, Hassenbein D, Leikauf GD. Ozone inhalation stimulates expression of a neutrophil chemotactic protein, macrophage inflammatory protein 2. Toxicol Appl Pharmacol. 1993 Apr;119(2):306-9.

8. Ellis AK, Keith PK: Nonallergic rhinitis with eosinophilia syndrome. Curr Allergy Asthma Rep. 2006 May;6(3):215-20.

9. Frischer TM, Kuehr J, Pullwitt A, Meinert R, Forster J, Studnicka M, Koren H. Ambient ozone causes upper airways inflammation in children. Am Rev Respir Dis. 1993 Oct;148(4 Pt 1):961-4.

10. Frischer T, Studnicka M, Halmerbauer G, Horak F Jr, Gartner C, Tauber E, Koller DY. Ambient ozone exposure is associated with eosinophil activation in healthy children. Clin Exp Allergy. 2001 Aug;31(8):1213-9.

11. Goldman DL, Li X, Tsirilakis K, Andrade C, Casadevall A, Vicencio AG. Increased chitinase expression and fungal-specific antibodies in the bronchoalveolar lavage fluid of asthmatic children. Clin Exp Allergy. 2012 Apr;42(4):523-30.

12. Gonlugur Ugur, Gonlugur TE. Non-allergic eosinophilic inflammation. Immunol Invest. 2006;35(1):29-45.

13. Harkema JR, Hotchkiss JA, Henderson RF. Effects of 0.12 and 0.80 ppm ozone on rat nasal and nasopharyngeal epithelial mucosubstances: quantitative histochemistry. Toxicol Pathol. 1989;17(3):525-35.

14. Harkema JR, Wagner JG. Epithelial and inflammatory responses in the airways of laboratory rats coexposed to ozone and biogenic substances: enhancement of toxicant-induced airway injury. Exp Toxicol Pathol. 2005 Jul;57 Suppl 1:129-41.

15. Harkema JR, Carey SA, Wagner JG. The nose revisited: a brief review of the comparative structure, function, and toxicologic pathology of the nasal epithelium. Toxicol Pathol. 2006;34(3):252-69.

16. Hellings PW, Hessel EM, Van Den Oord JJ, Kasran A, Van Hecke P, Ceuppens JL. Eosinophilic rhinitis accompanies the development of lower airway inflammation and hyper-reactivity in sensitized mice exposed to aerosolized allergen. Clin Exp Allergy. 2001 May;31(5):782-90.

17. Hiltermann TJ, de Bruijne CR, Stolk J, Zwinderman AH, Spieksma FT, Roemer W, Steerenberg PA, Fischer PH, van Bree L, Hiemstra PS. Effects of photochemical air pollution and allergen exposure on upper respiratory tract inflammation in asthmatics. Am J Respir Crit Care Med. 1997 Dec;156(6):1765-72.

18. Homer RJ, Zhu Z, Cohn L, Lee CG, White WI, Chen S, Elias JA. Differential expression of chitinases identify subsets of murine airway epithelial cells in allergic inflammation. Am J Physiol Lung Cell Mol Physiol. 2006 Sep;291(3):L502-11

19. Hotchkiss JA, Harkema JR, Sun JD, Henderson RF. Comparison of acute ozone-induced nasal and pulmonary inflammatory responses in rats. Toxicol Appl Pharmacol. 1989 Apr;98(2):289-302.

20. Hotchkiss JA, Harkema JR, Henderson RF. Effect of cumulative ozone exposure on ozone-induced nasal epithelial hyperplasia and secretory metaplasia in rats. Exp Lung Res. 1991 May-Jun;17(3):589-600.

21. Islam Z, Harkema JR, Pestka JJ. Satratoxin G from the black mold Stachybotrys chartarum evokes olfactory sensory neuron loss and inflammation in the murine nose and brain. Environ Health Perspect. 2006 Jul;114(7):1099-107.

22. Jang AS, Choi IS, Lee JH, Park CS, Park CS. Prolonged ozone exposure in an allergic airway disease model: adaptation of airway responsiveness and airway remodeling. Respir Res. 2006 Feb 13; 7:24.

23. Jin HM, Copeland NG, Gilbert DJ, Jenkins NA, Kirkpatrick RB, Rosenberg M.. Genetic characterization of the murine Ym1 gene and identification of a cluster of highly homologous genes. Genomics. 1998 Dec 1;54(2):316-22.

24. Johnston CJ, Stripp BR, Reynolds SD, Avissar NE, Reed CK, Finkelstein JN. Inflammatory and antioxidant gene expression in C57BL/6J mice after lethal and sublethal ozone exposures. Exp Lung Res. 1999 Jan-Feb;25(1):81-97.

25. Johnston CJ, Reed CK, Avissar NE, Gelein R, Finkelstein JN. Antioxidant and inflammatory response after acute nitrogen dioxide and ozone exposures in C57Bl/6 mice. Inhal Toxicol. 2000 Mar;12(3):187-203.

26. Kierstein S, Krytska K, Sharma S, Amrani Y, Salmon M, Panettieri RA Jr, Zangrilli J, Haczku A. Ozone inhalation induces exacerbation of eosinophilic airway inflammation and hyperresponsiveness in allergen-sensitized mice. Allergy. 2008 Apr;63(4):438-46.

27. Kumar V. Innate lymphoid cells. new paradigm in immunology of inflammation. Immunol Lett. 2014 Jan-Feb;157(1-2):23-37.

28. Larsen ST, Matsubara S, McConville G, Poulsen SS, Gelfand EW. Ozone increases airway hyperreactivity and mucus hyperproduction in mice previously exposed to allergen. J Toxicol Environ Health A. 2010;73(11):738-47.

29. Lee CG, Da Silva CA, Dela Cruz CS, Ahangari F, Ma B, Kang MJ, He CH, Takyar S, Elias JA. Role of chitin and chitinase/chitinase-like proteins in inflammation, tissue remodeling, and injury. Annu Rev Physiol. 2011;73:479-501.

30. Lee IT, Luo SF, Lee CW, Wang SW, Lin CC, Chang CC, Chen YL, Chau LY, Yang CM. Overexpression of HO-1 protects against TNF-alpha-mediated airway inflammation by down-regulation of TNFR1-dependent oxidative stress. Am J Pathol. 2009 Aug;175(2):519-32.

31. Li L, Xia Y, Nguyen A, Lai YH, Feng L, Mosmann TR, Lo D. Effects of Th2 cytokines on chemokine expression in the lung: IL-13 potently induces eotaxin expression by airway epithelial cells. J Immunol. 1999 Mar 1;162(5):2477-87.

32. Lu FL, Johnston RA, Flynt L, Theman TA, Terry RD, Schwartzman IN, Lee A, Shore SA: Increased pulmonary responses to acute ozone exposure in obese db/db mice. Am J Physiol Lung Cell Mol Physiol. 2006 May;290(5):L856-65.

33. McCusker C, Chicoine M, Hamid Q, Mazer B. Site-specific sensitization in a murine model of allergic rhinitis: role of the upper airway in lower airways disease. J Allergy Clin Immunol. 2002 Dec;110(6):891-8.

34. Nakanishi A, Morita S, Iwashita H, Sagiya Y, Ashida Y, Shirafuji H, Fujisawa Y, Nishimura O, Fujino M. Role of gob-5 in mucus overproduction and airway hyperresponsiveness in asthma. Proc Natl Acad Sci U S A. 2001 Apr 24;98(9):5175-80.

35. Nio J, Fujimoto W, Konno A, Kon Y, Owhashi M, Iwanaga T. Cellular expression of murine Ym1 and Ym2, chitinase family proteins, as revealed by in situ hybridization and immunohistochemistry. Histochem Cell Biol. 2004 Jun;121(6):473-82. Epub 2004 May 18.

36. Owhashi M, Arita H, Hayai N: Identification of a novel eosinophil chemotactic cytokine (ECF-L) as a chitinase family protein. J Biol Chem. 2000 Jan 14;275(2):1279-86.

37. Passalacqua G, Ciprandi G, Canonica GW. United airways disease: therapeutic aspects. Thorax. 2000 October; 55(Suppl 2): S26–S27.

38. Qureshi AM, Hannigan A, Campbell D, Nixon C, Wilson JB. Chitinase-like proteins are autoantigens in a model of inflammation-promoted incipient neoplasia. Genes Cancer. 2011 Jan;2(1):74-87.

39. Renauld JC. New insights into the role of cytokines in asthma. J Clin Pathol. 2001 Aug;54(8):577-89.

40. Rothenberg ME, Hogan SP. The eosinophil. Annu Rev Immunol. 2006;24:147-74.

41. Tran NP, Vickery J, Blaiss MS. Management of rhinitis: allergic and non-allergic. Allergy Asthma Immunol Res. 2011 Jul;3(3):148-56.

42. Van CE, Van Damme J, Opdenakker G. The MCP/eotaxin subfamily of CC chemokines. Cytokine Growth Factor Rev. 1999 Mar;10(1):61-86.

43. Wagner JG, Hotchkiss JA, Harkema JR. Effects of ozone and endotoxin coexposure on rat airway epithelium: potentiation of toxicant-induced alterations. Environ Health Perspect. 2001 Aug;109 Suppl 4:591-8.

44. Wagner JG, Hotchkiss JA, Harkema JR. Enhancement of nasal inflammatory and epithelial responses after ozone and allergen coexposure in Brown Norway rats. Toxicol Sci. 2002 Jun;67(2):284-94.

45. Young JT. Histopathologic examination of the rat nasal cavity. Fundam Appl Toxicol. 1981 Jul-Aug;1(4):309-12.

46. Zhao Q, Simpson LG, Driscoll KE, Leikauf GD. Chemokine regulation of ozone-induced neutrophil and monocyte inflammation. Am J Physiol. 1998 Jan;274(1 Pt 1):L39-46.

47. Zhu Z, Homer RJ, Wang Z, Chen Q, Geba GP, Wang J, Zhang Y, Elias JA. Pulmonary expression of interleukin-13 causes inflammation, mucus hypersecretion, subepithelial fibrosis, physiologic abnormalities, and eotaxin production. J Clin Invest. 1999 Mar;103(6):779-88.

CHAPTER 3

ROLE OF LYMPHOCYTES IN OZONE-INDUCED EOSINOPHILIC RHINITIS, USING RAG2(-/-) x γc(-/-) MICE AND C57BL/6 MICE

A. Introduction

In the previous chapter, I described my finding that a shift in cytokine gene expression from Th1 to Th2 profile accompanies the temporal development of eosinophilic rhinitis in the nasal mucosa of C57BL/6 mice exposed to intermittent ozone. A Th2 cytokine gene expression was concurrent with epithelial remodeling, hyalinosis and mucous cell metaplasia of the nasal mucosa.

Transgenic and immunocompromised mice strains defective in T-lymphocytes, B-lymphocytes and/or NK cells, are widely used in cancer studies as they do not reject allogenic or xenogenic stem cells. Several strains of immunocompromised mice of different background strains, such as BALB/c nude, ICR scid and NOD scid mice, are commonly used in research. In a recently published study, several mice strains including Rag2 x common gamma chain (γc)-deficient mice [double knockout, hereby described as RAG2(-/-) x γc(-/-)] were utilized to investigate the potential role of innate lymphoid type 2 cells in induction of eosinophilia and Th2 associated immune stimulation (Molofsky et al., 2013). In the present study, I used lymphoid depleted RAG2(-/-) x γc(-/-) mice, on C57BL/6 background, that lack both the common gamma chain (Il2rg or γc) and Rag2 (recombinase activating gene 2).

Lymphocytes serve a crucial role in recognizing and responding to antigenic stimulation via immunoglobulin (Ig) and T-cell receptor (TCR) molecules. Rag1 and Rag2 are recombinases that facilitate the process of V(D)J recombination which is essential for the development and maturation of lymphocytes (Jones et al., 2004), while the common gamma chain is essential for functional IL-2, IL-4, IL-7, IL-9 and IL-15, and development of T, B and NK cells (Asao et al., 2001; Kondo et al., 1997). As such, RAG2(-/-) x γc(-/-) mice are deficient in T, B and NK cells, and lack development of gut associated lymphoid tissue (GALT), peripheral lymph nodes,

intestinal intraepithelial lymphocytes and other lymphoid tissues such as splenic white pulp and thymus (Cao et al., 1995). Owing to their immunocompromised phenotype, the RAG2(-/-) x γc(-/-) mice are invaluable for xenograft transplant studies as well as stem cell research. As the RAG2(-/-) x γc(-/-) mice are on the same background strain as the animals used in my previous studies (C57BL/6 mice) and are lymphoid deficient, they were chosen to investigate the role of lymphoid cells in ozone-induced Th2 cytokine gene expression, eosinophilic rhinitis and nasal epithelial remodeling (e.g. mucous cell metaplasia)

I tested the hypothesis that lymphocytes, including innate lymphoid cells, are the major source for the Th2 cytokines associated with ozone-induced eosinophilic rhinitis and nasal epithelial remodeling. This study compared the epithelial changes, granulocyte influx and cytokine gene expressions in air and ozone-exposed RAG2(-/-) x γc(-/-) mice, with that of similarly exposed C57BL/6 mice.

B. Materials and Methods

1. Laboratory Animals

Specific pathogen free male C57BL/6 and transgenic RAG2(-/-) x γc(-/-) (nomenclature: B10;B6-*Rag2*^{tm1Fwa}*Il2rg*^{tm1Wjl}) mice (8 weeks of age; Taconics, Huson NY) were used in this part of study. Mice were housed in stainless steel wire cages, whole body inhalation exposure chambers (H-1000; Lab Products Marywood, NJ). Animals were provided free access to food (Harlan Teklad Irradiated 8940, Madison, WI) and water. Mice were maintained in Michigan State University (MSU) animal housing facilities accredited by the Association for Assessment and Accreditation of Laboratory Animal Care and according to the National Institutes of Health guidelines as overseen by the MSU Institutional Animal Care and Use Committee. Rooms were maintained at temperatures of 21°C–24°C and relative humidities of 45–70%, with a 12-h light/dark cycle starting at 7:30 A.M.

2. Experimental Design and Inhalation Exposures

Six mice per group [for each of C57BL/6 and RAG2(-/-) x γc(-/-) mice groups] were designated for histopathology and exposed to either filtered air or 0.5 ppm ozone for 9 days, at 4 hours of exposure per day. An additional 6 mice per group were similarly exposed and processed for nasal RNA extraction. Mice were euthanized 24 hours after the end of exposure (ozone or air). Animals were housed individually in stainless steel wire cages, and exposed in whole body inhalation exposure chambers (H-100; Lab Products Marywood, NJ). Ozone was generated with an OREC 03V1-Clone ozone generator (Ozone Research and Equipment Corp., AZ) using compressed air as a source of oxygen. Total airflow through the exposure chambers was 250

l/min (15 chamber air changes per hour). A Dasibi 1003 AH ambient air ozone monitor (Dasibi Environmental Corp., Glendale, CA) was used to monitor the chamber ozone concentrations.

3. Necropsies and Nasal Tissue Collection

At 24h post last exposure, mice were anesthetized with sodium pentobarbital (Vortech Pharmaceuticals, Ltd. Dearborn, MI) and sacrificed by exsanguination via the abdominal aorta. Immediately after death, the head of each animal was removed from the carcass. After the lower jaw and skin were removed, formalin or RNA-Later fluid was infused retrograde through the nasopharyngeal meatus. The head was immersed in 10% neutral buffered formalin for routine histology of the nasal cavity, or in RNA-Later (Sigma-Aldrich, an ammonium sulfate based RNA fixative/stabilizer) for nasal mucosal RNA extraction.

4. Tissue Processing for Light Microscopy, Histochemistry and Immunohistochemistry

Transverse tissue blocks of four anatomic sites from the heads of the mice were selected for light microscopy as previously described (Young 1981; Harkema et al. 2006; Islam et al. 2006). Briefly, the proximal section (T1) was taken immediately caudal to the upper incisor teeth; the middle section (T2) was taken at the level of the incisive papilla of the hard palate; the third nasal section (T3) was taken at the level of the second palatal ridge; and the most caudal nasal section (T4) was taken at the level of the intersection of the hard and soft palate, through the proximal portion of the olfactory bulb of the brain (see Figure 2 on page 25). Nasal tissue blocks were processed for histopathologic, immunohistochemical, and morphometric analyses. All of these blocks were embedded in paraffin, and the anterior face of each block was sectioned at a thickness of 5 microns and stained with hematoxylin and eosin for routine light microscopic

examination. Additional slides were stained with Alcian Blue (pH 2.5)/Periodic Acid Schiff (AB/PAS) to identify acidic and neutral mucosubstances stored in mucus-secreting cells of nasal airway surface epithelium.

For immunohistochemistry, slides were placed in Tris Buffered Saline for pH adjustment, followed by Heat Induced or Enzyme Induced Epitope Retrieval, and subsequently blocked for endogenous peroxidase using 3% Hydrogen Peroxide/Methanol. Following pretreatments standard Avidin, Biotin complex staining steps were performed at room temperature on the Dako Autostainer. Slides were blocked for non-specific protein in Normal Goat / Normal Rabbit Serum (Vector Labs – Burlingame, CA). Endogenous Biotin was blocked by incubation in Avidin D (Vector) and d-Biotin (SigmaAldrich – St.Louis, MO).

Sections were immunostained for mouse eosinophil specific major basic protein (MBP) using a rat antibody directed against murine MBP (1:10,000; Mayo Clinic, Scottsdale, AZ), and for neutrophils using Rat Anti-Mouse Neutrophil 7/4 Allotypic Marker (1:2500 AbD Seroterc Raleigh, NC). Sections were subsequently covered with secondary biotinylated antibodies, treated with alkaline phosphatase and visualized with Fast Red (Substrate Kit 1). For Ym1/2 immunohistochemistry, unstained and hydrated paraffin sections were incubated for one hour with rabbit polyclonal anti-Ym1 antibody at a dilution of 1:3,000. This antibody was a generous gift from Dr. Shioko Kimura (National Cancer Institute, Bethesda, MD) and was prepared by immunizing rabbits with 2 peptide sequences derived from eosinophilic crystals in gastric epithelium of CYP1A2 deficient mice. Immunoreactivity of Ym1/2 was visualized with Vector R.T.U. Elite ABC Peroxidase Reagent followed by Nova Red (Vector Laboratories Inc., Burlingame, CA). After immunohistochemistry, slides were dehydrated through ascending

grades of ethanol; cleared through several changes of xylene and cover-slipped using permanent mounting media.

5. Nasal Mucosal Morphometry

Amounts of epithelial mucosubstances, eosinophils and neutrophils in the mucosa, as well as epithelial Ym1/2 protein, were estimated quantified by standard morphometry techniques. All histological slides were scanned and digitalized with a slide scanner (VS110, Olympus) prior to quantification. Analysis of the virtual slides was performed with the newCast system (Visiopharm, Denmark). Briefly, images for analysis were sampled at the region of interest, i.e., entire length of the lateral walls in the T1 section, with a 100 % meander sampling at a 40x magnification.

For estimation of the amount of intraepithelial mucosubstances per length of basal lamina, a point-intercept grid was superimposed over the selected images. The point grids had an area/point of 16.90 μm^2 for estimating the area of mucosubstances per length of basal lamina. A line grid with an area/point of 563.20 μm^2 was used to estimate the corresponding surface density of the basal lamina.

The formula for the estimation of epithelial mucosubstances per basal lamina is described below. Density of mucosubstances ($\hat{V}_M$) was estimated by counting the number of points falling on epithelial areas staining positively for AB/PAS (P_M) multiplied by the area/point (a/p) and divided by the total number of point in all images (n) as shown in equation 1 (EQ1) .

$$\hat{V}_M = \frac{\sum P_M \times a/p}{n} \qquad \text{EQ 1}$$

The surface density of the basal lamina ($\hat{S}_{BL}$) in the selected images was estimated by counting the number of intercepts (I) of the line probe with the basal lamina of the lateral wall divided by

the length per point (l/p) and the number of points in all sampled images (n) as described in equation 2 (EQ2).

$$\hat{S}_{BL} = \frac{2 \times \sum I}{l / p \times n} \qquad \text{EQ2}$$

Stained mucosubstances per basal lamina of the lateral wall was then estimated by dividing $\hat{V}_M$ by $\hat{S}_{BL}$. For quantification of Ym1/2 labelling within nasal epithelium of lateral wall, the same formula and image analysis settings as that for mucus, with point grids area/point of 105.60 μm^2, were used.

The influx of neutrophil and eosinophil in the nasal mucosa was estimated by quantifying the amount of Major Basic Protein (MBP) immunolabelling for eosinophils, and the amount of rat anti-mouse neutrophil allotypic marker (clone 7/4) for neutrophils in the nasal mucosa of the lateral wall. A point grid with an area/point of 16.90 μm^2 was used to estimate the area of MBP and neutrophil marker respectively and a point grid with an area/point of 563.20 μm^2 was used to measure the reference space, i.e. the lamina propria and the epithelium of the lateral wall. The total number of points was the multiplied by the area/point for either MBP stain or neutrophil marker and for the reference space. The percentage of MBP or neutrophil marker per mucosa was calculated by dividing the area of the stain by the area of the reference space.

6. Total RNA Isolation from Nasal Mucosa

A longitudinal incision was made along the midline of individual RNA-Later preserved head of ozone-exposed and filtered air control group mice. The median septum was removed and the turbinates and lateral wall tissues were microdissected from both left and right nasal cavities (see Figure 2 on page 25). Tissues samples were removed and placed in RNALater and kept at 4ºC

for 24 hours then transferred to -80ºC until processed. Total RNA was extracted using RNeasy Mini Kit according to manufacturer's instructions (Qiagen, Valencia, CA). Briefly, tissues were homogenized in buffer RLT containing β -Mercaptoethanol with a 5mm rotor-sator Homogenizer (PRO Scientific, Oxford, CT) and centrifuged at 12,000g for 3 minutes. RNA was purified from the supernatant using the RNeasy capture column. Samples were treated with Qiagens Rnase-Free Dnase Set on the column (2X recommended concentration for 30min). Eluted RNA was quantified using a Genequant pro spectrophotometer (BioCrom, Cambridge, England).

7. Gene Expression Analysis

Reverse Transcription was performed using High Capacity cDNA archive Kit reagents (Applied Biosystems, Foster City, CA). RNA was incubated in GeneAmp PCR System 9700 Thermocycler PE (Applied Biosystems, Foster City, CA) at 25ºC for 10 Minutes, 37ºC for 2 hours and held at 4ºC. cDNA was diluted to 5ng/ul and 384 well reaction plates were set up robotically using the BioMek 2000 Automated Workstation (Beckman Coulter, Fullerton, Ca). Quantitative mRNA expression analysis was performed using the ABI PRISM 7900 HT Sequence Detection System using Taqman Gene Expression Assay reagents (Applied Biosystems). The cycling parameters were 48ºC for 2min, 95ºC for 10 min and 40 cycles of 95ºC for 15sec and 60ºC for 1min. The real-time PCR reaction was relatively quantified using the ΔΔCT method normalized to 18S, GAPDH and β-actin. Statistical analysis was performed in individual relative fold increase values using Sigma Stat (SPSS Inc, Chicago, IL). Hierarchical clustering of nasal mucosal gene expressions was performed in the TM4 Multiexperiment Viewer (MeV 4.8.1; (http://www.tm4.org) using Pearson correlation metric.

8. Statistical Analysis

Data are reported as mean ± SEM. Exposure related effects between air and ozone were assessed by a T-test for single comparisons where appropriate. Exposure and time related effects were determined by ANOVA, followed by Student-Newman-Keuls post hoc test, for multiple comparisons. Non-normal distributed data was analyzed by Kruskal-Wallis ANOVA on ranks. Specific statistical analysis for each data set is provided in each figure. Significance was assigned to p-values less than or equal to 0.05.

C. Results

1. Histopathology and Morphometry

Similar site specific ozone-induced nasal lesions were present in the C57BL/6 mice exposed to ozone for 9 consecutive weekdays, as previously described in the 9-day time course study. These changes were, again, characterized by granulocyte influx, epithelial hyperplasia and mucous cell metaplasia in the mucosa lining the lateral meatus of both proximal nasal passages. No nasal histopathology was present in mice exposed to filtered air. In both air-exposed and ozone-exposed RAG2(-/-) x γc(-/-) mice, there were scant granulocyte influx within the lamina propria and no epithelial remodeling, similar to that in the ozone-exposed C57BL/6 mice.

i. Eosinophil Infiltration

Eosinophilic rhinitis was present in the C57BL/6 mice exposed to 0.5 ppm ozone. There was no eosinophilic influx in the nasal mucosa of air control (0 ppm ozone) C57BL/6 mice, as well as in both air (0 ppm ozone) and 0.5 ppm ozone-exposed RAG2(-/-) x γc(-/-) mice (Figure 24). The morphometrically estimated quantities of eosinophils are shown in Figure 25. There was a significant increase in the mucosal density of eosinophils in the ozone-exposed C57BL/6 mice compared to all other groups. No eosinophils were detected in both air (0 ppm ozone) and 0.5 ppm ozone-exposed RAG2(-/-) x γc(-/-) mice.

Bone marrow within T1 to T4 sections of both air- and ozone-exposed mice were also examined histologically. MBP-laden eosinophils were present in the bone marrow of C57BL/6 mice as well as RAG2(-/-) x γc(-/-) mice, for both air and ozone exposure groups.

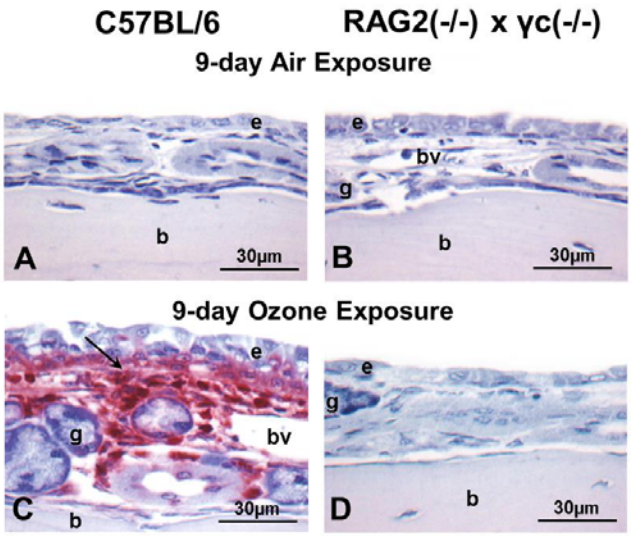

Figure 24. Eosinophil infiltration within the nasal mucosa of C57BL/6 mice and RAG2(-/-) x γc(-/-) mice after 9 weekdays of air (0 ppm) and ozone (0.5 ppm) exposures. **(A, B)** No eosinophils were present in the air-exposed animals for both mice strains. **(C)** Eosinophils, immunohistochemically labelled with Major Basic Protein (MBP) (solid arrow), predominate the granulocyte influx in the nasal mucosa of ozone-exposed C57BL/6 mice. **(D)** There were no eosinophils present in the nasal mucosa of ozone-exposed RAG2(-/-) x γc(-/-) mice. *(bv: blood vessel; e: epithelium; b:bone; g: gland)*

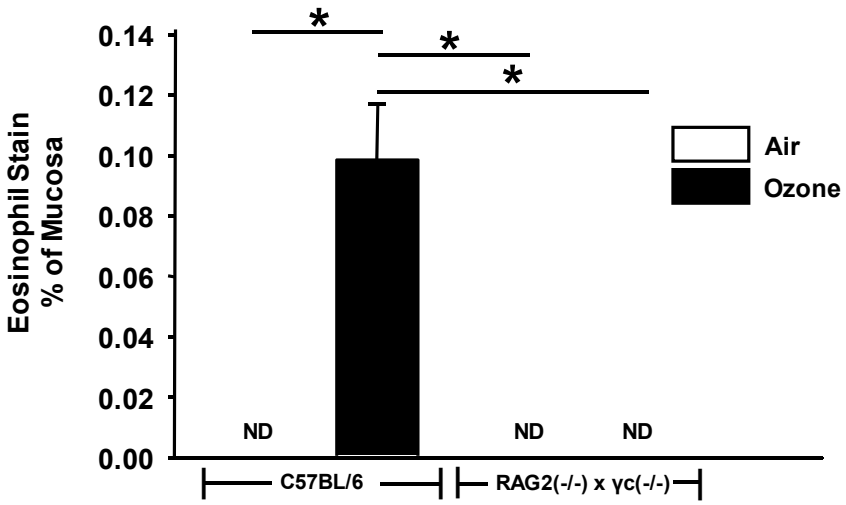

Figure 25. Morphometry of eosinophil infiltration in the mucosa of RAG2(-/-) x γc(-/-) and C57BL/6 mice after 9-weekdays inhalation exposure. There was a significantly greater eosinophilic influx in the ozone-exposed C57BL/6 mice compared to all other groups. No eosinophils were detected in both air (0 ppm ozone) and 0.5 ppm ozone-exposed RAG2(-/-) x γc(-/-) mice. ND = Not detected. *Statistically different, $p \leq 0.05$, by two-way ANOVA and Student-Newman-Keuls post hoc test. Data are expressed as mean ± SEM.

ii. Neutrophil Infiltration

Using rat anti-mouse neutrophil allotypic marker to label neutrophils, there was a very mild neutrophilic influx in the nasal mucosa of the ozone-exposed C57BL/6 mice. No or few neutrophils were present in the air-exposed (0 ppm ozone) C57BL/6 mice. In contrast, a conspicuous neutrophilic rhinitis was present in both air (0 ppm ozone) and ozone (0.5 ppm)-exposed RAG2(-/-) x γc(-/-) mice (Figure 26). Morphometrically estimated quantities of neutrophils in the nasal mucosa are shown in Figure 27. There was a significant difference in the neutrophilic infiltration in the ozone-exposed C57BL/6 mice compared to air control C57BL/6 mice. Both air and ozone-exposed RAG2(-/-) x γc(-/-) mice have significantly higher neutrophil infiltration within the nasal mucosa, compared to filtered air control C57BL/6 mice.

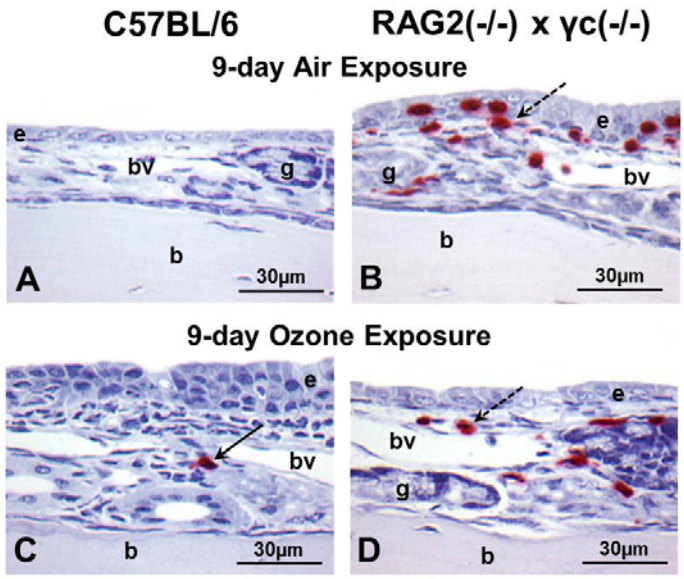

Figure 26. Neutrophils, immunohistochemistically labelled with rat anti-mouse neutrophil allotypic marker, within nasal mucosa of C57BL/6 mice and RAG2(-/-) x γc(-/-) mice after 9 weekdays of air (0 ppm) and ozone (0.5 ppm) exposures. **(A)** Neutrophils were absent in the air-exposed C57BL/6 mice. **(C)** Few neutrophils (solid arrows) were present in the ozone-exposed C57BL/6 mice. **(B, D)** Granulocyte influx in the nasal mucosa of the air-exposed and ozone-exposed RAG2(-/-) x γc(-/-) mice consisted of neutrophils (stippled arrows),. *(bv: blood vessel; e: epithelium; b:bone; g: gland)*

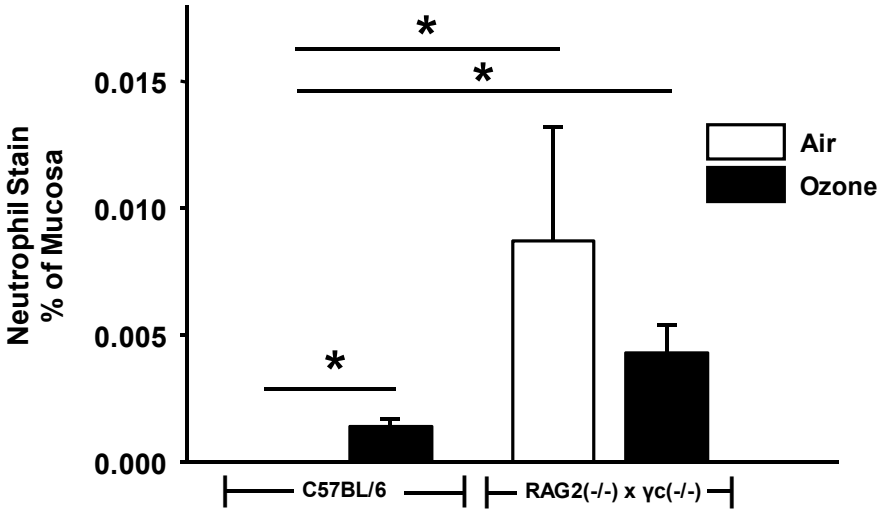

Figure 27. Morphometry of neutrophil infiltration in the mucosa of RAG2(-/-) x γc(-/-) and C57BL/6 mice after 9-weekdays inhalation exposure. There was a significant difference in the neutrophilic infiltration in the ozone-exposed C57BL/6 mice compared to air control C57BL/6 mice. Both air and ozone-exposed RAG2(-/-) x γc(-/-) mice had significantly greater neutrophil density in the nasal mucosa, compared to air control C57BL/6 mice. *Statistically different, $p \leq 0.05$, by two-way ANOVA and Student-Newman-Keuls post hoc test. Data are expressed as mean ± SEM.

iii. Epithelial Remodeling

On examination of the H&E sections, the previously described epithelial hyperplasia, hypertrophy and hyalinosis were, as expected, seen in the C57BL/6 mice exposed to 0.5 ppm ozone (Figure 28). These histological changes were not present in the air control C57BL/6 mice, and were also not seen in both air (0 ppm ozone) and 0.5 ppm ozone exposed RAG2(-/-) x γc(-/-) mice. The epithelium of both ozone and air-exposed RAG2(-/-) x γc(-/-) mice had no histopathological changes, and were similar to that of air-exposed C57BL/6 mice.

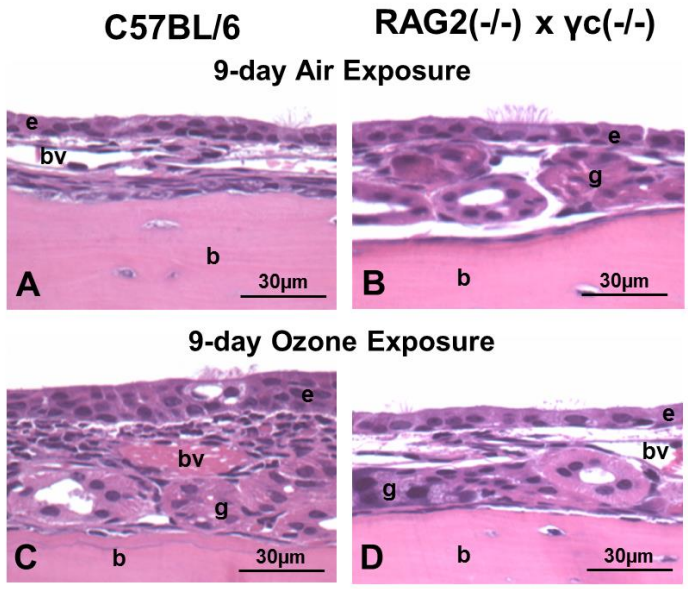

Figure 28. Light photomicrographs of nasal mucosa of C57BL/6 mice and RAG2(-/-) x γc(-/-) mice after 9-weekdays inhalation exposure. **(A, C)** There was mucosal epithelial hypertrophy/ hyperplasia and accumulation of eosinophilic hyaline material (hyalinosis) in the ozone (0.5 ppm)-exposed animals, but not in the air-exposed (0 ppm ozone) animals. **(B, D)** The nasal epithelium of both ozone- and air-exposed RAG2(-/-) x γc(-/-) mice had no histopathological changes, and were similar to that of air-exposed C57BL/6 mice. (Hematoxylin and Eosin). *(bv: blood vessel; e: epithelium; b:bone; g: gland)*

ix. Intraepithelial Mucosubstances

Using Alcian Blue PAS (pH 2.5) histochemical stain to highlight mucosubstances, an increase in amount of epithelial mucosubstances was observed in the apical aspect of the nasal epithelium lining the lateral wall in the ozone-exposed C57BL/6 mice, consistent with mucous cell metaplasia. Mucous cell metaplasia of the lateral wall mucosal epithelium was absent in air control (0 ppm ozone) C57BL/6 mice, as well as in both air (0 ppm ozone) and 0.5 ppm ozone-exposed RAG2(-/-) x γc(-/-) mice (Figure 29). Morphometrically estimated quantities of epithelial mucosubstances are illustrated in Figure 30. There were significant increases in the amount of epithelial mucosubstances in the ozone-exposed C57BL/6 mice compared to air-exposed C57BL/6 mice and both air- and ozone-exposed RAG2(-/-) x γc(-/-) mice (Figure 30).

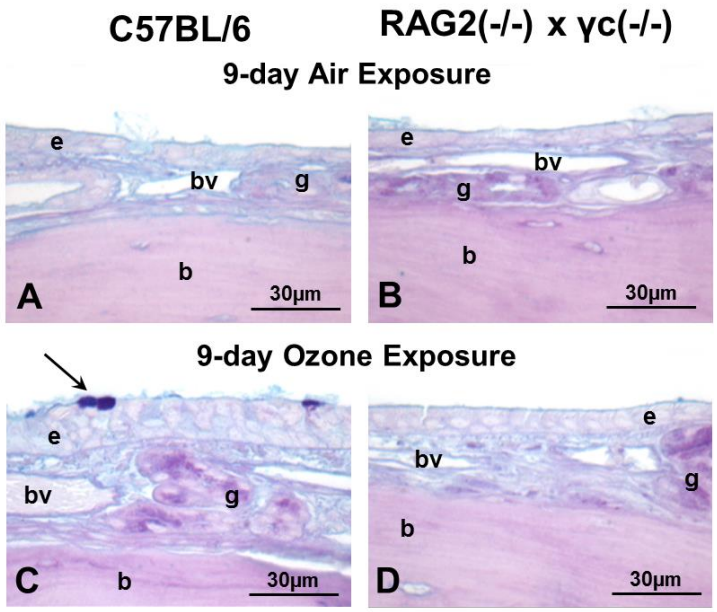

Figure 29. Intraepithelial mucosubstances in the mucosa lining the proximal nasal airways of RAG2(-/-) x γc(-/-) mice and C57BL/6 mice after 9-weekdays inhalation exposure. **(A, C)** There was an increase in the amount of apical intraepithelial mucosubstances in the ozone-exposed C57BL/6 mice (solid arrow), but was not present in the mucosa of air control (0 ppm ozone) C57BL/6 mice. **(B, D)** The epithelium of both ozone and air-exposed RAG2(-/-) x γc(-/-) mice had no intraepithelial mucosubstances. (Alcian Blue, pH 2.5 PAS) *(bv: blood vessel; e: epithelium; b:bone; g: gland)*

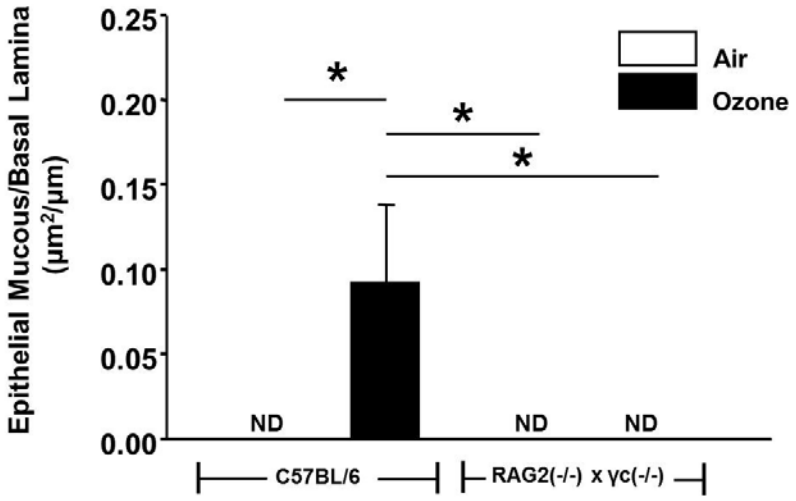

Figure 30. Morphometry of intraepithelial mucosubstances in the mucosa lining the proximal nasal airways of RAG2(-/-) x γc(-/-) mice and C57BL/6 mice after 9-weekdays inhalation exposures. There was a significant increase in the amount of epithelial mucosubstances in the ozone-exposed C57BL/6 mice, compared to air-exposed C57BL/6 mice and both air and ozone-exposed RAG2(-/-) x γc(-/-) mice. ND = Not detected *Statistically different, $p \leq 0.05$, by two-way ANOVA and Student-Newman-Keuls post hoc test. Data are expressed as mean ± SEM.

x. Intraepithelial Ym1/2 Protein

Ym1/2 immunohistochemistry revealed marked epithelial Ym1/2 protein accumulation in the ozone-exposed C57BL/6 mice. In contrast, scant amounts of Ym1/2 proteins were present in air (0 ppm ozone) control C57BL/6 mice, as well as in both air and ozone-exposed RAG2(-/-) x γc(-/-) mice (Figure 31). The amount of intraepithelial Ym1/2 (area of Ym1/2-stained protein per length of airway basal lamina) was morphometrically estimated (Figure 32). Marked increases in Ym1/2 protein were present in the 9 days ozone-exposed C57BL/6 animals, and was significantly greater than that in air (0 ppm ozone) control C57BL/6 mice, as well as that in both groups of RAG2(-/-) x γc(-/-) mice.

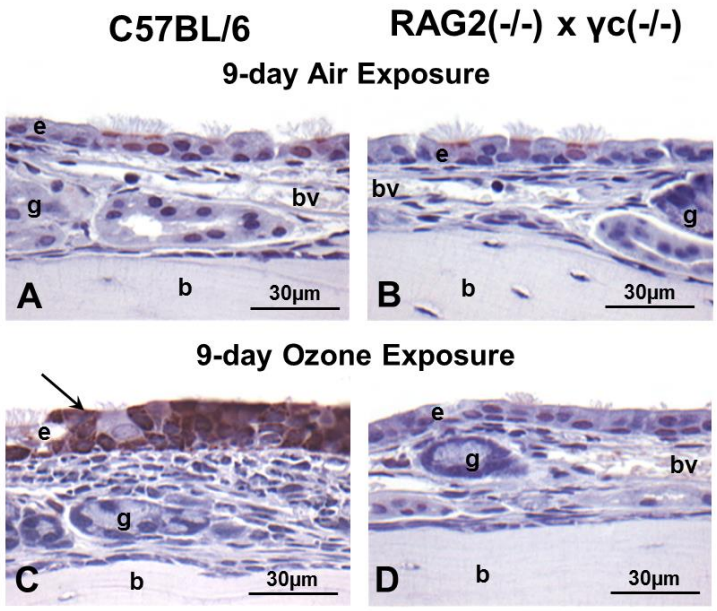

Figure 31. Epithelial Ym1/2 protein in nasal mucosa of C57BL/6 mice and RAG2(-/-) x γc(-/-) mice after 9-weekdays of inhalation exposures. **(A, C)** There was marked epithelial Ym1/2 protein in the nasal epithelium of ozone-exposed C57BL/6 mice (solid arrow), but only scant amounts of Ym1/2 protein was present in epithelium of air control (0 ppm ozone) C57BL/6 mice. **(B, D)** Nasal epithelium of both ozone- and air-exposed RAG2(-/-) x γc(-/-) mice had scant Ym1/2 protein within the apical portion of the epithelium, and similar to that in air control C57BL/6 mice. (rabbit polyclonal anti-Ym1 antibody) *(bv: blood vessel; e: epithelium; b:bone; g: gland)*

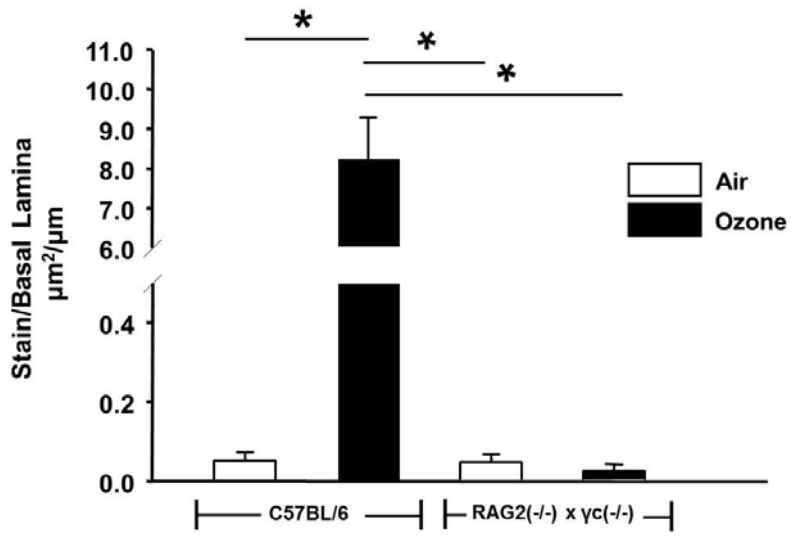

Figure 32. Morphometry of epithelial Ym1/2 in nasal mucosa of RAG2(-/-) x γc(-/-) mice and C57BL/6 mice after 9-weekdays of inhalation exposures. A marked increase in Ym1/2 protein was present in the ozone-exposed C57BL/6 animals, and this was significantly elevated compared to air (0 ppm ozone) control C57BL/6 mice, as well as compared to both groups of RAG2(-/-) x γc(-/-) mice. *Statistically different, $p \leq 0.05$, by two-way ANOVA and Student-Newman-Keuls post hoc test. Data are expressed as mean ± SEM.

2. Cytokine Gene Expression in Nasal Mucosa

i. Cytokine Gene Expression in Nasal Mucosa of RAG2(-/-) x γc(-/-) Mice and C57BL/6 Mice

Fold changes in cytokine gene expression in nasal mucosa of C57BL/6 mice and RAG2(-/-) x γc(-/-) mice after 9-day exposures to air and ozone are shown in Table 3 (Appendix). Values were expressed as mean ± standard error of the mean, relative to air group within each individual time point.

ii. Unsupervised Hierarchical Clustering of Gene Expression

There were two main branches within the hierarchical tree (Figure 33), representing Th1 and Th2 gene expression clusters. Compared to air control C57BL/6 mice, both air- and ozone-exposed RAG2(-/-) x γc(-/-) mice overexpressed Th1 cytokine genes (Saa3, IL-1β, RANTES and Tnf-α), whereas ozone exposed C57BL/6 mice had expression of Th2 cytokines (Arg1, Muc5AC, Ym2, Eotaxin, IL-10, IL-13, Gob-5, IL-5 and IL-4). There was a decrease in expression of Th2 cytokines (Ym2, IL-13, Gob-5, IL-5) in the RAG2(-/-) x γc(-/-) mice, relative to air control C57BL/6 mice.

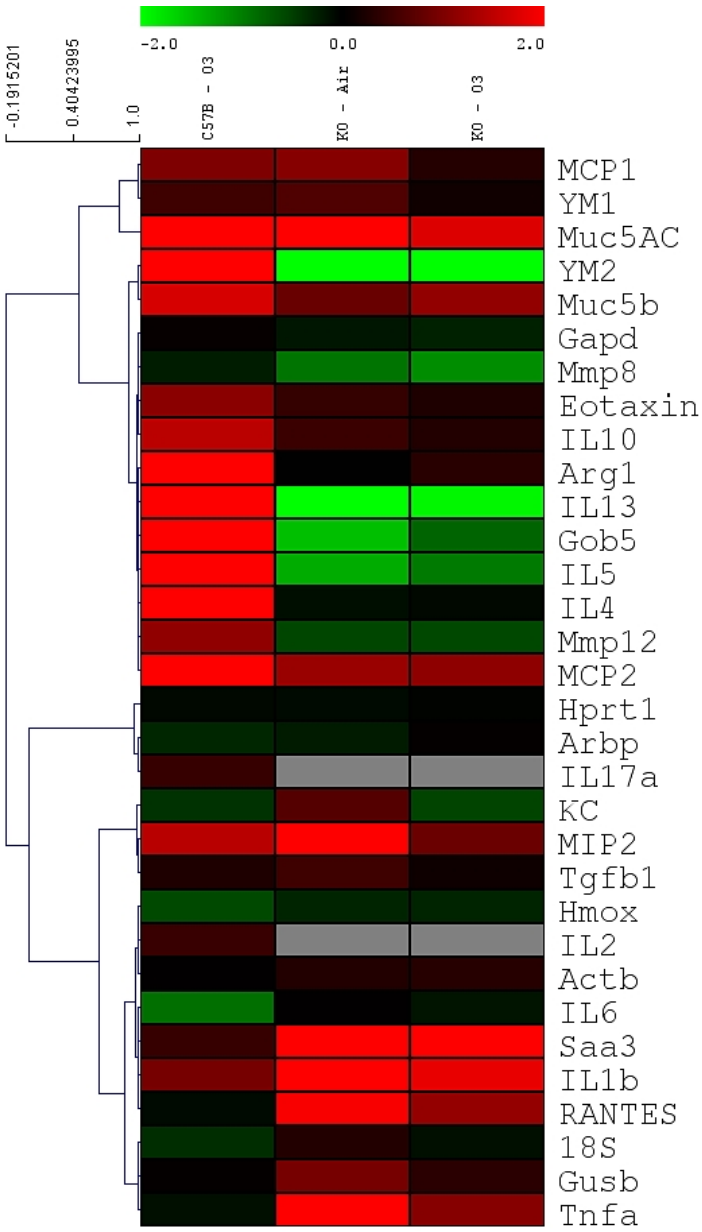

Figure 33. Unsupervised hierarchical clustering of changes in ozone-induced gene expression in nasal mucosa of RAG2(-/-) x γc(-/-) mice and C57BL/6 mice, relative to air-exposed C57BL/6 mice, after 9-weekdays of inhalation exposures

Red intensity = Degree of up-regulation vs. air-exposed controls.
Green intensity = Degree of down-regulation vs. air-exposed controls.
Hierarchical clustering was performed in the TM4 Multiexperiment Viewer (MeV 4.8.1; (http://www.tm4.org) using Pearson correlation metric.

iii. Th2 Cytokine Gene Expression

The fold changes in Arg1, Eotaxin, IL-10, IL-13, IL-5, MCP2 and Ym2 gene expressions, for both air and ozone-exposed RAG2(-/-) x γc(-/-) mice and C57BL/6 mice, were statistically analysed and graphically represented (Figure 34). These cytokine gene expressions were significantly elevated in the ozone-exposed compared to air-exposed C57BL/6 mice. In contrast, these genes were only insignificantly elevated or have negative fold changes, in both air and ozone-exposed RAG2(-/-) x γc(-/-) mice.

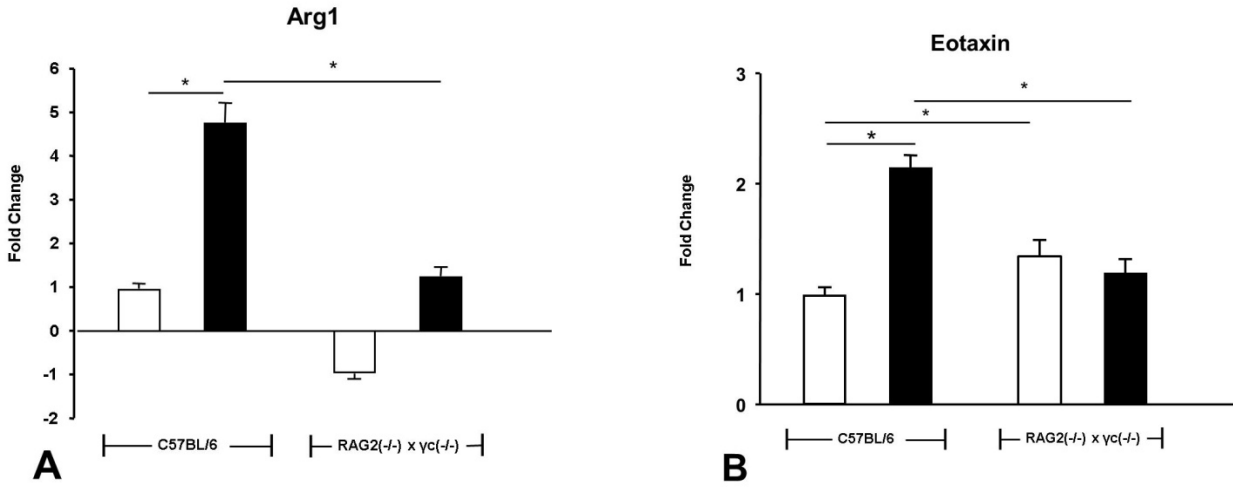

Figure 34. Fold changes in gene expressions in nasal lateral wall of RAG2(-/-) x γc(-/-) mice and C57BL/6 mice after 9-weekdays inhalation exposure, for selected Th2 cytokine genes. **(A, B, C, D, E, F, G)** Compared to air-exposed C57BL/6 mice, ozone exposed C57BL/6 mice had marked increases in the expression of Arg1, Eotaxin, IL-10, IL-13, IL-5, MCP2 and Ym2 cytokine genes. In contrast, these genes were not overexpressed or had negative fold changes, in both air and ozone-exposed RAG2(-/-) x γc(-/-) mice. *Statistically different from air-control group, $p \leq 0.05$, by two-way ANOVA and Student-Newman-Keuls post hoc test. Data are expressed as mean ± SEM.

Figure 34 (cont'd)

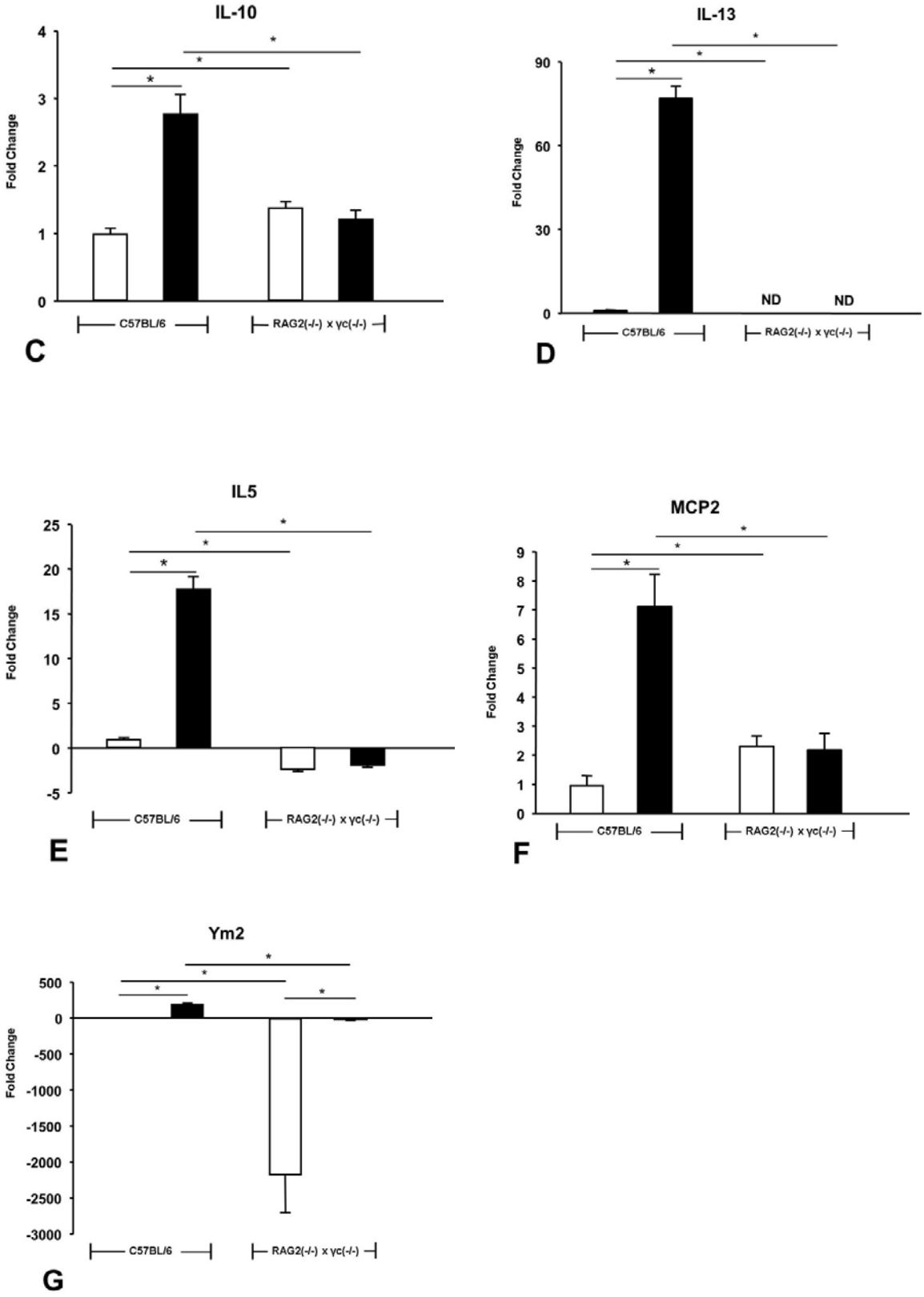

ix. Gob5, Muc5AC and Muc5b Cytokine Gene Expression

The fold changes in Muc5AC, Muc5b and Gob5 gene expression were statistically analysed and graphically represented (Figure 35). These cytokine gene expressions were significantly elevated in the ozone-exposed compared to air-exposed C57BL/6 mice. These genes were not overexpressed in either air- or ozone-exposed RAG2(-/-) x γc(-/-) mice.

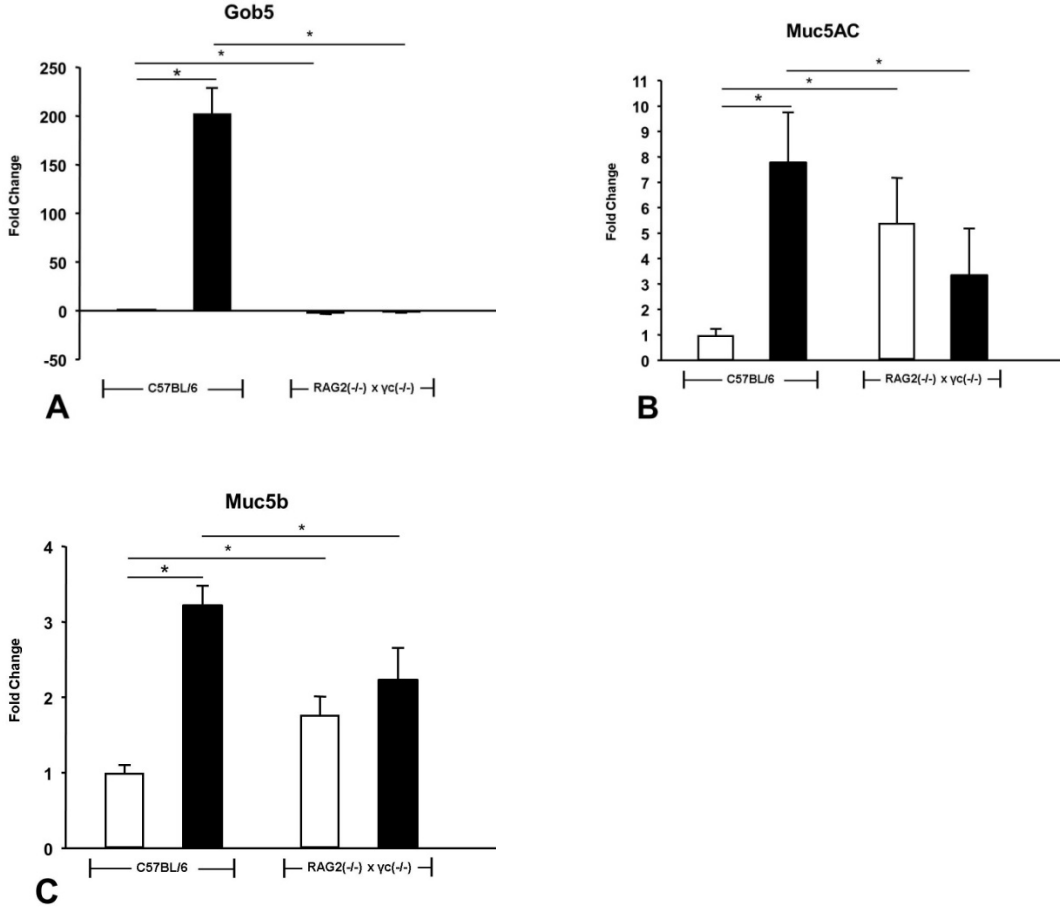

Figure 35. Fold changes in gene expressions in nasal lateral wall of RAG2(-/-) x γc(-/-) mice and C57BL/6 mice after 9-weekdays inhalation exposures, for Muc5AC, Muc5b and Gob5 genes. The gene expression of these three cytokines were significantly elevated in the ozone-exposed compared to air-exposed C57BL/6 mice. **(A)** Gob5 cytokine gene expression had negative fold changes in both air and ozone-exposed RAG2(-/-) x γc(-/-) mice. **(B, C)** Muc5AC and Muc5b cytokine gene expressions were not overexpressed in either air- or ozone-exposed RAG2(-/-) x γc(-/-) mice. *Statistically different from air-control group, $p \leq 0.05$, by two-way ANOVA and Student-Newman-Keuls post hoc test. Data are expressed as mean ± SEM.

D. Discussion

Based on the results of this study, lymphocytes play a crucial role in the development of eosinophilic rhinitis, nasal epithelial remodeling, mucous cell metaplasia and elevated Ym1/2 protein in the nasal epithelium of mice exposed to ozone. Th2 cytokines were overexpressed in ozone-exposed C57BL/6 mice, along with these epithelial changes. Overexpression of Th2 cytokines, nasal epithelial remodeling and mucous cell metaplasia were absent in both air- and ozone-exposed RAG2(-/-) x γc(-/-) mice.

Ozone-induced overexpression of Th2 cytokine genes was absent in the RAG2(-/-) x γc(-/-) mice, indicating that lymphoid cells are the source of these cytokines. In addition, these lymphoid depleted mice lacked overexpression of eotaxin, Gob5, IL-10, IL-13, IL-5, MCP-2 and Muc5AC after exposure to ozone. Eotaxin and IL-5 are related to recruitment of eosinophils, while Gob5 and Muc5AC are related to goblet cells hyperplasia/metaplasia. The absence of an increase in eotaxin and IL-5 cytokine gene expressions in the ozone-exposed RAG2(-/-) x γc(-/-) mice were correlated with the absence of eosinophilic rhinitis in these mice. The presence of eosinophils within the bone marrow of RAG2(-/-) x γc(-/-) mice suggested that these animals are not defective in the production of eosinophils, and that the absence of ozone-induced eosinophilic rhinitis in these mice was most likely due to a lack of Th2 cytokines, IL-5 and eotaxin that are responsible for eosinophil chemotaxis.

Likewise, the absence of mucous cell metaplasia and reduced expression of Muc5AC and Gob5 genes in the ozone-exposed RAG2(-/-) x γc(-/-) mice was most likely due to an absence of lymphocyte derived Th2 cytokines such as IL-13. Epithelial Ym1/2 protein accumulation in the nasal mucosal epithelium was also absent in the RAG2(-/-) x γc(-/-) mice in both exposure groups. It is interesting to note that the RAG2(-/-) x γc(-/-) mice had a much lower Ym2 gene expression in both exposure groups compared to the ozone exposed C57BL/6 mice. The level of

Ym2 expression in the RAG2(-/-) x γc(-/-) mice was likely too low to result in Ym1/2 protein accumulation that was seen in the ozone exposed C57BL/6 mice. As the expression of both Ym1 and Ym2 in mice are dependent on IL-13, the absence of lymphocyte derived Th2 cytokines such as IL-13 in RAG2(-/-) x γc(-/-) mice would most likely have resulted in the reduced expression of Ym1 and Ym2.

This study also demonstrated that neutrophils were the predominant inflammatory cells present in both the air and ozone exposed RAG2(-/-) x γc(-/-) mice. This could be due to the absence of a Th2 cytokine gene expression that is known to dampen Th1 gene expression. Saa3, Tnf-α and IL-1β cytokine gene expressions are associated with an acute inflammatory response, and are related to the recruitment of neutrophils (Helen et al., 2010; Rider et al., 2011; Saber et al., 2013). There was overexpression of these cytokines in the RAG2(-/-) x γc(-/-) mice compared to the C57BL/6 mice, and this correlated with the neutrophilic influx present in the nasal submucosal of the RAG2(-/-) x γc(-/-) mice. The nose is not sterile, and is constantly exposed to inhaled particles (e.g. dust, pollen) as well as to resident microflora (i.e. commensal bacteria). In response to these agents, the immunocompromised RAG2(-/-) x γc(-/-) mice may have mounted a persistent and compensatory innate immune response (dominated by neutrophils), and were unable to generate a Th2 cytokine driven adaptive immune response.

The absence of epithelial remodeling could be associated with the lack of development of eosinophilic rhinitis in ozone-exposed RAG2(-/-) x γc(-/-) mice. Eosinophils have been shown to play an important role in airway remodeling and fibrosis in asthma via activation of epithelium and mesenchymal cells, possibly via the role of TGF-β1 and other cytokines (Kariyawasam et al., 2007). Subcytotoxic levels of eosinophil cationic proteins (e.g. MBP) have also been shown to induce bronchiolar epithelial cells to synthesize remodeling molecules such as transforming

growth factors (TGFs), matrix metalloproteinases (MMPs) and platelet-derived growth factor (PDGFs) (Pégorier S et al, 2006). These factors, released by eosinophils during ozone-induced rhinitis, could have similar effects on the nasal epithelium and be the driving forces behind the nasal mucosal epithelial hyperplasia. In fact, in this study, expression levels of both MMP8 and MMP12 were decreased in the RAG2(-/-) x γc(-/-) mice compared to C57BL/6 mice.

In my previous study, the early expression of IL-5 and IL-13 observed in the ozone-exposed mice may have been an early cytokine responses induced by innate lymphoid cell population. Innate lymphoid cell Type 2 is a subtype of innate lymphoid cells that produces Th-2 cytokines including IL-5 and IL-13, which play a role in infections, asthma and allergy, as well as inflammatory bowel disease (Walker et al., 2013). These cells have been reported in the mesenteric lymph node, spleen, liver and bone marrow of mice (Hams et al., 2012).

Based on the results of this study, innate lymphoid (ILC2) cells and/or T-helper cells are likely to the main lymphoid cells responsible for inducing ozone-induced eosinophilic rhinitis and epithelial remodeling. CD4+ T-helper cells have been classically grouped as Th1, Th2, Th17 and regulatory T-cells (Mirchandani et al., 2014). Innate lymphoid cells, a unique and distinct class of lymphoid cells, have only been recently described. When stimulated, these cells produce several of the cytokines that were initially thought to be produced by the above-mentioned T-helper cells (Walker et al., 2013). Three subsets, Group 1, 2 and 3, of innate lymphoid cells of innate lymphoid cells (ILCs) have been described. Group 1 ILCs include NK cells and ILC1s, and produce predominantly Th1 cytokines. Group 2 ILCs include nuocytes, innate helper 2 cells (ILC2s) and produce mainly Th2 cytokines. Group 3 ILCs include lymphoid tissue-inducer (LTi) cells and ILC3s, and are associated with the production of IL-17a and IL-22 (Walker et al., 2013; Kumar et al., 2014). ILC2s play important roles in allergy and asthma with regards to pathology

and homeostasis, which is just beginning to be elucidated (Walker et al., 2013). In mice, ILC2s are found in the airways and characterized by expression of CD45, IL17-RB, IL-33R and Thy-1, CD117, CD25, CD69, CD90, among other markers (Mirchandani et al., 2014; Halim et al., 2013). ILCs have been shown to boost CD4+ T-helper cell responses to immune stimulation (Mirchandani et al., 2014), are also present in the lungs, and appear to be one of first responders that subsequently drive the Th2 cascade (Halim et al., 2013). These cells are also an important innate source of type 2 cytokines such as IL-5 and IL-13, which are involved in the pathogenesis of asthma (Li et al., 2013). In human studies, it is suggested that innate immune response through the action of innate T-helper cell (IL2) is responsible for IL-5, eotaxin and IL-33 production (Kwon et al., 2013).

A previous study showed that experimentally induced Th2 cytokine response in mice, via the infusion of IL-25, resulted in eosinophilic infiltration, increased mucus production and epithelial cell hyperplasia/hypertrophy in the lung of mice (Fort et al., 2001). More recently, IL-25 has been described as a cytokine that can be released from damaged epithelial cells damage (Li et al., 2013), subsequently acting as an alarmin and driving ILC2 mediated Th2 cytokine response. In my current series of studies, Th2 cytokine gene expression within the upper airways was associated with nasal mucosal epithelial hyperplasia and eosinophilic rhinitis. The absence of these cytokines, source of which could be Th2-helper cells or innate lymphoid cells (Type 2, of which produce Th2 cytokines), may have been associated with the lack of development of nasal epithelial remodeling and eosinophilic rhinitis in the RAG2(-/-) x γc(-/-) exposed to ozone.

Through this series of experiments, it is evident that ozone induced eosinophilic rhinitis, epithelial hyperplasia and mucous cell metaplasia, as well as overexpression of Ym1/2 protein, are lymphoid dependent. Lymphocytes may not be the sole source of cytokine production in

upper airway disease however, and the role of epithelium in airway defense may be more than a physical barrier. It has been shown that IL-33, an alarmin that is constitutively expressed in nucleus of several mouse tissues, is released during epithelial cell injury or necrosis. The cytokine IL-33, as well as IL-25 and TSLP, can be released by airway epithelial cells in response to stimuli or damage. Innate lymphoid cells (Type 2) (ILC2) are major responders to alarmin release from damaged tissues (Pichery et al., 2012; Bartemes et al., 2012), and ILC2 could be orchestrating the subsequent downstream pathway that involves eosinophilic rhinitis (via IL-4, IL-5, IL-13) and nasal epithelial remodeling.

The possibility of ILC2 cells playing a role in ozone-induced nasal pathology forms the basis for further studies, and a proposed pathway could be adapted from the recent paper by Li et al. (Li et al., 2013). Ozone-induced epithelial damage in the nasal airways signals the release of TSLP, IL-25 and IL-33 (alarmins) from the nasal epithelial cells. These cytokines activate ILC2 cells, which subsequently produce IL-4, IL-5 and IL-13, which then stimulate plasma cells to produce IgE, as well as induce an eosinophilic rhinitis. Eosinophils, being a source of Th2 cytokines, augment the Th2 cytokine overexpression initiated by ILC2. Eosinophil cationic proteins, released by eosinophils, cause epithelial hyperplasia and remodeling with increasing time of ozone exposure. Obliteration of the lymphoid population, including the ILC2s, will eliminate this pathway of ozone-induced rhinitis and epithelial changes.

The absence of epithelial remodeling, sustained epithelial damage, mucous cell metaplasia or eosinophilic rhinitis in the RAG2(-/-) x γc(-/-) histologically, despite ozone exposure begs the question of whether these responses are indeed beneficial to the ozone-exposed immunocompetent subjects, or whether these responses are an exaggerated immune response to a noxious stimulant. Extending this newly described paradigm of lymphoid

dependent, ozone-induced eosinophilic rhinitis (likely involving the role of ILC2s) beyond inhalation toxicology, one might speculate that ILC2s could play a role in other conditions/diseases characterized by eosinophilic influx in humans (e.g. asthma) (Saglani et al., 2014) and animals [e.g. canine eosinophilic bronchopneumopathy in dogs (Clercx et al., 2007), eosinophilic granuloma complex in cats]. In the next and last chapter, I will summarize and further discuss my current findings.

APPENDIX

APPENDIX

Gene	C57B6 - Air	C57B6 - O3	Rag2GammaC - Air	Rag2GammaC - O3
Arbp	1.00+/-0.18	-1.23+/-0.19	-1.16+/-0.26	1.03+/-0.22
Hmox	1.00+/-0.12	-1.49+/-0.08 (*)	-1.22+/-0.06	-1.21+/-0.07
Hprt1	1.00+/-0.03	-1.05+/-0.05	-1.06+/-0.06	-1.02+/-0.06
Mmp8	1.00+/-0.23	-1.17+/-0.33	-1.88+/-0.29	-2.17+/-0.19
KC	1.00+/-0.38	-1.31+/-0.44	1.60+/-0.51	-1.45+/-0.19
IL6	1.00+/-0.56	-1.83+/-0.46	1.02+/-0.26	-1.12+/-0.21
Arg1	1.00+/-0.12	4.78+/-0.44 (*)	-1.01+/-0.12	1.26+/-0.21 (#)
Gob5	1.00+/-0.25	202.65+/-26.33 (*)	-2.82+/-0.32 (#)	-1.74+/-0.31 (#)
IL13	1.00+/-0.19	76.92+/-4.33 (*)	-6.48+/-2.00 (#)	-3.83+/-1.31 (#)
IL5	1.00+/-0.17	17.78+/-1.39 (*)	-2.56+/-0.17 (#)	-1.95+/-0.20 (#)
IL4	1.00+/-0.39	4.78+/-1.19	-1.08+/-0.01	-1.05+/-0.02
Gapd	1.00+/-0.05	1.04+/-0.08	-1.13+/-0.09	-1.20+/-0.07
Mmp12	1.00+/-0.21	2.21+/-0.66 (*)	-1.47+/-0.55	-1.48+/-0.27 (#)
YM2	1.00+/-0.56	193.15+/-15.72 (*)	-2,183.08+/-520.62 (#)	-17.70+/-15.09 (*,#)
IL1b	1.00+/-0.14	1.91+/-1.02	4.98+/-1.46 (#)	3.56+/-0.89 (#)
Gusb	1.00+/-0.06	1.03+/-0.11	1.91+/-0.21 (#)	1.27+/-0.12 (*)
MCP1	1.00+/-0.15	1.00+/-0.19	2.09+/-0.58	1.23+/-0.26
MIP2	1.00+/-0.54	2.74+/-2.38	4.84+/-1.51 (#)	1.80+/-0.74
IL17a	1.00+/-0.54	1.35+/-1.24	N/D	N/D
IL2	1.00+/-0.12	1.37+/-0.28	N/D	N/D
Actb	1.00+/-0.03	1.02+/-0.04	1.21+/-0.03	1.24+/-0.02
Tgfb1	1.00+/-0.09	1.19+/-0.12	1.42+/-0.15 (#)	1.09+/-0.08
YM1	1.00+/-0.16	1.42+/-0.26	1.55+/-0.33	1.10+/-0.16
Eotaxin	1.00+/-0.07	2.14+/-0.11 (*)	1.34+/-0.15 (#)	1.19+/-0.12 (#)
IL10	1.00+/-0.08	2.78+/-0.28 (*)	1.38+/-0.09 (#)	1.21+/-0.13 (#)
Muc5b	1.00+/-0.10	3.22+/-0.26 (*)	1.77+/-0.25 (#)	2.23+/-0.42 (#)
Muc5AC	1.00+/-0.30	7.78+/-1.98 (*)	5.37+/-1.85 (#)	3.35+/-1.83 (#)
MCP2	1.00+/-0.32	7.13+/-1.10 (*)	2.31+/-0.36 (#)	2.18+/-0.57 (#)
Saa3	1.00+/-0.34	1.35+/-0.82	18.25+/-4.41 (#)	12.13+/-4.52 (#)
RANTES	1.00+/-0.18	-1.06+/-0.09	3.90+/-0.89 (#)	2.26+/-0.85 (*)
Tnfa	1.00+/-0.11	-1.09+/-0.24	7.67+/-2.33 (#)	2.09+/-0.48 (*,#)

Table 3. Gene expression in nasal mucosa of RAG2(-/-) x γc(-/-) mice and C57BL/6 mice after 9 days of ozone inhalation exposure. Values are expressed as fold changes, relative to C57BL/6 air group. N/D = undetected. * = statistically different within mouse strain. # = statistically different from C57BL/6 mouse, within exposure group

REFERENCES

REFERENCES

1. Asao H, Okuyama C, Kumaki S, Ishii N, Tsuchiya S, Foster D, Sugamura K. Cutting edge: the common gamma-chain is an indispensable subunit of the IL-21 receptor complex. J Immunol. 2001 Jul 1;167(1):1-5.

2. Bartemes KR, Kita H. Dynamic role of epithelium-derived cytokines in asthma. Clin Immunol. 2012 Jun;143(3):222-35.

3. Cao X, Shores EW, Hu-Li J, Anver MR, Kelsall BL, Russell SM, Drago J, Noguchi M, Grinberg A, Bloom ET, et al. Defective lymphoid development in mice lacking expression of the common cytokine receptor gamma chain. Immunity. 1995 Mar;2(3):223-38.

4. Clercx C, Peeters D. Canine eosinophilic bronchopneumopathy. Vet Clin North Am Small Anim Pract. 2007 Sep;37(5):917-35, vi.

5. Fort MM, Cheung J, Yen D, Li J, Zurawski SM, Lo S, Menon S, Clifford T, Hunte B, Lesley R, Muchamuel T, Hurst SD, Zurawski G, Leach MW, Gorman DM, Rennick DM. IL-25 induces IL-4, IL-5, and IL-13 and Th2-associated pathologies in vivo. Immunity. 2001 Dec;15(6):985-95.

6. Halim TY, McKenzie AN. New kids on the block: group 2 innate lymphoid cells and type 2 inflammation in the lung. Chest. 2013 Nov;144(5):1681-6

7. Hams E, Fallon PG: Innate type 2 cells and asthma. Curr Opin Pharmacol. 2012 Aug;12(4):503-9.

8. Harkema JR, Carey SA, Wagner JG: The nose revisited: a brief review of the comparative structure, function, and toxicologic pathology of the nasal epithelium. Toxicol Pathol. 2006;34(3):252-69.

9. Helen L. Wright, Robert J. Moots, Roger C. Bucknall, and Steven W. Edwards. Neutrophil function in inflammation and inflammatory diseases. Rheumatology. 2010. 49 (9): 1618-1631

10. Islam Z, Harkema JR, Pestka JJ. Satratoxin G from the black mold Stachybotrys chartarum evokes olfactory sensory neuron loss and inflammation in the murine nose and brain. Environ Health Perspect. 2006 Jul;114(7):1099-107.

11. Jones JM, Gellert M. The taming of a transposon: V(D)J recombination and the immune system. Immunol Rev. 2004 Aug;200:233-48.

12. Kariyawasam HH, Robinson DS. The role of eosinophils in airway tissue remodelling in asthma. Curr Opin Immunol. 2007 Dec;19(6):681-6.

13. Kondo M, Akashi K, Domen J, Sugamura K, Weissman IL. Bcl-2 rescues T lymphopoiesis, but not B or NK cell development, in common gamma chain-deficient mice. Immunity. 1997 Jul;7(1):155-62.

14. Kumar V. Innate lymphoid cells: new paradigm in immunology of inflammation. Immunol Lett. 2014 Jan-Feb;157(1-2):23-37.

15. Kwon BI, Hong S, Shin K, Choi EH, Hwang JJ, Lee SH. Innate type 2 immunity is associated with eosinophilic pleural effusion in primary spontaneous pneumothorax. Am J Respir Crit Care Med. 2013 Sep 1;188(5):577-85.

16. Li BW, Hendriks RW. Group 2 innate lymphoid cells in lung inflammation. Immunology. 2013 Nov;140(3):281-7.

17. Mirchandani AS, Besnard AG, Yip E, Scott C, Bain CC, Cerovic V, Salmond RJ, Liew FY. Type 2 Innate Lymphoid Cells Drive CD4+ Th2 Cell Responses. J Immunol. 2014 Jan 27.

18. Molofsky AB, Nussbaum JC, Liang HE, Van Dyken SJ, Cheng LE, Mohapatra A, Chawla A, Locksley RM. Innate lymphoid type 2 cells sustain visceral adipose tissue eosinophils and alternatively activated macrophages. J Exp Med. 2013 Mar 11;210(3):535-49.

19. Pégorier S, Wagner LA, Gleich GJ, Pretolani M. Eosinophil-derived cationic proteins activate the synthesis of remodeling factors by airway epithelial cells. J Immunol. 2006 Oct 1;177(7):4861-9.

20. Pichery M, Mirey E, Mercier P, Lefrancais E, Dujardin A, Ortega N, Girard JP: Endogenous IL-33 is highly expressed in mouse epithelial barrier tissues, lymphoid organs, brain, embryos, and inflamed tissues: in situ analysis using a novel Il-33-LacZ gene trap reporter strain. J Immunol. 2012 Apr 1;188(7):3488-95.

21. Rider P, Carmi Y, Guttman O, Braiman A, Cohen I, Voronov E, White MR, Dinarello CA, Apte RN. IL-1α and IL-1β recruit different myeloid cells and promote different stages of sterile inflammation. J Immunol. 2011 Nov 1;187(9):4835-43.

22. Saber AT, Lamson JS, Jacobsen NR, Ravn-Haren G, Hougaard KS, Nyendi AN, Wahlberg P, Madsen AM, Jackson P, Wallin H, Vogel U. Particle-induced pulmonary acute phase response correlates with neutrophil influx linking inhaled particles and cardiovascular risk. PLoS One. 2013 Jul 24;8(7).

23. Saglani S, Lloyd CM. Eosinophils in the pathogenesis of paediatric severe asthma. Curr Opin Allergy Clin Immunol. 2014 Feb 4.

24. Young JT. Histopathologic examination of the rat nasal cavity. Fundam Appl Toxicol. 1981 Jul-Aug;1(4):309-12.

25. Walker JA, Barlow JL, McKenzie AN. Innate lymphoid cells--how did we miss them? Nat Rev Immunol. 2013 Feb;13(2):75-87

CHAPTER 4

SUMMARY, CONCLUSIONS AND FUTURE DIRECTIONS

In the first chapter, I introduced ground level ozone as a common secondary gaseous air pollutant and a principal oxidant air pollutant of photochemical smog. Ozone exerts adverse health effects on the respiratory tract of humans, associated with increased morbidity and mortality (Bell et al., 2004; Burnett et al., 2001; Gryparis et al., 2004; Jerrett et al., 2013), as well as impairment of pulmonary function (Bromberg et al., 1995). Children and infants are at higher risk to the adverse effects of airway injury from air pollution (Kim, 2004), and exposure of children to unhealthy levels of ozone at a young age can cause injury to the respiratory system and result adverse health effects later in life. I also discussed the ozone inhalation toxicity studies in animals**,** and highlighted differences in gross structure and distribution of nasal epithelium between species.

In the second chapter, I described the temporal changes in nature of inflammatory cell infiltration, mucosal epithelial remodeling, as well as localized cytokine expression in the nasal cavity of mice, induced by subacute ozone exposure. A marked eosinophilic rhinitis was observed in mice that received the longer-term episodic exposures to ozone for nine or 24 consecutive weekdays. As murine granulocytes are often indistinguishable via routine H&E, specific immunohistochemical markers for murine neutrophils and eosinophils were used to differentiate these two granulocytic populations. Transmission electron microscopy was also used to identify the ultrastructural features of eosinophils, further confirming the infiltrating granulocytes as eosinophils. The temporal changes in epithelial remodeling were characterized by epithelial hyperplasia, Ym1/2 protein accumulation as well as increase in epithelial mucosubstances. These changes were morphometrically analysed for mice exposed to 1, 2, 4, 9 and 24 days of ozone and filtered air. I also described an early Th1 followed by predominantly Th2 cytokine gene expression profile in the nasal mucosa of ozone-exposed mice, which

accompanied the temporal development of eosinophilic rhinitis and epithelial remodeling. Expression of Th1 cytokines was restricted to mice that had received 1 or 2 day exposures to ozone, while Th2 cytokines expression was seen in mice exposed to ozone in the later time points after 4 to 9 days of exposure. The Th2 cytokine gene expression was observed along with the epithelial remodeling, hyalinosis and mucous cell metaplasia of nasal mucosa. The biphasic pattern of expression in IL-5, IL-10, eotaxin and IL-13 genes prompted further investigation into the possible role of lymphoid cells as an early source of Th2 cytokines that subsequently drives the Th2 cytokine directed immune response and epithelial remodeling.

In the third chapter, I conducted studies that were designed to test the hypothesis that ozone-induced eosinophilic rhinitis is dependent on Th2 cytokines produced by lymphoid cells. RAG2(-/-) x γc(-/-) mice, which are deficient in T-lymphocytes, B-lymphocytes and NK cells, do not develop eosinophilic rhinitis when subjected to 9 days of ozone inhalation exposures. The presence of eosinophils within bone marrow of both air and ozone exposed RAG2(-/-) x γc(-/-) mice suggested that the absence of ozone-induced eosinophilic rhinitis is most related to lack of eosinophil chemotaxis rather than eosinophil production. In both the air and ozone exposed RAG2(-/-) x γc(-/-) mice, neutrophils were the predominant inflammatory cells present. RAG2(-/-) x γc(-/-) mice exposed to 9-day ozone, also do not develop nasal epithelial remodeling, mucous cell metaplasia nor overexpression of Th2 cytokines. These studies showed that lymphocytes play a crucial role and are the primary source of Th2 cytokines associated with the development of ozone-induced eosinophilic rhinitis, nasal epithelial remodeling, mucous cell metaplasia and Ym1/2 protein accumulation in the nasal mucosa of mice.

The results of this study provided an insight into the question of how the eosinophilic rhinitis and epithelial remodeling due to repeated ozone exposure in mice, could be related to the

injury to the respiratory tract and to the development of chronic diseases in humans. The early nasal changes seen in C57BL/6 mice exposed to 0.5 ppm ozone, characterized by neutrophilic rhinitis and epithelial injury, are very similar to that seen in humans subjected to short term ozone exposure (Bascom et al., 1990; Koren et al., 1989). The nasal changes seen at the later time-points in these mice, characterized by Th2 cytokine expression, epithelial remodeling and eosinophilic rhinitis, mimic changes seen in human respiratory diseases with eosinophilic inflammation such as asthma, allergic and non-allergic rhinitis. Epidemiological studies have reported associations between elevated ambient ozone concentrations and the increase in eosinophil-derived proteins (e.g., eosinophil cationic protein and eosinophil protein X) in the urine of both asthmatic and non-asthmatic children, suggesting that repeated ozone exposures is associated with eosinophilic, rather than neutrophilic, airway inflammation in humans (Frischer T et al, 1993; Frischer T et al., 2001; Hiltermann et al., 1997). While ozone by itself is not an allergen, studies have shown that ozone has a priming effect in nasal airways of humans to allergen (Peden DB et al, 1995) and has been associated with increased allergic sensitization and asthma in children, as well as increased prevalence of atopy and susceptibility to the ozone-induced rhinitis (Kim et al., 2012; Pénard-Morand et al.; 2005; Peden et al., 2001).

Ym1/2 proteins, demonstrated in this study to accumulate within mucosal epithelium of mice repeatedly exposed to ozone, have been shown to be chemotactic for eosinophils and to play a role in airway remodeling in the allergic lung of mice (Webb DC, 2001). It has also been suggested that these proteins act as an auto-antigen in mice (Qureshi et al, 2011). Based on these literature and the current results, one can further postulate that nasal epithelial Ym1/2 proteins could be an ‘auto-antigen’ that induce an eosinophilic rhinitis that is markedly enhanced by ozone exposure in mice.

The findings of this study on ozone induced eosinophilic rhinitis and epithelial remodeling, along with currently available literature, suggests a hypothetical pathway (mode of action or pathogenesis) for ozone-induced airway inflammation and remodeling in mice (Figure 36), partially adapted from the recent paper by Li et al (Li et al., 2013). Nasal mucosal epithelium is normally lined by ciliated cells and a protective mucus layer. Ozone, with its oxidizing properties, exhausts the anti-oxidant capabilities of this protective layer and generates free radicals that subsequently cause lipid peroxidation of the epithelial cell membranes. In the early stage of ozone-exposure, damaged epithelial cells are unable to maintain osmotic balance and hence exhibit vacuolar swelling and degeneration. Early epithelial damage by ozone also stimulates an innate immune response typified by neutrophilic influx within the lamina propria. Epithelial damage in the nasal airways also signals the release of TSLP, IL-25 and IL-33 (alarmin) from the nasal epithelial cells. These cytokines activate lymphoid cells (possibly ILC2s), which then produce an early increase in IL-5, eotaxin and IL-13, subsequently inducing an eosinophilic rhinitis. The expression of IL-13 and mucous genes also initiate mucous cell metaplasia and increased epithelial mucosubstances lining the nasal mucosal epithelium. Ym1/2 protein within the nasal epithelium could act as a chemotactic agent for eosinophils, as well as an auto-antigen which then generate a persistent and marked eosinophilic rhinitis with repeated ozone exposure. Eosinophils, also a source of Th2 cytokines, augment the Th2 cytokine overexpression initiated by the lymphoid cells. Eosinophil cationic proteins (e.g. MBP) released by eosinophils could induce nasal epithelial cells to synthesize remodeling molecules such as TGFs, MMPs and PDGFs, which subsequently cause epithelial hyperplasia and remodeling. Obliteration of the lymphoid population (including the ILC2s) in the RAG2(-/-) x γc(-/-) mice, may not alter the initial epithelial damage of ozone, but my study with these mice did

demonstrate that lymphoid cells are crucial for the development of ozone-induced eosinophilic rhinitis and epithelial remodeling, including mucous cell metaplasia, Ym1/2 overexpression.

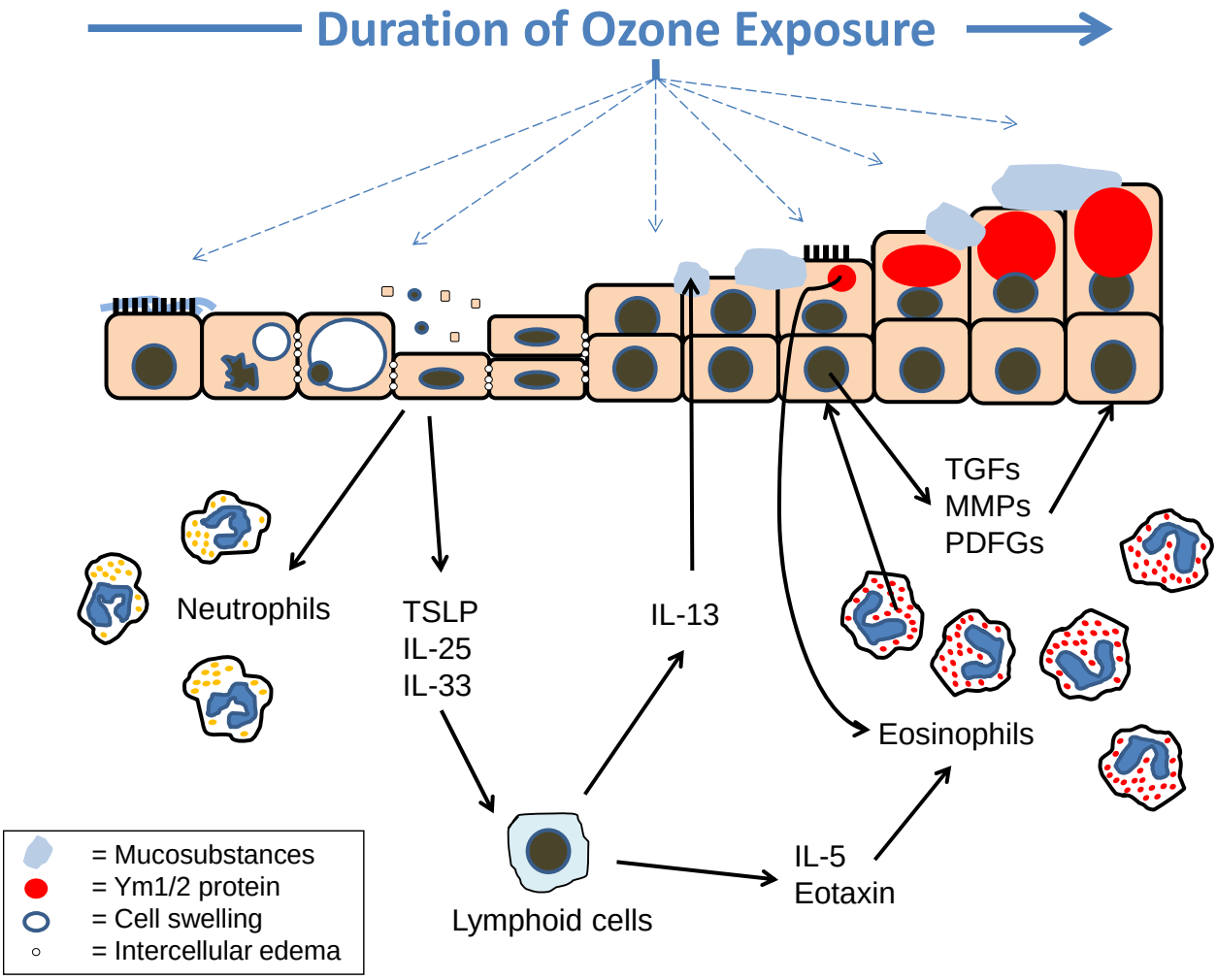

Figure 36. Ozone-Induced Airway Inflammation & Remodeling in Mice. In the early stage of exposure, ozone exhausts the anti-oxidant capabilities of the protective layer lining airway epithelium, and generates free radicals that subsequently cause cell membrane lipid peroxidation, vacuolar swelling and degeneration, as well as intercellular edema. Early epithelial damage by ozone also stimulates a neutrophilic rhinitis. Epithelial damage in the nasal airways also signals the release of TSLP, IL-25 and IL-33 from the nasal epithelial cells, which then activate lymphoid cells to produce an early increase in IL-4, IL-5, eotaxin and IL-13. IL-4, IL-5 and eotaxin induce an eosinophilic rhinitis, while expression of IL-13 along with mucus genes results in mucous cell metaplasia and increased production of epithelial mucosubstances. Generation of Ym1/2 proteins within the nasal epithelium may be acting act as a chemotactic agent for eosinophils. Eosinophil cationic proteins (e.g. MBP) released by eosinophils, induce nasal epithelial cells to synthesize remodeling molecules such as TGFs, MMPs and PDGFs, which subsequently cause epithelial hyperplasia and remodeling.

Further investigations are needed to support, amend, modify and/or supplement my proposed pathway. These include the roles of ILC2, IgE in ozone-induced eosinophilic rhinitis, effects of eosinophilic cationic proteins on nasal epithelial cells, as well as role of nociceptors (sensory nerve endings) in the nasal cavity of mice exposed to ozone.

Based on the current studies, innate lymphoid (ILC2) cells and/or T-helper cells appear to be part of a pathway in driving ozone-induced eosinophilic rhinitis and epithelial remodeling. Specifically, Group 2 ILCs, which play important roles in allergy and asthma, and produce mainly Th2 cytokines, could be the major source of innate IL-5 and IL-13 seen in the early time points of these studies. Interestingly, Rag2 (-/-) mice, in contrast to RAG2(-/-) x γc(-/-) mice, still have functional common gamma chain which is required for development of T, B and NK cells. As development of ILC2s (also known as nuocytes and natural helper cells) is also dependent on the expression of gamma C surface receptor (Hwang YY et al, 2013), one could postulate that via the use of Rag2 (-/-) mice, the role of ILC2 in the temporal development of ozone-induced eosinophilic rhinitis could be further elucidated. If ozone exposed Rag2 (-/-) mice developed the previously described epithelial, inflammatory and gene expression changes similar to those seen in C57BL/6 mice, it would suggest that ILC2 cells, rather than T- lymphocytes, are essential for the Th2 cytokine production, development of ozone-induced eosinophilic rhinitis and epithelial remodeling. In fact, a study by Halim et al., the authors used adoptive transfer of Type 2 innate lymphoid cells into Rag2GammaC double knockout mice, and restored the allergic phenotype in lungs of these mice (Halim TY et al, 2012). At the time of that report, these cells were called ‘lung natural helper cells’. The classification and nomenclature of these newly described cells has been actively changing as new discoveries are made.

We know that IL-5 is a major factor for the maturation, activation, recruitment and survival of eosinophils. Via the use of IL-5 knockout mice, one would expect that ozone exposure will not induce an eosinophilic rhinitis. However, it would be difficult to differentiate if this absence of eosinophilic influx is due to the lack of production/maturation of eosinophils in the bone marrow, or due to the lack of eosinophil chemotaxis.

The IgE level of mice in this study was not investigated. In humans, allergic and non-allergic rhinitis have been described. Allergic rhinitis is differentiated from its counterpart by the elevation of systemic IgE level in affected patients. Non-allergic rhinitis, on the other hand, is associated with chronic nasal symptoms in response to a non-allergen (e.g. cigarette smoke) and a negative allergen test. Hence, determining whether or not mice with ozone-induced eosinophilic have elevated IgE levels, could help associate the findings of this study as a being a better representation and perhaps model for human allergic or non-allergic rhinitis.

Epithelial remodeling could be related to the presence of subcytotoxic levels of eosinophil cationic proteins (e.g. MBP), which have been shown to induce bronchiolar epithelial cells to synthesize remodeling molecules such as transforming growth factors (TGFs), matrix metalloproteinases (MMPs) and platelet-derived growth factor (PDGFs) (Pégorier S et al, 2006). A similar mechanism of action could perhaps, be extrapolated to this study with regards to the nasal epithelial remodeling in response to ozone. However, further experiments are required to support this postulation.

The nose is innervated by trigeminal free nerve endings and solitary chemosensory cells (SCC) that facilitate protective reflexes in the nasal passage (Saunders CJ et al, 2014). A possible role of solitary chemosensory cells (SCC) in development of non-allergic rhinitis in human was discussed in a recent paper by Saunders CJ et al, 2014. In that study, a pathway involving

nociceptive fibers stimulation by airway irritant and subsequent release of Substance P, followed by stimulation of mast cell degranulation by Substance P, was proposed. Although no increase in mast cells was identified in the mucosa of mice exposed to ozone in our present study, these cells are also associated with eosinophilic airway disease and may have a role in ozone-induced changes in the nasal passages.

In summary, repeated inhalation exposures to ozone in mice cause a temporal development of eosinophilic rhinitis, overexpressed Ym1/2 protein, mucous cell metaplasia, and Th2 cytokines gene expression, all of which are lymphoid dependent. The possible role of ILC2s as major sources of these Th2 cytokines, involved in ozone-induced eosinophilic rhinitis and nasal epithelial remodeling, warrants further investigation in the near future.

REFERENCES

REFERENCES

1. Bascom R, Naclerio RM, Fitzgerald TK, Kagey-Sobotka A, Proud D: Effect of ozone inhalation on the response to nasal challenge with antigen of allergic subjects. Am Rev Respir Dis. 1990 Sep;142(3):594-601.

2. Bell M, McDermott A, Zeger S, Samet J, Dominici F. Ozone and short-term mortality in 95 US urban communities, 1987–2000. JAMA 2004;292:2372–2378

3. Bromberg PA, Koren HS: Ozone-induced human respiratory dysfunction and disease. Toxicol Lett. 1995 Dec;82-83:307-16.

4. Burnett RT, Smith-Doiron M, Stieb D, Raizenne ME, Brook JR, Dales RE, Leech JA, Cakmak S, Krewski D. Association between ozone and hospitalization for acute respiratory diseases in children less than 2 years of age. Am J Epidemiol 2001;153:444–452.

5. Frischer TM, Kuehr J, Pullwitt A, Meinert R, Forster J, Studnicka M, Koren H. Ambient ozone causes upper airways inflammation in children. Am Rev Respir Dis. 1993 Oct;148(4 Pt 1):961-4.

6. Frischer T, Studnicka M, Halmerbauer G, Horak F Jr, Gartner C, Tauber E, Koller DY. Ambient ozone exposure is associated with eosinophil activation in healthy children. Clin Exp Allergy. 2001 Aug;31(8):1213-9.

7. Gryparis A, Forsberg B, Katsouyanni K, Analitis A, Touloumi G, Schwartz J, Samoli E, Medina S, Anderson HR, Niciu EM, et al. Acute effects of ozone on mortality from the "Air Pollution and Health: A European Approach" project. Am J Respir Crit Care Med 2004;28:28.

8. Halim TY, Krauss RH, Sun AC, Takei F. Lung natural helper cells are a critical source of Th2 cell-type cytokines in protease allergen-induced airway inflammation. Immunity. 2012 Mar 23;36(3):451-63

9. Hiltermann TJ, de Bruijne CR, Stolk J, Zwinderman AH, Spieksma FT, Roemer W, Steerenberg PA, Fischer PH, van Bree L, Hiemstra PS. Effects of photochemical air pollution and allergen exposure on upper respiratory tract inflammation in asthmatics. Am J Respir Crit Care Med. 1997 Dec;156(6):1765-72.

10. Hwang YY, McKenzie AN. Innate lymphoid cells in immunity and disease. Adv Exp Med Biol. 2013;785:9-26.

11. Jerrett M, Burnett RT, Beckerman BS, Turner MC, Krewski D, Thurston G, Martin R, von Donkelaar A, Hughes E, Shi Y, Gapstur SM, Thun MJ, Pope CA 3rd. Spatial

Analysis of Air Pollution and Mortality in California. Am J Respir Crit Care Med. 2013 Jun 27.

12. Kim BJ, Hong SJ. Ambient air pollution and allergic diseases in children. Korean J Pediatr. 2012 Jun;55(6):185-92.

13. Kim JJ; Ambient air pollution: health hazards to children. American Academy of Pediatrics Committee on Environmental Health. Pediatrics. 2004 Dec;114(6):1699-707.

14. Koren HS, Devlin RB, Graham DE, Mann R, McGee MP, Horstman DH, Kozumbo WJ, Becker S, House DE, McDonnell WF: Ozone-induced inflammation in the lower airways of human subjects. Am Rev Respir Dis. 1989 Feb;139(2):407-15.

15. Peden DB, Setzer RW Jr, Devlin RB. Ozone exposure has both a priming effect on allergen-induced responses and an intrinsic inflammatory action in the nasal airways of perennially allergic asthmatics. Am J Respir Crit Care Med. 1995 May;151(5):1336-45.

16. Peden DB. Effect of pollutants in rhinitis. Curr Allergy Asthma Rep. 2001 May;1(3):242-6.

17. Pégorier S, Wagner LA, Gleich GJ, Pretolani M. Eosinophil-derived cationic proteins activate the synthesis of remodeling factors by airway epithelial cells. J Immunol. 2006 Oct 1;177(7):4861-9.

18. Pénard-Morand C, Charpin D, Raherison C, Kopferschmitt C, Caillaud D, Lavaud F, Annesi-Maesano I. Long-term exposure to background air pollution related to respiratory and allergic health in schoolchildren. Clin Exp Allergy. 2005 Oct;35(10):1279-87.

19. Qureshi AM, Hannigan A, Campbell D, Nixon C, Wilson JB. Chitinase-like proteins are autoantigens in a model of inflammation-promoted incipient neoplasia. Genes Cancer. 2011 Jan;2(1):74-87.

20. Saunders CJ, Christensen M, Finger TE, Tizzano M. Cholinergic neurotransmission links solitary chemosensory cells to nasal inflammation. Proc Natl Acad Sci U S A. 2014 Apr 7.

21. Webb DC, McKenzie AN, Foster PS. Expression of the Ym2 lectin-binding protein is dependent on interleukin (IL)-4 and IL-13 signal transduction: identification of a novel allergy-associated protein. J Biol Chem. 2001 Nov 9;276(45):41969-76.